Aalto University
School of Chemical
Engineering

MIIKA MARTISKAINEN

INVESTIGATING THE EFFECTS OF PROCESS CONDITIONS ON THE CAPTURING CAPACITY OF GUARD MATERIALS

Master´s Programme in Chemical, Biochemical and Materials Engineering

Major in Chemical Engineering

Master's thesis for the degree of Master of Science in Technology submitted for inspection, Espoo, 27 September, 2020.

Supervisor: Professor Ville Alopaeus

Advisors: Dr. rer. nat. Sylvia Albersberger

Dr. Sc. Salla Likander

Aalto University
School of Chemical
Engineering

Aalto University, P.O. BOX 11000, 00076 AALTO
www.aalto.fi

Abstract of master's thesis

Author Miika Martiskainen

Title of thesis Investigating the effects of process conditions on the capturing capacity of guard materials

Degree Programme Master's programme in Chemical, Biochemical and Materials Engineering

Major Chemical and Process Engineering

Thesis supervisor Professor Ville Alopaeus

Thesis advisor(s) / Thesis examiner(s) Doctor Sylvia Albersberger, Doctor Salla Likander

Date 27.9.2020 **Number of pages** 130 **Language** English

Abstract

The utilization of a guard bed can potentially mitigate fouling and poisoning of the catalysts by removing the impurities from the process stream before the catalyst. The purpose of this Master's thesis was to be a pre-study for the removal of impurities by utilizing the guard bed technology. This work investigated the effect of temperature, pressure and space velocity on the impurity removal. Based on the evaluation of the experiments a test run procedure for future studies is proposed.

This thesis focused mainly on the removal of two impurities (phosphorus and silicon) using γ-alumina as the guard material. The investigation of the topic was undertaken by performing test runs with bench scale tube reactors packed with the guard material. The two feeds were used in the test runs. One had phosphorus and the other one had silicon as the primary impurity. The test runs consisted of a reference run and three conditions change runs where one process condition was altered in each. The liquid products were analysed primarily using ICP-MS and the guard materials were characterized mainly with XRF.

Test runs with the phosphorus rich feed showed that the phosphorus removal occurs mainly by formation of salts and subsequent collection in the reactor bed. The results showed that the temperature had the most influence on the phosphorus removal. Lower temperature decreased the removal and higher space time increased it. In the test runs using the silicon rich feed the removal of silicon seemed to occur mostly by decomposition of silicon compounds to volatile compounds. From the results it was difficult to distinguish the effects of condition changes due to the leaching of metals and silicon from the reactor bed or the equipment by the feed. A temperature decrease seemed to increase silicon removal by decreasing the leaching. A lower feed rate possibly favoured the removal of silicon via adsorption than the evaporation. Pressure had no major effect on the phosphorus and silicon removal.

The temperature could be increased in further test runs with phosphorus rich feed while the other conditions could be kept the same as in the reference test run. γ-alumina occurred not to be a suitable guard material for the silicon rich feed due to its leaching by the feed. Without feed pretreatment, the process conditions which mitigate the leaching should be used meaning lower temperature and the space time should not be increased. For future test runs with both feeds the reactor packing should be improved. The guard beds should also be prewashed before test runs to mitigate leaching from the fixed bed.

Keywords Guard bed, Process conditions, Impurity removal, Renewable and recycled feedstocks, Phosphorus, Silicon, Alumina

.

Aalto University
School of Chemical
Engineering

Aalto University, P.O. BOX 11000, 00076 AALTO
www.aalto.fi

Abstract of master's thesis

Author Miika Martiskainen

Työn nimi Tutkimus prosessiolosuhteiden vaikutuksesta suojamateriaalien talteenottokapasiteettiin

Koulutusohjelma Master's programme in Chemical, Biochemical and Materials Engineering

Pääaine

Työn valvoja Professori Ville Alopaeus

Työn ohjaaja(t)/Työn tarkastaja(t) Tohtori Sylvia Albersberger, Tohtori Salla Likander

Päivämäärä 27.9.2020 **Sivumäärä** 130 **Kieli** Englanti

Tiivistelmä

Suojapetien käyttö voi mahdollisesti vähentää katalyyttien likaantumista ja myrkyttämistä poistamalla epäpuhtaudet prosessivirrasta ennen katalyyttipetiä. Tämän opinnäytetyön tarkoituksena oli olla esitutkimus epäpuhtauksien poistamiseksi suojapetiteknologiaa hyödyntämällä. Työssä tutkittiin lämpötilan, paineen ja tilavuusajan vaikutusta epäpuhtauksien poistoon. Työhön liittyvien kokeiden tuloksien perusteella ehdotettiin koeajometodeja jatkotutkimuksia varten.

Opinnäytetyö keskittyi pääasiassa kahden epäpuhtauden (fosforin ja piin) poistamiseen käyttämällä suojamateriaalina γ-alumiinia. Aiheen tutkiminen suoritettiin koeajoilla pienen mittakaavan putkireaktoreilla, joihin suojapetimateriaali oli pakattuna. Työn koeajoissa käytettiin kahta eri syöttöä, joissa yhdessä oli suuri määrä fosforia ja toisessa piitä. Koeajot koostuivat referenssiajoista ja kolmesta koeajosta, joissa muutettiin yhtä prosessiolosuhdetta verrattuna referenssiajoon. Koeajojen nestemäiset tuotteet analysoitiin pääasiassa ICP-MS:llä ja suojapetimateriaalit karakterisoitiin pääosin XRF:llä.

Koeajoissa fosforirikkaalla syötöllä osoitettiin, että fosfori poistui syötöstä pääasiassa muodostamalla suoloja, jotka kerääntyvät reaktoripetiin. Tulokset näyttivät, että lämpötilalla oli eniten vaikutusta fosforin poistoon kuin muilla olosuhteilla. Matalampi lämpötila laski fosforin poistamista ja taas korkeampi tilavuusaika tehosti sitä. Piirikkaan syötön koeajoissa piin poistuminen tapahtui suurimmalta osin piin yhdisteiden hajoamisella haihtuviksi yhdisteiksi. Tuloksista oli vaikea erottaa olosuhteiden muutosten vaikutuksia, mikä johtui metallien ja piin liukenemisesta syöttöön reaktoripedistä tai laitteistosta. Lämpötilan laskeminen näytti lisäävän piin poistoa vähentämällä sen liukenemista. Pienentämällä syöttönopeutta piin poistaminen näyttää mahdollisesti tapahtuvan haihtumisen sijaan enemmän adsorption avulla. Paineella ei ollut merkittävää vaikutusta fosforin ja piin poistamiseen.

Jatkotutkimuksissa fosfori rikkaalla syötöllä lämpötilaa voitaisiin nostaa ja taas muut olosuhteet voitaisiin pitää samoina kuin referenssikoeajossa. γ-alumiinioksidia ei vaikuttanut olevan sopiva suojamateriaali piirikkaan syöttöä varten johtuen sen liukenemisesta syöttöön. Jos syöttöä ei esikäsitellä, seuraavissa koeajoissa tulisi käyttää liukenemista lieventäviä prosessiolosuhteita eli matalampaa lämpötilaa ja mahdollisimman suurta tilavuusaikaa. Tulevia koeajoja varten molempien syöttöjen koeajojen reaktorinpakkaamismenetelmää olisi parannettava. Suojapedit tulisi myös esihuuhdella reaktoripedin liukenemisen vähentämiseksi.

Avainsanat Suojapeti, Prosessiolosuhteet, Epäpuhtauksien poistaminen, Uusiutuvat ja kierrätetyt raaka-aineet, Fosfori, Pii, Alumiinioksidi

Table of contents

Symbols and Abbreviations

BET (isotherm)	Brunauer-Emmett-Teller isotherm
BJH (isotherm)	Barrett-Joiner-Halenda isotherm
C_{Ag}	Concentration of compound A in the fluid phase (gas)
C_{As}	Concentration of compound A at the external surface of the catalyst
$C_{CO \cdot S}$	Concentration of the adsorbate CO on the surface of the adsorbent
C_t	Total concentration of active sites
D_4	Octamethylcyclotetrasiloxane
EDS	Energy Dispersive X-ray Spectroscopy
FT-IR	Fourier-Transform Infrared Spectroscopy
GC	Gas chromatography
GPC	Gel Permeation Chromatography
HDO	Hydrodeoxygenation
ICP	Inductively Coupled Plasma
K_A	Adsorption equilibrium constant
LHSV	Liquid Hourly Space Velocity
M	Active metal site
MS	Mass Spectrometry
P_{CO}	Concentration or partial pressure of adsorbate CO in bulk fluid
PDMS	Polydimethylsiloxane
RI (detector)	Refractive index detector
SEM	Scanning Electron Microscope
TAN	Total Acid Number /mg KOH/g

TGA	Thermogravimetric Analysis
UV (detector)	Ultraviolet detector
X_i	Conversion of the species i
x_{if}	Concentration molar fraction of the species i in the feed
x_{ip}	Concentration of molar fraction of the species I in the products
XRD	X-ray Diffraction
XRF	X-ray Fluorescence
$\theta_{(pore)}$	Thiele modulus (for a pore)

1 INTRODUCTION

The demand of renewable feedstocks is increasing as the fossil-based material resources are diminishing. Substituting the use of fossil-based materials in chemical, pharmaceutical and plastic industries with ones produced from renewable sources, such as renewable oils and fats, would reduce the greenhouse gas emissions. This in turn would have a positive effect on the climate change. The use of fossil-based feedstocks still possesses some challenges as the feedstocks commonly contain sulphur, nitrogen, silicon and metal containing impurities. Renewable and recycled feedstocks can contain as many impurities as fossil derived feeds. Additionally, they can contain high amount of phosphorus, alkali and alkaline earth metals. These impurities are an issue in processing renewable and recycled feeds because they are able to cause pressure drop and deactivate the catalyst. The pressure drop can be partially mitigated by decreasing the feed flow rate to the reactor and continue running at lower capacity until the next turnaround. However, this would mean reduced production and in turn loss of profit. The other way to alleviate the pressure drop would be to skim and replace the most plugged parts of the reactor bed, which is usually the top of the reactor bed. The poisoned catalyst, however, would require a total change of the reactor inventory. Skimming and catalyst replacement results in a loss of production time and the cost of new reactor fillings. In principle, these problems could be avoided, if the impurities are removed from the feed before they enter the main catalyst. A possible method to remove feed impurities is the utilization of guard beds which function as adsorbent beds and/or filters to trap the impurities. [1-4]

As information about the impact of reaction conditions on the function of guard beds is scare, the purpose of this thesis is to offer new information about the influence of process conditions, such as temperature, pressure and space velocity, on the removal of the different impurities present in renewable feedstocks. Moreover, a testing protocol for future studies of guard materials will be established to potentially optimize the guard bed conditions.

The literature study of the thesis focuses on the reasons and mechanisms of catalyst deactivation caused by different impurities occurring in the renewable feed-

stocks and the mitigation of catalyst deactivation with guard materials. The literature study also comprises the most abundant impurities present in renewable and recycled feedstocks.

The removal of impurities from a phosphorus and a silicon rich renewable and recycled feedstock has been investigated in the experimental part of this work. The guard material for the experiments was chosen to be γ-alumina (γ-Al_2O_3). The main emphasis has been put on the impact of the reaction conditions on the removal of phosphorous and silicon but removal of some alkali and alkaline earth metals, such as sodium, potassium and calcium, have been additionally followed. Study of the thermal stability of a phosphorus rich feed has also been included in this work to gain knowledge about the effect of temperature on the composition of the feed and along with that the behaviour of the impurity containing molecules. The experiments have been carried out with bench scale tube reactors. The composition of the liquid products has been analysed mainly with ICP-MS and the fresh and spent γ-alumina has been characterized using XRF, XRD and SEM-EDS. In addition to the impact of the reaction conditions on the removal of impurities from both feeds, the capacity of alumina to uptake phosphorous and silicon, respectively, have been studied.

2 LITERATURE PART

2.1 Importance of catalysis for chemical industry

Catalysts can be considered as the backbone of the chemical industry. It has been estimated that catalysts are used in approximately 85–90 % of all chemical processes in industry which is why catalysis affects one quarter of the gross domestic products of developed countries. Catalysts are essential in the production of nearly all chemicals, fuels, polymers and fibres. In 2001, the world market for catalysts was around 10 billion dollars which was nearly equally distributed over refining, polymerization, chemicals, and environmental implementation. [5-7]

The primary reason for the high use of catalysts is their ability to allow reactions to occur more rapidly and/or with higher selectivity by providing reaction pathways a less energy demanding mechanism. These reactions can require lower temperatures and pressures than the non-catalysed routes, which would need such severe process conditions that they would not be economically viable for an industrial production. [5,7]

Catalysis can be categorized into three different subcategories: heterogeneous catalysis, homogeneous catalysis and biocatalysis. Homogenous catalysis comprises reactions where the catalyst is in the same phase as at least one reactant. These reactions occur usually in liquid phase and acids/bases or organometallic compounds are used as catalysts. An example for a homogeneous gas phase catalyst is nitrogen oxides (NO_x) in the lead chamber process. Catalysts used in homogeneous catalysis possess high efficiency and selectivity. Homogeneously catalysed reactions usually occur at relatively low temperatures (50 – 200 °C). However, a disadvantage of homogeneous catalysis is that the catalysts have to be separated from the reaction products. Thus, recycling and reuse of homogenous catalyst as well as the purification of the product phase can be challenging and costly. [7,8]

Enzymes are large complex proteins and known as biocatalysts. They have a very specifically shaped site where only similarly shaped reactants (substrates) or their transition states can connect. After the catalytic reaction the product disconnects

from the active site of the enzyme. The enzyme and the substrate behave similar to a lock and a key meaning different enzymes only catalyse reactions with specific substrates. Enzymes are highly efficient and require mild conditions. They however are temperature and pH sensitive and their separation from the products is also difficult. [7,8]

Heterogeneously catalysed reactions often have a lower selectivity and mass and heat transfer limitations compared to the other two subcategories. Although, they can be applied in a wide array of processes and they are easy to separate from the products which is why 80 % of all catalytic processes in the industry utilize heterogeneous catalysis. Typically, heterogeneous catalysis requires higher temperatures (above 250 °C) compared to homogeneous catalysis. The subsequent literature study is focused only on heterogeneous catalysts which are explained more in detail in the following section. [7,9]

2.2 Heterogeneous catalysts

In heterogeneous catalysis the catalysts are in a different phase than the reactants, in most cases they are solid, for instance, metals or metal oxides, and the reactants are in gas and/or liquid phase. The catalytic reaction itself takes place on a so-called active site on the surface of the catalyst for example on an acidic site. Reactants are able to form a chemical bond with this active site and then undergo a reaction. The more active sites are available for the reactants, the more of these reactions can occur. This is why industrial catalysts tend to be porous materials with large surface areas so that the quantity and accessibility of the active sites is maximized. [5,7]

2.2.1 Structure of supported catalysts

Industrial catalysts commonly used in heterogeneous reactions consist of three components: an active material, a support and in some cases a promoter. These kinds of catalysts are referred to as supported catalysts, where the active material and promoter are dispersed as microcrystallites over the surface of a porous support. Catalysts can also be unsupported metals which consist of an active material with a possible added promoter. [5,7,8]

2.2.1.1 Active materials of supported catalysts

The active material of a catalyst contains the active sites, thus making it the most important part of the catalyst. Noble metals, transition metals and their oxides, sulphides, carbides and nitrides are often used as active materials. They are able to effortlessly donate or accept electrons, which allows them to form or break chemical bonds. In Table 1, the most common active phases together with their components and the reactions they typically catalyse are summarized. [5,7]

Table 1. Typical catalytically active materials and the industrial reactions where they are used. [5]

Active phase	**Elements and compounds**	**Industrial reactions**
Metals	Fe, Co, Ni Cu, Ru, Rh, Pd, Ir, Pt, Au	Hydrogenation, steam reforming, oxidation, ammonia synthesis, Fischer-Tropsch process
Oxides	Oxides of V, Mn, Fe, Cu, Mo, W, Al, Si, Sn, Pb, Bi	Acid-catalysed reactions, oxidation of hydrocarbons
Sulphides	Sulphides of Co, Mo, W, Ni	Hydrotreating, hydrogenation
Carbides	Carbides of Fe, Mo, W	Hydrogenation, Fischer-Tropsch process

2.2.1.2 Support materials

Supports (also known as carriers) are usually porous materials with a high surface area which are relatively inert. Their purpose is to provide a large surface area where the active material can be widely dispersed and thus allowing a higher number of accessible active sites. They also improve the thermal stability of the catalysts, thus avoiding thermal degradation, sensitivity that the non-supported catalysts have. Supports are most commonly metal oxides or carbons such as alumina, silica and active carbon. [5,7]

Alumina (Al_2O_3) is frequently used as a support material. It is discussed more in detail in Subsection 2.5.1.1. [5]

Silica (SiO_2) is used to a minor extent than alumina due to its lower thermal stability which is why it is applied in processes with a relatively low temperature (below 300 °C). Silica also tends to produce volatile hydroxides at high temperature when exposed to steam which can lead to equipment corrosion. Additionally, silica is difficult to press into pellets. The pore size, particle size and surface area of silica

are relatively easy to adjust to specific requirements by their preparation method. .Consequently, the properties can differ by a large range, for example they can have effective surface between 300 – 900 m^2/g. Silica is mainly used as support material in hydrogenation, polymerization and oxidation reactions. Silica is favoured upon alumina for processes with sulphur rich feedstocks because it is more resistant to reactions between its surface and sulphur containing compounds. These reactions would produce surface sulphate species which could result in catalyst deactivation. [5,7]

Another support material applied in the industry is carbon which is prepared through the pyrolysis of natural sources such as trees and plants. The pyrolysis is done in inert gas, carbon dioxide (CO_2) and steam. The nature of the carbon sources and the pyrolysis conditions affect the properties of the carbon support. Carbon produced at pyrolysis temperatures between 800 – 1500 °C and by subsequent treatment in oxygen is called active carbon. It has a surface area up to 1000 – 1500 m^2/g and it is considered to be an ultrahigh surface area support. Higher temperatures during synthesis lead to graphitic carbon which has a lower surface area than active carbon. In general, carbon is used as a support for noble catalysts in hydrogenation reactions of organic compounds in the fine chemical industry as it is thermally stable in reducing atmosphere. Additionally, the noble metals are easy to disperse on the surface of the carbon. [5,7]

Zeolites are natural or synthetic crystalline aluminosilicates. They have a well-defined open structure and a high surface area (500 – 1000 m^2/g), which is why they possess a high reproducibility in production. They are shape selective as only the substrates smaller than their nearly uniform pore size can enter the pore and thus react. Additionally they are thermally very stable up to 600 °C. Due to these reasons they are attractive support materials. In addition to catalysis, they have applications in adsorption and ion exchange processes. The acid sites of zeolites are also another important property of them. The zeolites can exhibit two types of acid sites: Lewis acid and Brønsted acid sites (Figure 1). Lewis acid sites are ions or molecules who are able to accept an electron pair whereas Brønsted acid sites are per definition ions or molecules being able to donate protons (H^+). Both sites can catalyse multiple reactions. [5,7]

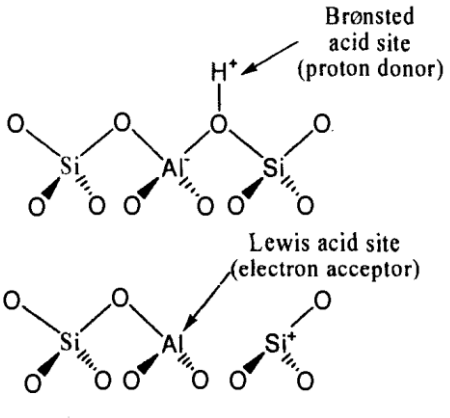

Figure 1. Depiction of Lewis and Brønsted acid sites on a zeolite. [5]

2.2.1.3 Promoters

Promoters are so-called catalyst spices with the purpose to enhance and maintain catalyst properties such as dispersion of active material and stability. The amount of a promoter is relatively small, usually 1–5 wt. %. The promoters are mixed to the active material or the support during preparation. They can be categorized into textural and chemical promoters. The textural promoters aid the preparation of adequate and stable dispersion of the active material also under reaction conditions. A support can, in general, act as a textural promoter. Chemical promoters, in contrast, increase the activity or selectivity of the catalysts. Alkali and alkaline earth metals as well as metal oxides are frequently used as chemical promoters. For example, in the ammonia synthesis, electronical interaction of potassium oxide (K_2O) with the active iron phase enhances the adsorption properties. This increases dissociative adsorption of N_2 on the active iron site. [5,7]

2.2.2 Catalyst properties

In this chapter different properties of catalysts are discussed. The catalysts properties can be divided into dynamic, chemical and physical characteristics. [5,7]

2.2.2.1 Dynamic properties of catalyst

The dynamic properties comprise the performance of the catalyst during the reaction. The activity of the catalyst is used to describe the acceleration of reaction rate by the catalyst. A catalyst potentially promotes simultaneous reaction pathways which produce different products. The selectivity of the catalyst describes the ratio between the desired reaction routes to the competing pathways. It is usually ex-

pressed as percentage of the desired product or comparative rates. Chemical reactions and process conditions can change the physical and chemical properties of the catalyst which can result in the loss of activity. The stability of the catalyst is the ability of the catalyst to resist these changes. It is commonly specified by types such as thermal and poison stability. [5,7]

2.2.2.2 Chemical properties of catalyst

The chemical properties of the catalyst are mainly determined by the surface properties of the catalyst such as composition, oxidation state of the active metal, chemical environment and acidity. The acidity of the catalyst is a major factor in many catalytic reactions. They are especially important in reactions of hydrocarbons, for example cracking, isomerization and polymerization. The fore mentioned zeolites are one of the catalysts that possess acid sites. [5,7]

2.2.2.3 Physical properties of catalyst

Density, porosity and surface area are the most important physical properties of catalysts. Pores are important for the performance of catalyst because they often contain the majority of the surface area. The pores are interlinked void channels or cages in the catalyst particle. Porosity describes the percentage of pore voids from the total volume of a solid. [5,7]

In general, pores can be classified by their pore diameters [5,7]:

- micropores (< 2 – 3 nm),
- mesopores (2 – 3 nm and < 50 nm.),
- macropores (50 < nm).

The pore size distribution varies depending on the catalyst and the support. The pore volume is defined as the total volume of the pores. Materials with high pore diameter usually have high pore volumes which allow the reactants to enter the pores more easily than in the case of smaller pores. With high pore volumes and large pore diameters, the active sites are highly accessible for substrates. However, the total surface areas of the high-volume pores are smaller than with smaller pore volumes meaning a smaller number of active sites. [5,7]

The total surface area of the catalyst consists of the outer surface and the area inside the pores of the catalyst. The importance of the surface area has been pointed out in Subsection 2.2.1.2, however, the whole surface area does not contribute to the catalytic reaction. The area portion containing the active sites is called

active surface area. The dispersion of the active sites within this area is defined by the ratio of the number of active atoms or molecules on the surface and the total amount of atoms and molecules of the surface. [5,7]

2.3 Cycle of heterogeneous catalysis

A catalysed reaction can be described as a continuous and repeatable cycle consisting of different elementary steps. The catalyst participates in the reaction and then returns to its original state after every cycle without getting consumed in the reaction. [10]

The elementary steps of a heterogeneous catalytic reaction are [5]:

1. external diffusion of the reactants to the catalyst surface
2. internal diffusion of the reactants to the inside of a pore of the catalyst
3. adsorption of the reactants on the active site
4. surface reaction
5. desorption of the products from the active site
6. internal diffusion of the products to the outside of a pore of the catalyst
7. external diffusion of the products from the catalyst surface.

A depiction of these steps can be seen in Figure 2 which shows that the reactants must first reach the external surface of the catalyst. This happens by bulk diffusion through the boundary layer of the catalyst particle. The reactions most likely occur inside the pores of the catalyst because the pores contain the majority of surface area and thus most of the active sites. This is why the reactants have to diffuse from the surface to the active sites inside the pore. The reactants then adsorb on the active site forming a chemical bond. This changes the reactants in such a way that the reaction is more feasible to occur. After the reaction, the formed products desorb from the active site and exit the catalyst pores and the boundary film by internal and external diffusion, respectively. All these steps happen with different rates. The slowest step in the cycle is considered to be the rate-determining step and is therefore limiting the overall reaction rate. The steps will be elaborated even further in the following parts of this literary study. [5,7,11]

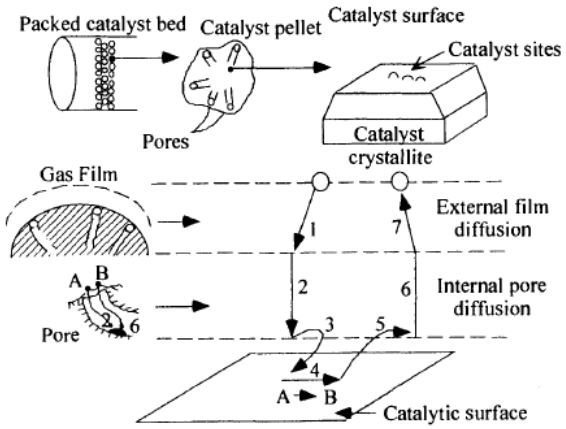

Figure 2. Depiction of the elementary steps involved in a heterogeneous catalytic reaction. [5]

The main reason why catalysts are able to increase the reaction rate and/or selectivity is because they offer an alternative pathway for the reaction. Figure 3 depicts the potential energies along the reaction coordinate of a catalytic and a non-catalytic reaction. It can be seen that the catalytic route has a significantly smaller potential energy requirement. According to the collision theory this means that the amount of successful collisions increases and thus the reaction rate increases accordingly. Note that the catalysis does not affect the initial and final state energetics of the reactants and products. Thus, a catalyst cannot force thermodynamically unfavourable reactions to happen or change the equilibrium of the reaction. [5,10]

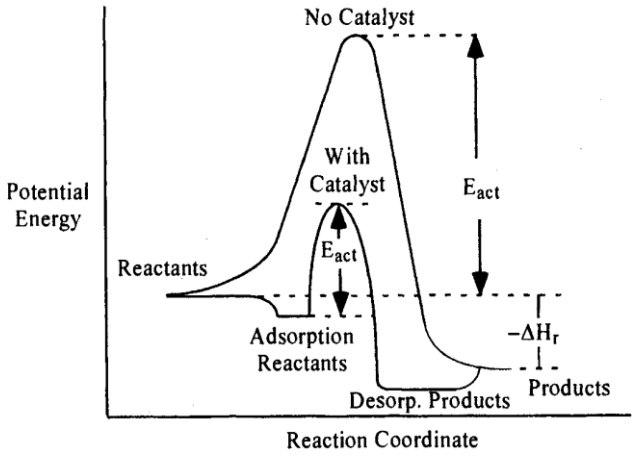

Figure 3. Depiction of potential energies along the reaction coordinate for catalysed and non-catalysed pathways. [5]

2.3.1 Diffusion in the heterogeneous catalysis

Molecular diffusion is a mass transfer phenomenon where the concentration gradient is the driving force for transportation of substances such as atoms or molecules, through a stagnant medium via the random thermal motion. The direction of transport occurs from a high level of concentration to a low one causing the concentration differences to reach equilibrium. In general, diffusion can be divided into external and internal diffusion. [5,12]

2.3.1.1 External diffusion

As stated before, industrial catalysts tend to be highly porous solid particles which possess active sites on their exterior surface but mostly inside their pores. A simple pore model for diffusion is shown in Figure 4. From the model, it can be seen that the reactants need to diffuse first from the bulk fluid to the exterior surface. This is referred as external diffusion or film diffusion. A concentration-position curve from the bulk to the inside of a pore (Figure 5) demonstrates the concentration difference between the bulk (C_{Ag}) and the catalyst exterior (C_{As}). This is caused by diffusion resistances, which are inhibiting the mass transfer and are considered to exists primarily as a thin layer (film) surrounding the catalyst particle. This boundary layer with finite thickness is inversely proportional to mass transfer coefficient, being the relation between diffusion rate and concentration difference. The film thickness is affected by process conditions and the particle size of the catalyst. For example, the film tends to be thick when the velocity of the fluid over the particle is low. A larger film thickness results in a smaller mass transfer coefficient, thus the rate of diffusion will be slow. This can affect the overall reaction rate and make the rate limited by the external diffusion. [5,8,12,13]

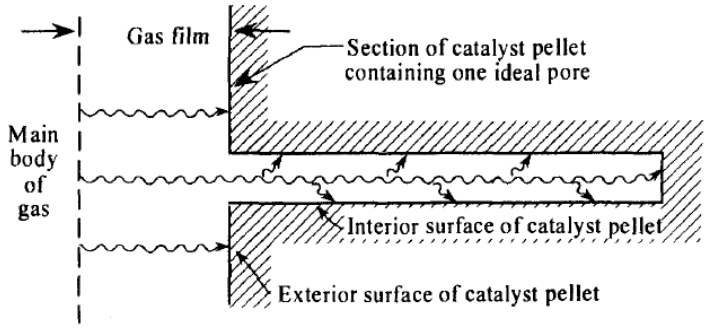

Figure 4. Simple pore model where the different stages of diffusion can be seen. [5]

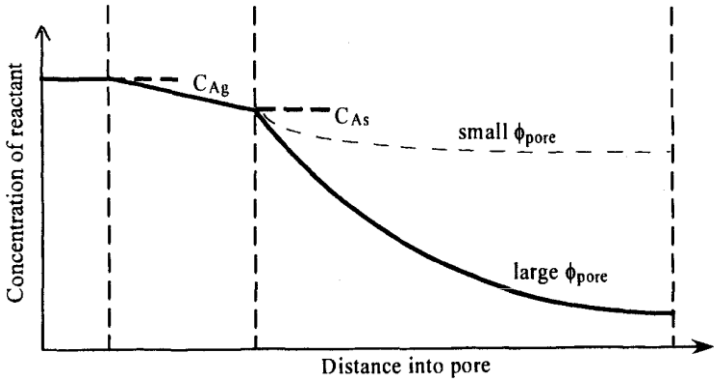

Figure 5. Concentration profile of reactant A from the bulk fluid phase (C_{Ag}) to the external surface of catalyst (C_{As}) and two different concentration profiles of reactant A inside the pore considering a small and a large Thiele modulus (Φ_{pore}). [5]

2.3.1.2 Internal diffusion

Once the reactants have reached the outer surface of the catalyst particle, either external surface reaction or diffusion to the catalyst pore (internal diffusion or pore diffusion) occurs. Similarly to external diffusion the pore also resists diffusion, which is why the concentration of reactant decreases even further (Figure 5). The Thiele modulus (Φ) is a commonly used parameter to describe the relation between the reaction rate and the rate of diffusion. As can be seen from Figure 5, when the value of Thiele modulus is small, meaning the rate of surface reaction is much larger than rate of diffusion, the concentration difference in the pore is small. A large Thiele modulus, in contrast, indicates that the internal diffusion is limiting the reaction rate. Internal diffusion is affected by the size and the shape of the catalyst particle and the reaction temperature but it is independent of the bulk fluid velocity. [5,8,13]

2.3.2 Adsorption and desorption in the heterogeneous catalysis

Adsorption is a surface phenomenon, where a liquid or gaseous component (adsorbate) adheres on the surface of a solid (adsorbent). Desorption is the reverse process of this, where the adsorbed component leaves the solid surface into the fluid. In industry, adsorption is frequently applied in separation processes such as purification of water and waste water treatment. [5,12,13]

Adsorption of reactants and desorption of the formed products are vital steps in the catalytic cycle. The purpose of a high surface area of the catalyst is to provide widely dispersed active sites, where reactants are able to adsorb. The adsorption

phenomenon itself is based on minimization of the surface energy of unsaturated surface bonds. [5]

There are two different types of adsorption: physical adsorption and chemical adsorption. Commonly, these are referred to as physisorption and chemisorption, respectively. [5]

2.3.2.1 Physisorption

Physisorption is caused by van der Waals forces which do not involve electron transfer between the adsorbent and adsorbate. The interaction between them is relatively weak, which is why physisorption is highly reversible. The atomic distances are typical to the van der Waals radiuses and the heat of absorption is rather low, less than 15 – 20 kJ/mol which is in the same range as the heat of evaporation of the adsorbate. Physisorption can function in low temperature ranges and the adsorption rate is very high. The absorbent can form multiple layers and its adsorption is non-specific, meaning that it does not require specific sites, such as active sites, to occur. [5,8,12]

2.3.2.2 Chemisorption

Chemisorption is a monolayer adsorption which happens on specific sites of the catalyst. In chemisorption, electron transfer between an adsorbent and an adsorbate occurs forming a chemical bond. The heat of adsorption is much higher than in the case of physisorption, around 50 – 300 kJ/mol. Because of the strong interaction between the adsorbent and adsorbate, chemisorption is often irreversible. Chemisorption generally requires higher temperatures and the rate of adsorption is strongly affected by the temperature. Chemisorption can be dissociative, when a chemical bond of the adsorbate breaks to form two or more adsorbed molecular fragments. This can happen when the energy gain from the interaction between adsorbent and adsorbate is higher than the binding energy of the molecular bonds of the adsorbent. Dissociative chemisorption is common with diatomic molecules, such as dihydrogen and it is probably preceded by a physisorption precursor state. The opposite of dissociative chemisorption is associative or molecular chemisorption, where the whole molecule adsorbs on to the surface site without dissociation. Usually, molecules with multiple bonds or free electron pairs adsorb in this way. [5,8,13]

2.3.2.3 Impact of process conditions on adsorption

In both types of adsorption, pressure and temperature have a strong effect on the equilibrium between adsorption and desorption rates. A high pressure and a low temperature favour adsorption while the desorption rate increases at a higher temperature and lower pressure. How the temperature affects both types of adsorption can be seen in Figure 6, where the amount of physisorbed gas is high at low temperatures and it begins to decrease strongly as the temperature increases. However, the amount of chemisorbed gas reaches its maximum at moderate temperatures but when the temperature increases further the equilibrium is shifted towards desorption. [5,12]

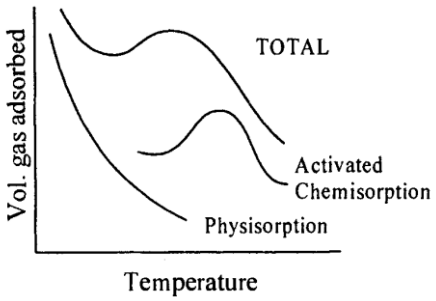

Figure 6. Effect of temperature on volume of physisorbed and chemisorbed gas. [5]

2.3.2.4 Adsorption isotherms

The concentration of species adsorbed on the adsorbent cannot be measured directly. Their amount is related to measurable quantities such as the partial pressure of the adsorbate species in a gas phase or the concentration in a liquid phase. Isotherms relate the surface concentration or the amount absorbed to the partial pressure or the concentration of adsorbate at a constant temperature. Physicochemical parameters of isotherms can also provide information about the adsorption mechanism and surface properties. This will be presented in the follow Subsection 2.3.2.4.2. [5,12]

2.3.2.4.1 Langmuir isotherm

The Langmuir isotherm is the most frequently applied isotherm for monolayer adsorption. It is an empirical model which is based on following assumptions:

1. Species are chemisorbed in a monolayer and one site can only hold one species.

2. The adsorption surface is homogeneous, meaning it is completely flat without channels and the site distribution is the same, implying that the sites are intrinsically the same.
3. The sites do not interact, meaning the adsorption energy is the same on all sites and independent of the environment and the coverage.
4. The equilibrium between adsorption and desorption exists. [5,13,14]

As an example, a simplified Langmuir isotherm expression for associative adsorption of carbon monoxide (CO) is presented in Equation 1:

$$C_{CO\cdot S} = \frac{K_A P_{CO}}{1+K_A P_{CO}} C_t \qquad (1)$$

where $C_{CO\cdot S}$ is the concentration of the adsorbate CO on the surface of the adsorbent,
K_A is the adsorption equilibrium constant,
P_{CO} is the concentration or partial pressure of adsorbate CO in bulk fluid,
C_t is the total concentration of active sites. [13]

For many adsorption cases, Langmuir isotherms do not apply over the entire coverage range but it is usually valid for limited ranges. The reason for this is the assumptions made in Langmuir isotherm are based on ideal adsorption conditions. In real cases, the catalyst surface is not uniform and the sites interact with each other and with the adsorbate. [5,13]

Other monolayer isotherms, such as the Freundlich isotherm, have been developed to take the limitations of Langmuir isotherm into account. The Freundlich isotherm can be used in adsorptions where the surface sites have different adsorption energies. The sites with the strongest binding energy are covered first which causes an exponential decrease of the adsorption energy. The Freundlich isotherm can describe the adsorption of many systems. [12,14]

2.3.2.4.2 Brunauer–Emmett–Teller isotherm

As stated before, physisorption can be multilayered which requires an isotherm that is able to take that into account. One example of such an isotherm is the Brunauer–Emmett–Teller isotherm (BET). It is the most commonly used multilayer isotherm and based on the same assumptions as the Langmuir isotherm but with

some exceptions. The BET isotherm assumes that the firstly adsorbed layer acts as adsorption sites for the second layer and that rate of adsorption of one layer is equal to the desorption rate of the next layer. BET isotherms can provide a lot of insight about the adsorbent for instance: surface area, pore volume, pore sizes and their distribution as well as the pore structure can be determined. [5,12]

2.3.3 Surface reaction in the heterogeneous catalysis

Reactions are able to occur after the reactant has chemisorbed on the active site. Various models have been developed to explain surface reaction mechanisms. Amongst them, the Langmuir–Hinshelwood and Eley–Rideal models are the most prominent ones and will therefore be outlined in the following. [13]

2.3.3.1 Langmuir–Hinshelwood reaction mechanism

In the Langmuir–Hinshelwood reaction mechanism the reactions occur between species absorbed on the catalyst surface. The reaction mechanism can be split into two categories depending on the number of active sites involved in the reaction. [13]

In a single site mechanism, only one active site is involved in the reaction. Isomerization or decomposition reactions can, for example, be catalysed in that way. A projection of a single site mechanism can be seen in Figure 7, where the adsorbed substrate A reacts to the adsorbed substrate B. [13]

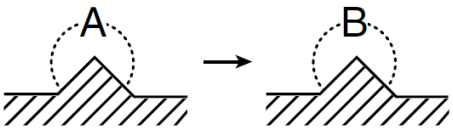

Figure 7. Single site Langmuir–Hinshelwood mechanism reaction of the adsorbed substrate A to the adsorbed substrate B. [13]

The dual site mechanism can occur in three different ways. Two of these are shown in Figure 8. In the first way, an adsorbed species A reacts with another vacant active site (1). The reaction can yield in a vacant site and an adsorbed product B or two adjacent sites with adsorbed products. In the second option, two adsorbed species A and B react with each other and form two species C and D (2). The third possibility is similar to the second one but the reactants are adsorbed on different types of active sites. All mechanisms possess the same active site assumptions

as with the Langmuir adsorption model which was discussed in subchapter 2.3.2.4.1. [13]

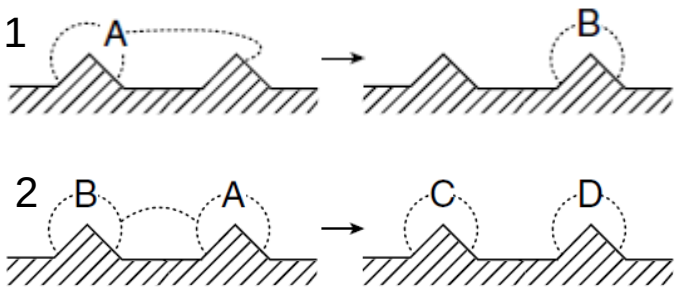

Figure 8. Double site Langmuir–Hinshelwood mechanism reactions: Reaction of an adsorbed species with a vacant active site and the reaction of two neighbouring adsorbed species. [13]

2.3.3.2 Eley–Rideal mechanism

Figure 9 shows the Eley–Rideal mechanism projection involving a singular active site where an adsorbed species A directly reacts with a second reactant B from the gas phase thus forming adsorbed product C. [13]

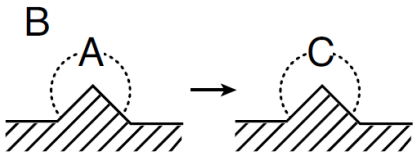

Figure 9. Eley–Rideal mechanism reaction. [13]

2.4 Deactivation of heterogeneous catalysts

Catalysts will inevitably start to lose their activity and/or selectivity over time on stream. This phenomenon is known as deactivation. Despite the regeneration of the catalyst after one reaction cycle as described in Section 2.3, the catalyst tends to go through changes that affects its activity after a certain time on stream. [5,15]

Deactivation of catalysts is a major concern in the chemical industry because catalysts have to be eventually replaced and usually the replacement requires a process shutdown. These issues can in total cost billions of dollars per year to the

chemical industry. The deactivation of catalyst has to be taken into account in the process from its research and development to its actual production. [16,17]

The catalyst lifetime describes the amount of completed catalytic cycles before the catalyst deactivates too severely, for example, when the temperature requirement to increase the conversion becomes too high for the process. The catalyst typically goes through an initial activity change after it has been on stream for 50 – 100 h. The catalyst lifetime can vary largely depending on the catalyst, the process conditions and the feeds. The reasons for deactivation can be physical or chemical in nature. The frequently recognized deactivation mechanisms, which are discussed in this literature part, are: poisoning, fouling and thermal degradation. Other methods that can cause deactivation are mechanical failure of the catalyst and volatilization of catalytic metals. [5,15,16]

2.4.1 Poisoning of heterogeneous catalysts

The activity loss of the catalyst can happen because of a strong chemisorption of catalyst poisons on the active sites. Any chemical species can be considered as poison if it is not the desired reactant and possesses a higher adsorption strength compared to other competing species for the same active site. In the case of a strong interaction between poisons and actives sites, even a small amount of a poison is able to rapidly decrease the activity of the catalyst. [5,15]

The chemisorption of a poison can have multiple effects on a catalyst. These effects can act individually or as a combination. Figure 10 shows a conceptual model for catalyst poisoning, where the poison blocks the access to the active sites. [5,16]

Effects of catalyst poisoning [5,16]:

- The adsorbed poison can limit the availability of active sites by physically blocking multiple sites on the surface of the catalyst.
- The poison can block the access of other adsorbed species to each other which prevents any reactions between the species.
- The poison may have such a strong chemical bonding that it has an electronic effect on the nearby active sites leading to altered adsorption and/or dissociation of other species.
- The poison may modify the active sites of the catalyst. The modification can change the chemical nature of catalyst and result in huge changes of the catalytic properties.

- The poison can inhibit surface diffusion of other species by decelerating or preventing the diffusion completely.

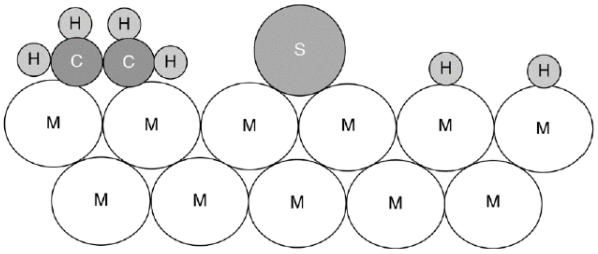

Figure 10. Conceptual model of sulphur poisoning on an active metal site M. [17]

Catalyst poisons can be categorized by their chemical structure, selectivity for active sites and the types of reactions they poison. Common catalyst poisons divided according to their chemical structure are listed in Table 2. [5,17]

Table 2. Usual catalyst poisons categorized by their chemical structure. [17]

Chemical type	**Examples**
Group 5 and Group 16	N, P, As, Sb, O, S, Se, Te
Group 7	F, Cl, Br, I
Toxic heavy metals and their ions and iron	As, Pb, Hg, Bi, Sn, Cd, Cu, Fe
Molecules that adsorb with multiple bonds	CO, NO, HCN, benzene, acetylene, other unsaturated hydrocarbons

Catalyst resistance, extent of poisoning and catalyst tolerance are common parameters which are used in discussions about the catalyst poisoning. Catalyst resistance describes how quickly the poison deactivates the catalyst. The extent of poisoning tells how much the catalyst needs to be poisoned before it becomes too severely deactivated. Poisoning of the catalyst does not necessarily cause complete deactivation of the whole surface. The surface of the catalyst can still possess some amount of activity. Catalyst tolerance is a measure of the activity during the saturation coverage of poison on the catalyst. [5,17]

Poisoning of catalysts can be non-selective, selective or anti-selective. The effect of the concentration of three differently selective poisons on the total catalytic activity is depicted in Figure 11. The Figure shows that non-selective poisoning occurs evenly around the catalyst surface, thus decreasing the activity linearly (case A). Selective poisoning (case B), in opposite, affects active sites with strong characteristics, such as high activity or acidity, before poisoning other sites. This

can be seen in Figure 11, where the activity decreases quickly as highly active sites are poisoned first (case B). Anti-selective poisons (case C) acts opposite to the selective deactivation, preferably poisoning sites with the weakest catalytic activity first. Thus, the activity in case C (Figure 11) initially decreases slowly before it plummets. This is caused by the most active sites start to deactivate. [16,17]

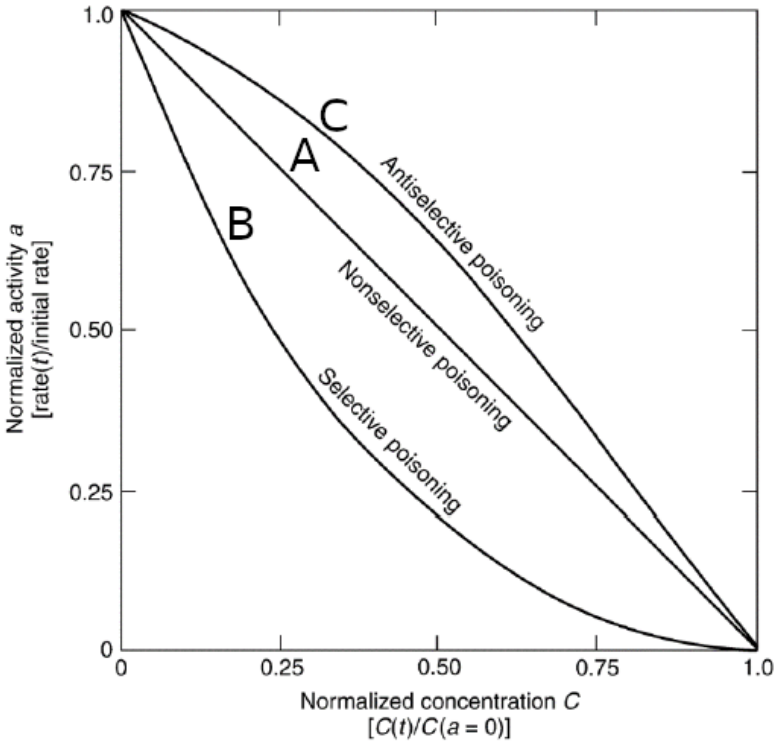

Figure 11. Effect of concentration of differently selective poisons (cases A, B and C) on catalyst activity. [17]

However, a behaviour similar to the ones in Figure 11 are rarely witnessed in typical industrial processes. A reason for this is that it would require the surface reaction to be the rate-determining step and poisoning is occurring uniformly meaning diffusional resistances would need to be very small. Industrial processes tend to have such a high temperature and pressure usually causing a high pore diffusional resistance in the main and/or poisoning reaction. [5,16]

If catalyst poisoning affects all active sites evenly, a decreasing activity should not impact the selectivity of a catalyst. However, multifunctional catalysts often have sites which can promote different reactions simultaneously. Consequently, selective poisoning can have a strong effect on the product selectivity of the catalyst

because some of the active sites can be unaffected by the poisoning. This phenomenon is utilized in catalyst tempering, where selective poisoning of active sites promotes a certain reaction pathway increasing the selectivity towards the desired product. For example, a Pt/Al_2O_3 catalyst used in reforming reactions consist of an active metal (platinum) promoting hydrogenation–dehydrogenation reactions and its support (alumina) which can catalyse isomerization and cracking reactions because of its acid sites. Basic nitrogen containing compounds are used to selectively poison the active acid sites of alumina to decrease isomerization and cracking reactions and in turn increase the selectivity towards hydrogenation–dehydrogenation reactions. [16]

Catalyst poisoning can be reversible or irreversible depending on the strength of the chemisorption of the poison on the adsorption site of the catalyst. A weak interaction between the poison and the active site is in principle reversible. Thus, desorption of the poison and regeneration of the catalyst can occur if the process conditions are changed for example temperature. In case of weak interaction, and if the poisoning species is removed from the feed before the reactor, the catalyst may regenerate as the poisons desorb from the catalyst. In the case of irreversible poisoning, prevention is usually the better option than regeneration of the catalyst because regeneration can be difficult and specific catalysts often require specific treatments. [15]

2.4.2 Fouling of the catalyst bed

Fouling causes loss of activity by physically blocking active sites and pores of the catalyst with feed deposits. This may lead to destruction of the catalyst particles and blocking of voids in the catalyst bed which can increase the pressure drop and finally plug the reactor. The species which can lead to fouling are typically coke and carbon and other insoluble deposits. These are discussed in detail in the following subsections. [5,18]

2.4.2.1 Catalyst fouling by coking

Processes forming coke and carbon include chemisorption of carbons or carbon containing compounds which can behave similar to catalyst poisons. The difference between coke and carbon is arbitrary. The product of CO disproportion is commonly considered to be carbon while coke consist of polymerized heavy hydrocarbons produced by decomposition (cracking) and condensation of hydrocarbons. [16,17]

Carbon and coke can foul supported catalysts by:

- blocking the access to active sites by chemisorption or physisorption,
- completely covering the catalyst particle causing it to deactivate,
- plugging micro- and mesopores of the catalyst,
- collecting filamentous carbon deposits to the pores to such an amount that in the long run the stress breaks up the catalyst support. [16,17]

Reactions can be coke-sensitive or coke-insensitive. The abovementioned fouling effects influence the coke-sensitive reactions. In the coke-insensitive reactions, coke precursors can be removed by gasifying agents such as hydrogen. Example processes for both types are: catalytic cracking and hydrolysis for coke-sensitive as well as catalytic reforming and methanol synthesis for coke-insensitive reactions. [16,17]

Coke and carbon deposits have many different structures which are affected by the reaction, the catalyst and the reaction conditions. The mechanism of coke formation is different between the catalyst types, for example, its formation on metal type catalyst is significantly different from the formation on metal oxide and sulphide supports. [16,17]

Formation of coke on metal supported catalysts, for example on nickel, can happen in the following way. CO dissociates on nickel and produces different forms of carbon depending on the process conditions and catalyst composition. These carbon deposits can be seen in Table 3. Nickel coking in steam reforming of hydrocarbons can produce three different kinds of carbon species. An encapsulating film is formed by slow polymerization of C_nH_n radicals under 500 °C and causes progressive deactivation. Formation of whisker-like coke occurs below 450 °C by nickel separating from the support and growing into whiskers with coke. This can cause breakdown of the catalyst and increase the pressure drop. Below 600 °C, pyrolytic carbon is formed by cracking of hydrocarbons. In this case, the carbon encapsulates the catalyst particle while causing deactivation and increasing in the pressure drop. [5,16]

Table 3. Carbon forms of decomposed CO formed on a catalyst with nickel as the active material. [17]

Type of carbon/coke structure	Formation temperature / °C
Adsorbed, atomic (surface carbide)	200 – 400
Polymeric, amorphous films or filaments	250 – 500
Vermicular filaments, fibres, and/or whisk-ers	300 – 1000
Nickel carbide (bulk)	150 – 250
Graphite (crystalline) platelets or films	500 – 550

Coke formation on sulphide and oxide supports is caused by cracking reactions of coke precursors, such as olefins and aromatics, catalysed by Brønsted acid sites. The suggested routes for coke formation involve dehydrogenation and cyclization reactions proceeding via carbonium ion intermediates formed on acid sites. The produced aromatic compounds react further to polynuclear aromatic compounds and finally condense to coke. [16,17]

Coke formation can be controlled by adapting the properties of the catalyst and process conditions. The aim is to achieve equilibrium between coke production and coke removal by gasifying agents such as the hydrogen. If the coke removal is not sufficient, coke begins to build up on the catalyst surface. Regeneration of catalysts with coke deposits can be done by gasification with hydrogen, water or oxygen. [17]

2.4.2.1 Insoluble deposits

The source of insoluble deposits can be precipitates formed from components of the feed formed under reaction conditions. Examples of these deposits are asphaltenes, which can separate from hydroprocessing feeds, after the feed loses its ability to keep them dissolved due to its hydrogenation. The decomposition of unstable feed components or reaction intermediates can also lead to the formation of heavy foulants which can deposit on the catalyst. This can be an issue with biomass feedstocks because they usually contain compounds with many different functional groups, which are highly reactive. For example, sugars can decompose by caramelization and then deposit on to the catalyst. [18,19]

Other sources of insoluble deposits can be corrosion products such as, ceramics or iron, from the preceding equipment. [15,19]

The reason why insoluble deposits can collect to the reactor beds is that the packed bed reactors behave similar to filters. The filtering effect of the reactor bed depends on the flow path and the void fraction of the bed. The flow path is the area between catalyst particles while the void fraction is the volumetric fraction of the bed which is not covered by the reactor bed particles compared to total bed volume. The sizes of flow paths in the reactor bed depend mainly on the diameter of the bed particles and their sizes and determines the size of the captured deposits. The amount of deposits that the bed can capture depends on the void fraction which is affected by the particle shape. The particulates flow through the reactor bed until the flow path becomes narrow enough for them to be captured. The capturing decreases the void fraction and creates a new more narrow flow paths, which enables capturing of even smaller particulates. As a consequence, the pressure drop increases eventually leading to reactor plugging. Once the void volume of the reactor bed decreases to 20 – 25 % of the original void volume, the pressure drop increase changes from linear progression to exponential. This means that the pressure drop starts to increase more rapidly which may lead to unplanned shutdown of the process. [3,20]

Insoluble foulants are typically either difficult or impossible to remove from the catalysts economically. Thus, in most cases, catalysts need to be replaced. Due to this reason fouling should be prevented by utilizing guard beds to remove these impurities. [19]

2.4.3 Thermal degradation

Temperature is one of the most important process control parameters. Usually the catalysts can function at relatively high temperatures, however, with time on stream, the temperature (usually above 500 °C) can negatively affect the catalyst resulting in deactivation. Commonly, this is caused by changes of the structure of the catalyst induced by temperature. [5,15,17]

The effects of temperature on the catalyst are for example [5,17]:

- The crystallites of the active material begin to grow resulting in decreasing the active surface area.

- The pores of the catalyst start to collapse which reduces the surface area and pore volume. Active material can become trapped inside the collapsed pore.
- Solid state transformations of the catalyst can occur, for example from γ-alumina to δ-alumina which has lower surface area above 800 °C.
- Transformation of the active material to non-active.

The first two of the listed effects are typically referred to as sintering. Sintering occurs at relatively high process temperatures, usually at temperatures above 500 °C. Two mechanisms for the crystallite growth have been proposed: atomic migration and crystallite migration. [5,17]

Figure 12 shows the conceptual model for crystallite growth by migration. The metal–metal bonds of the larger crystallites are more stable than the metal–support bonds of the smaller ones. This causes smaller crystallites to decrease in their size while the size of the larger ones grows. In the atomic migration (A), as can be seen from the model image in Figure 12, atoms detach from their deposited metal crystallites and migrate over the surface and are finally captured by larger crystallites. Crystallite migration (B) occurs with similar principle to atomic migration, but in this case the entire crystallites migrate over the support surface before the crystallites collide with each other resulting in coalescence. The metal crystallites can only migrate if they are smaller than 5 nm and not too strongly attached to the surface of support. It is very likely that both of these mechanisms happen simultaneously. [5,15,17]

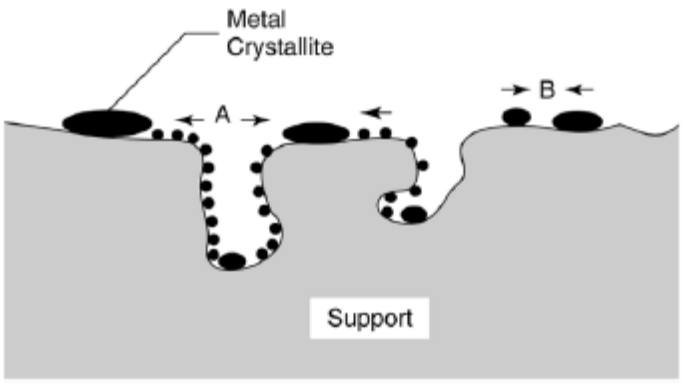

Figure 12. Conceptual model for (A) atomic migration and (B) crystallite migration. [17]

The primary factors affecting the catalyst sintering are: temperature, atmosphere, metal type, promoters, impurities of the feed and support properties. The impact of temperature on sintering of metal and metal oxide particles increases exponentially. Temperature causes reorganization of the catalyst structure by diffusion. The temperature where sintering begins to influence the particles of the catalyst can be estimated using Hüttig and Tamman temperatures. They are multipliers for the melting point of the support. A temperature increase enhances the mobility of the atoms on the surface of the catalyst due to the increasing thermal vibration. Close to Hüttig temperatures (0.2 – 0.3 times the melting point), the mobility becomes significant on the catalyst surface, which means that the weakly bounded surface atoms start to migrate and the surface accordingly gets smoother. Close to Tamman temperatures (0.5 times the melting point), volume diffusion gains importance as migration of the bulk atoms is additionally initiated. [15,17]

It has been noticed that oxygen atmosphere increases the sintering rate of noble metal catalysts whereas hydrogen atmosphere decreases the rate. In processes containing water vapour, the sintering rate of supported metals is accelerated. Reducing atmospheres tend to decrease the melting temperature of metals, which increases the instability of metal crystallites. In an oxidizing atmosphere, the stability of crystallites is affected by the volatility of the metal oxide and the strength of interaction with the support. [5,17]

Promoters and impurities can further influence the sintering rate. For example, chlorine and sulphur can increase the rate whereas oxygen, calcium and caesium can decrease it because they possess higher melting points and obstruct dissociation and diffusion of other species. [5,17]

The support properties which affect sintering are, for instance, surface area, texture, and porosity. Surface defects and pores of supports can impede the mobility on the surface of catalysts. This is particularly the case with pore diameters close to the diameters of metal crystallites (micropores and mesopores). The strength of the metal-support interaction also influences how mobile the metals are on the surface. [5,17]

High temperature can cause solid-solid reactions between the active material and the support or the promoter. For example, nickel and alumina can form nickel aluminate resulting in similar effects as poisoning. Temperature can also lead to the

transition of metals or the support to other phases. For example, at high temperatures (above 1300 °C) γ-alumina (surface area: 150 – 300 m^2/g) can be transformed to α-alumina (surface area: ~2 m^2/g), which has a significant effect on the catalyst activity. [5,15]

The prevention of thermal degradation is important because it is mostly irreversible or very difficult to reverse. Altering the process conditions by, for example, lowering the temperature or decreasing the amount of water vapour in presence of metal oxide catalysts, can decrease the sintering rate. Another way to increase the thermal stability of the catalyst is to add promoters like the base metal to noble metals. [16,17]

2.5 Utilization of guard beds for impurity removal

As it has been previously stated (Section 2.4) that catalyst poisoning, fouling and coking are major issues for catalyst deactivation in the chemical industry. They may cause an early shutdown of the process by deactivating the catalyst and increasing the pressure drop in the reactor. The remedies in these cases may be the total change of the inventory of the reactor or partial skimming of the reactor bed. This may result in economic losses due to a unit shutdown time and replacing the reactor packing. The pretreatment to remove the harmful substances from the feed before the catalyst bed, such as filtering, is the way to decrease the rate of deactivation. In some cases filtering may not be effective enough to remove impurities such as dissolved impurities or particulates smaller than 5 – 20 µm. Another method to remove the impurities from the feed is the use of guard beds. They are beds of an adsorbent placed upstream from the catalyst to protect the subsequent catalyst bed. Guard beds function by adsorbing and filtering catalyst poisons (such as metals) and insoluble particulates from the feed. Thus, the effects of fouling and poisoning occur in them instead of the expensive main catalyst. The following subsections discuss about some potential guard materials for the impurity removal and different guard bed technologies. [3,5,20,21]

2.5.1 Guard materials

Guard materials are generally inexpensive as they are used to capture catalyst poisons and foulants, meaning their replacing should be cost effective. The choice

of guard material depends on the feed and its impurities which are desired to be removed.

Active guard materials are usually low cost supported catalysts. Typically, group VI metals (such as molybdenum and tungsten) and group VIII metals (such as nickel and cobalt). Partially deactivated main catalyst can also be used as active guard material.

In some cases inert guard materials are enough for the impurity removal. Inert materials can be utilized by physisorption of impurity containing compounds and upholding the particulates. They may also possess active sites on which the impurities can adsorb. Examples of such inert materials are e low cost solids like alumina or clays which are discussed in the following subsections. [22-24]

2.5.1.1 γ-alumina

Alumina (Al_2O_3) is often used as catalyst support material due to its high thermal stability and typically high surface area. Alumina has several distinct amorphous or crystalline structures, for instance γ-Al_2O_3 and α-Al_2O_3. The structure and properties of alumina can be influenced by its preparation, dehydration, thermal treatment and purity. The different alumina structures can have very different surface areas, pore sizes, pore size distributions and acidities. [5,7]

Figure 13 shows different structures of alumina including pathways used for their preparation. Alumina precursors (gibbsite and bayerite {$Al(OH)_3$} as well as boehmite {AlOOH}) are produced by precipitation from acidic or basic solutions at relatively low temperature. In Figure 13, the pathways a and b are for the preparation of fine crystals and wet and coarse particles, respectively. Dehydration of the precursors at high temperature can transform them into different alumina crystalline phases (Figure 13). Other phases than α-Al_2O_3, are commonly referred to as transitional alumina. They possess porous structures and have both a high surface area and Lewis and Brønsted acid sites. α-Al_2O_3, in opposite, is nonporous and produced by applying temperatures 800 – 1200 °C. It is the most stable alumina with the lowest surface area (50 – 150 m^2/g) and acidity. [5,7]

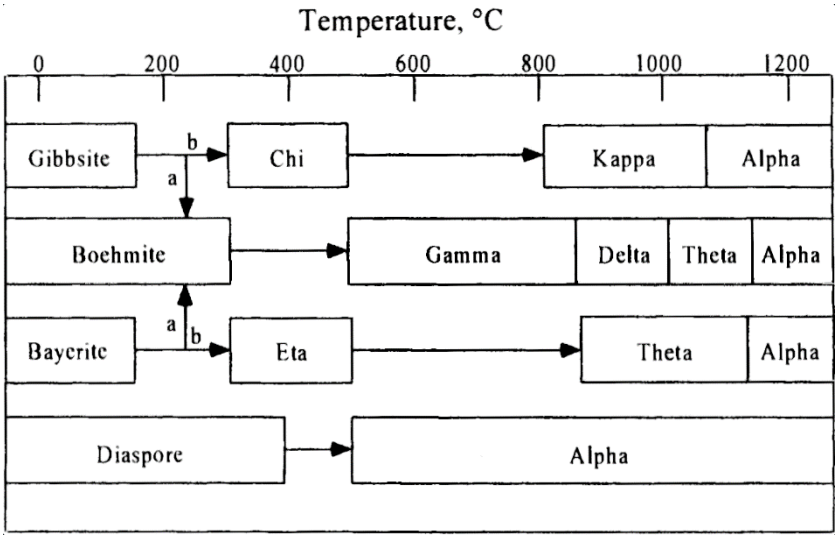

Figure 13. Alumina phases at different dehydration temperatures: (a) route for fine crystals and (b) route for wet or coarse particles. [5]

The most frequently used transitional alumina in industry is γ-Al_2O_3 as catalyst support because it has a relatively high surface area (150 – 300 m^2/g), is thermally stable in most process temperatures and can be shaped and processed into mechanically stable extrudates and pellets. In addition, it is moderately acidic, which is why it can also act as catalyst, for instance in catalytic reforming and catalytic cracking. Moreover, it has applications in separation processes, for example adsorption which makes it attractive to be used as a potential guard material. [5]

γ-Al_2O_3 crystallizes in a deformed spinel-type structure. Its surface is a complex combination of aluminium, oxygen and hydroxyl sites. The aluminium cation sites can act as strong Lewis acid sites and the hydroxyl sites (Al–OH) are Brønsted acid sites. Oxygen and aluminium are connected by an ionic bond (Al^+–O^-), which makes the oxygen ion a Lewis base site. [25-27]

2.5.1.2 Clays

Clays are hydrophilic fine-grained natural minerals that have many applications in the industry. They are used for their inertness and stability and additionally due to their catalytic activity. [28,29]

Clays are part of phyllosilicates which is one of the subclasses of silicates. Phyllosilicates consist of anionic $[SiO_4]^{4-}$ groups in tetrahedral shape and bivalent cations (e.g., Mg^{2+}, Fe^{2+}) or trivalent cations (mainly Al^{3+}). They are structured so that six $[SiO_4]^{4-}$ groups are arranged in a hexagonal structure around a hydroxyl group

which are connected by sharing three of their edge apical oxygen with another tetrahedral. This forms a 2D layer where the non-linked oxygen atoms point to the same direction. This structure has a negative charge which is neutralized by a cation layer formed by the bivalent cations and is located on top of the non-linked apical oxygen groups. This structure can have different structural types. Figure 14 shows an example of a montmorillonite type structure. The montmorillonite has two $[SiO_4]^{4-}$ groups in hexagonal structure surrounding the aluminium atom. The cation sheet of montmorillonites is between two silicon sheets, which are bound by van der Waals forces and the charge of the exchangeable cations in the cation sheet. [28,29]

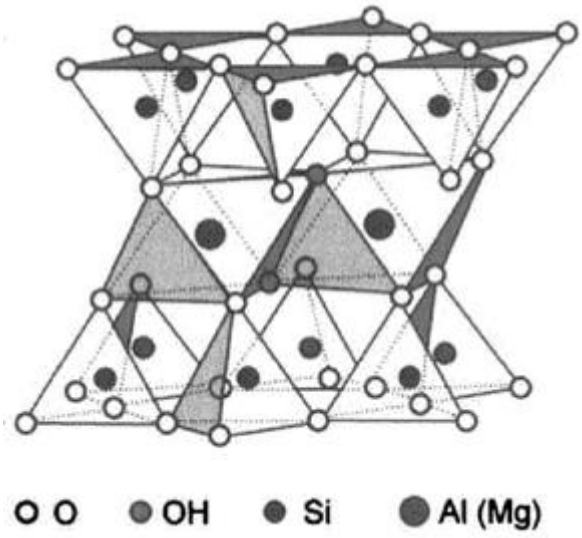

Figure 14. Projection of the montmorillonite structure. [30]

Kaolin and bentonite clay families are typically used in adsorption and reactive applications. The adsorption capabilities of clays are based on the negative charge of the silicon sheets, which can be neutralized by cations from external sources. Kaolins are used to synthesise zeolites which were discussed in the subsection 2.2.1.2. The bentonites are mostly formed from montmorillonite (Figure 14). However, naturally occurring clays usually consist of more than one structure type. Bentonites are used in adsorption due to their low cost and availability. Furthermore, they have a high surface area (up to 800 m^2/g). The bonds of montmorillonite are easily broken by water, other polar fluids or cationic fluids. This allows an easy exchange of the cations. [28,29]

Clays can be modified to enhance their properties by acid treatment or by thermally. In the acid activation, the clay mineral, which is usually bentonite with calcium cations, reacts with acids, for example hydrogen chlorine (HCl) and sulphuric acid (H_2SO_4). The acid causes dehydroxylation of the central hydroxide groups. The addition of acids removes the bivalent cations from the cation layer and replaces them with monovalent hydrogen ions thus making it more catalytically active. These cause changes to the structure of montmorillonite thus their pore volume enlarges which in turn increases the surface area and adsorption capacity. The acid activated bentonites are for example used in bleaching or decolourizing applications. In the thermal treatment of clays, they are treated by freeze-drying or by dehydration. The freeze-drying causes clays to become more macroporous than the air dried clays. The removal of water increases their acidity. Dehydration by heating can increase the porosity and surface are of the clays. Heating increases the acidity of the clay and changes the ratio of Brønsted to Lewis acid sites. Bentonites can also be treated with amines to gain clays that can uptake oils and grease. [28-30]

2.5.2 Guard bed technologies

Guard beds are usually placed in the reactor as a layer on top of the main catalyst bed or in a separate vessel before the actual reactor. Placing the guard material before the main catalyst may be done if the amount of catalyst poisons or reactor plugging substances in the feed are not significant enough to fill the capacity of the guard material too rapidly. The placement to the reactor could also be applied if retroactively adding a guard bed to an already existing process is needed. Because of the placement, the guard material takes up reactor volume from the main catalyst thus decreasing the possible maximum amount of catalyst which means a lower conversion unless a larger reactor is acquired. The problem can be diminished by employing guard beds which have guard material with some catalytic activity to start the catalysis already in the guard layer. An additional disadvantage of the placement into the main reactor is that the guard materials are exposed to the same process conditions as required by the main catalyst. Because the guard materials can remove impurities by adsorption, the removal is affected by the process conditions such as temperature as discussed in Section 2.3.2. This is why the reaction conditions in the main reactor may be suboptimal to reach the maximum uptake of impurities of the guard material. With typical fixed bed reactors, the guard

material cannot be exchanged during the operation. Thus shutdown would be needed if the breakthrough point of the guard material is reached. [21,23,31-33]

Placing guard materials into the separate guard vessels allows a separate adjustment of process conditions. Therefore, the process conditions for a maximum uptake of impurities can be achieved. The separate guard material vessel should be preferred if the sufficient removal of impurities requires a long guard bed which would require a large portion of the reactor volume. The continuous renewal of the guard material during the operation is possible by employing multiple guard bed vessels in a swing arrangement. In operation mode, one of the vessels is used until the breakthrough point of impurities of the guard material is reached or the pressure drop over the reactor gets too high. The vessel is taken off stream and the feed is switched to pass through a parallel guard bed vessel. Subsequently the guard material can be renewed. The separate guard bed unit might be a less attractive option for impurity removal compared to the placement of the guard material in the main reactor because it has the higher acquisition and operation costs. [21,22,34]

The guard beds can be composed of multiple layers, which are able to capture different kinds of impurities. Their performance to remove impurities and prevent pressure drop issues can be enhanced by utilizing a method called grading, where the layers consist of different particle sizes and/or shapes. These layers are organized in such a way that the pore void fraction of the particles decrease in axial direction. The particles can also be graded similarly by their pore volume and by their catalytic activity so that their pore volume progressively increases. In addition, two different guard materials can be mixed within one layer to produce intermediate grading between the two. [24,35-38]

Size grading can alleviate the pressure drop issue. As the void fraction decreases axially, the bed particles capture different size particulates in different parts of the bed. Larger particulates are captured at the top of the bed and the smaller ones at the bottom. This distributes the clogging particulates more evenly in the reactor bed instead of gathering them in one dense layer. The grading is additionally able to improve the fluid distribution. The shape choices for the large void fraction layers are typically rings, wagon wheels or particles with several inner channels. Shapes with a low void fraction are cylinders, trefoils, quadrilobes or spheres. [20,24,38,39]

Grading by the pore volume allows collection of more impurities before the pores get plugged by the impurities. This increases the impurity trapping capacity providing longer runs. Guard materials with a large pore volume are beneficial for trapping impurities, like iron, which tend to plug pores. The activity grading is beneficial for highly exothermic reactions. As only the most reactive substances are converted by low the activity grading, the heat load produced by the reaction is spread through the reactor evenly. This allows better temperature control over the whole reactor and also decreases the thermal degradation of the catalyst. Additionally with the activity grading, a more controlled conversion can be achieved to minimize the possible coke and gum formation. The activity loading is preferred in reactions that produce solid products as they are spread more evenly in the reactor. [24,35-38,40]

Table 5 shows an example of a graded guard bed. The first layer is dedicated to hold the catalyst down to prevent catalyst attrition. The second layer possesses very large void fraction to capture particles from the feed such as iron. The third, fourth and fifth layers possess catalytic activity to uptake contaminants that require it. They may also contribute to the main catalytic reaction and thus resulting in a more controlled conversion and heat distribution. The void fraction also decreases from layer to layer for the distributed filtering effect. The fifth layer has higher activity than the others to make the change to the highly active main catalyst (sixth layer) smoother by distributing the heat increase and conversion further. [40]

Table 4. An example of a graded guard bed filling. [40]

Example picture	Pellet size	Pore size	Void fraction	Activity
	5/8"	Very large	55 %	No
	1/2"	Very large	61 %	No
	3/16" Rings	Large	53 %	Low
	1/8" Rings	Large to medium	53 %	Low to medium
	1/10" Quadrilobes	Medium	48 %	Medium
	1/20" Catalyst	Small	47 %	High

2.6 Renewable feedstocks and their impurities

The term renewable feedstocks comprises of non-depletable raw materials which are able to replenish naturally. The materials that are considered renewable are the ones acquired from sources based on photosynthesis or are connected to photosynthesis through food chains. This means feedstocks that can be produced from plants, animals and microbiological biomass. The main renewable feedstocks groups are starch, triglycerides and lignocellulose-based materials. These materials can be converted to biofuels, bioplastics and useful platform chemicals such as glycerol. [1,8,41]

The problems with biomass derived feedstocks can be even more complex concerning contaminates as with the fossil derived feedstocks. Renewable feedstocks also tend to be over functionalized and thermally unstable and their process may need polar/aqueous and corrosive conditions. The removal of impurities and or other catalyst poisoning compounds from the feeds is important for a long catalyst lifetime. [2,18]

2.6.1 Common impurities in renewable feedstocks and their removal

Common impurities in the renewable feedstocks are phosphorus, silicon, alkali and earth alkaline metals as well as iron. In this section, the harmful effects on catalysts of these impurities are discussed and routes for their removal via guard beds and grading are pointed out.

2.6.1.1 Phosphorus containing impurities

In renewable feedstocks, phosphorus is present in the form of organic phospholipids (from animal fats and vegetable oils) and inorganic salts. Phospholipids can thermally decompose to phosphate anions which can deactivate catalysts by a condensation reaction with the hydroxyl groups on the catalyst surface. This reaction is depicted in the first picture of Figure 15, where the phosphate anion reacts with the alumina surface. First, the phosphate anion consumes the basic hydroxyl sites and then acidic hydroxyl sites on the surface of alumina. As can be seen in the first and the second picture of Figure 15, the phosphate-surface reaction creates two acid sites on the phosphate thus increasing the catalyst acidity. Eventually the phosphate can form a monolayer covering the whole catalyst extrudate as depicted in the third picture of Figure 15. The adjacent phosphorus species on the

surface react with each other by further condensation reaction to form linear di- and triphosphate chains. This leads to a loss of the double acid sites on the phosphate and thus decreasing the overall acidity of the surface. [42-45]

The phosphate anion can also form phosphate alkali salts if counter cations such as sodium or potassium are available in the feed. The formed salts can deposit as precipitates in the reactor bed and block or poison the active sites of the catalyst. The decomposition of the phospholipids may also produce phosphoric acids which can act as catalysts for unwanted oligomerization and polymerization reactions. [44,45]

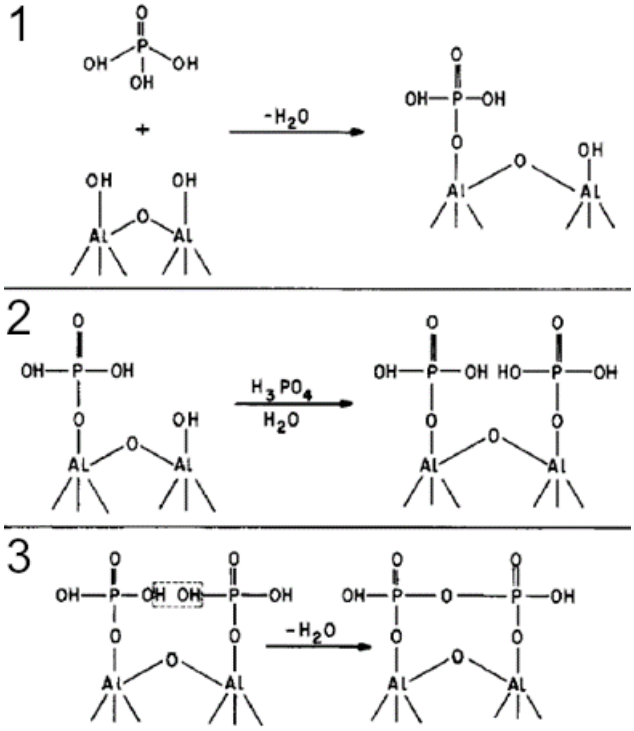

Figure 15. Mechanism of adsorption of a phosphate anion on the alumina (1) and reaction between adjacent phosphorus species (2 and 3). [43]

Aforementioned, phosphorus containing compounds can form a thick layer around the catalyst particle via condensation reactions which is able to block the pores of the catalyst as it deposits mainly on the external surface of catalyst. Phosphorus poisoning can cause diffusional limitations and disturb the uptake of other metals on the guard materials. The phosphorus layer decreases the void fraction which can lead to a pressure drop build-up.[46]

The phospholipids and free fatty acids (in bio-derived fats and oils) can react to gums. These are phosphatides which have similar structure than triglycerides except they have a phosphate group in instead of one of the fatty acid chains. The formed gums can be harmful for processes. For example, they are able to inhibit transesterification reaction and destroy the catalyst in the biodiesel production. Furthermore, they can disturb the separation of biodiesel esters from glycerol resulting in lower product yield. [47]

The guard material for the phosphorus removal should have some activity as the phosphates react with the basic sites and acid sites of the material. The guard material should also possess large pores so that both, diffusion of the phosphorus containing compound and the impurity capture capacity of the materials, are high. [40,46]

2.6.1.2 Silicon containing impurities

The primary source of silicon in renewable feeds is assumed to be polydimethylsiloxane (PDMS), which is typically employed as a foaming suppressant. The PDMS molecule is thermally stable up to 300 °C. When it decomposes, it forms mostly cyclic siloxanes but other silicon containing compounds are formed in addition, such as silanes, linear siloxanes or silanols. PDMS and the cyclic siloxane octamethylcyclotetrasiloxane (D_4) are depicted in Figure 16. The decomposition products of PDMS can be volatile, like trimethylsilanol which can react to siloxanes by self-condensation. PDMS degradation and its products are affected by the process conditions. Thus the nature of the silicon containing species governs the effect on the catalyst. For example, cyclic siloxanes and silanols can react via condensation reactions with hydroxyl groups of the catalyst. Adsorption of silicon containing compounds can lead to a complete coverage of the whole available surface of the catalyst. This means coverage of the active sites and pore volume decrease. Silicon containing compounds form a strong irreversible bond with the catalyst surface and thus the catalyst cannot be regenerated. A monolayer can cover the whole catalyst surface leading to pore mouth plugging. It also has been noticed that this kind of poisoning can change the catalyst behaviour by transforming Brønsted acid sites to Lewis acid sites. [31,48-51]

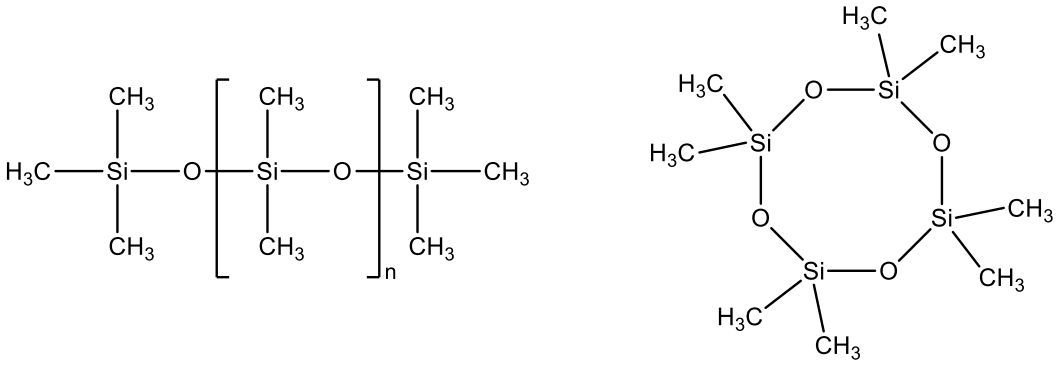

Figure 16. Polydimethylsiloxane (PDMS) and octamethylcyclotetrasiloxane (D4) which is one of its cyclic siloxane decomposition products. [51]

The removal of silicon containing compounds requires an active guard material with hydroxyl groups such as alumina. The guard material should have a high surface area leading to a high concentration of active sites. If using $NiMo/Al_2O_3$ as guard material, the pore diameter of the material should be 130 Å for highest silicon uptake. Higher pore diameters would have a minimal effect on the capturing amount. [46,52,53]

2.6.1.3 Alkali and alkaline earth metal impurities

Common alkali and alkaline earth metals in the renewable feedstocks are cations of sodium, potassium, calcium and magnesium. These electropositive impurities are able to neutralize Brønsted acid sites of catalysts by ion exchange with protons. Sodium is especially severe for such a type of reaction. In organic form, it is able to penetrate the whole catalyst particle consuming the active acid sites. Inorganic sodium tends to produce a crust around the surface of the catalyst. The other alkali metals and alkaline earth metals behave similar to sodium but their effect is not as severe as the one of sodium. The metal cations can also cause pressure drop in the reactor bed by collecting as precipitate to the bed voids by forming insoluble salt. Some of the alkali metals, such as sodium, can further increase the rate of sintering as it was discussed in Subsection 2.4.3. [44,46,54,55]

A guard material to adsorb alkali and alkaline earth metals requires acid sites as the cations adsorb to the surface of the material by ion exchange. Grading should be utilized if phosphates or other counter anions are present in the feed retaining the produced salt deposition to the guard bed. [38,40,46]

2.6.1.4 Iron containing impurities

Renewable feedstocks typically do not contain a high amount of iron. The origin of iron is usually from corrosion of preceding equipment and piping which is why the iron containing compounds are commonly seen in the presence of acidic feeds. Iron can be present in insoluble particulates of the feed, which are able to collect in the voids of the catalyst bed. The pressure drop over the reactor bed starts to increase as the void fraction in the bed decreases. Iron containing impurities are able to deactivate the metal catalyst by deposition on their surface and thus plugging the catalyst pores. Iron may also form salts that are collected in voids of the reactor. [31,35,46]

The guard material for the removal of iron containing contaminants can be inert. It should have high pore volume so that it has a higher capacity to capture iron containing compounds. The material should have a high void fraction as iron forms salts which tend to block the voids between the particles. [40,46]

3 EXPERIMENTAL PART

The experiments carried out in this Master's thesis focused mainly on the removal of two impurities being phosphorus and silicon. The removal by guard bed technology was studied using alumina as the guard material. Additionally, the collection of sodium, potassium and calcium using guard beds were also investigated.

The test runs were performed with two different feedstocks in two bench scale tube reactor systems. The feeds used in the experiments were a phosphorus rich feed and a silicon rich feed. In this thesis, the performed experiments included the determination of the capturing capacity of the guard bed material as well as test runs where the reaction conditions were changed. The capacity tests were carried out to study the maximum uptake of the impurities of alumina. The same test run was used as a reference test run to which the other the test runs which altering conditions were compared to. In the condition change test runs, the impact of temperature, pressure and feed rate on the ability of alumina to remove impurities was investigated. In this chapter the materials, the test run equipment and the experimental procedures which have been used are described.

3.1 Materials

3.1.1 Reactor bed materials

The reactor packing used in both test equipment consists of γ-alumina (γ-Al_2O_3) and silicon carbide (SiC). The alumina was chosen as the studied guard material due to its acidity and affordability which makes it an ideal guard material. It was provided by Sasol. The alumina was sieved to obtain extrudates with a length in the range of 2 – 5 mm. Silicon carbide was used to dilute the alumina, to close up voids in the guard bed for better wetting and as a structural support to keep the guard beds in the isothermal area of the reactor. SiC was acquired from Hiomaaine Oy. In the experiments three sizes of SiC were used: SiC 100 (0.106 - 0.150 mm), SiC 30 (0.500 - 0.710 mm) and SiC 16 (1.000 - 14.00 mm). SiC can be considered to be inert but may allow physisorption. Appendix 1 contains the analysis of the fresh alumina.

3.1.2 Feedstocks and cleaning solvents

All test feeds were acquired from Neste Oyj. The phosphorus rich feed contained approximately 7 ppm of phosphorus. The silicon rich feed contained about 30 ppm of Silicon.

For washing and shutdown an aromatic free gas oil and xylene were used. In some of the runs *n*-heptane (≥ 99.3 %) was employed for washing which was acquired from VWR.

3.1.3 Process gases

In the test runs, hydrogen (99.9 %) was used to keep the pressure in the reactor stable and decrease any possible coking. Helium (99.996 %) was employed in the leak test prior to each test run. Nitrogen was used for clean-up and drying. All gasses were acquired from Linde gas.

3.2 Test run equipment

The test runs were performed in two bench scale tube reactor systems: Lotta and Hansu. Lotta was used for the phosphorus removal experiments and Hansu for the silicon removal experiments. In the following section, these reactor systems are described in more detail.

The process flow diagram of the process equipment and instrumentation for the phosphorus removal test run is exemplary shown in Figure 17. The equipment used in the silicon test runs was very similar and thus it is not shown. The differences between the equipment are explained in text.

All lines, the pump and the filters were heated with trace heating. The vessels in the system were jacketed and heated by thermostatic oil baths.

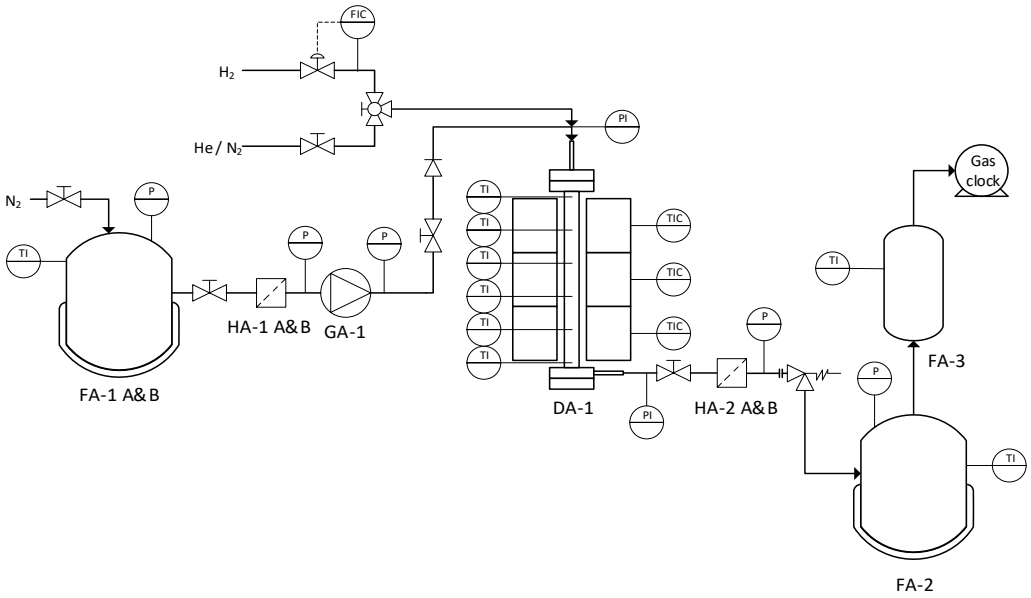

Figure 17. Process flow diagram of the test run equipment used in the phosphorus removal test run.

All lines, the pump and the filters were heated with trace heating. The vessels in the system were jacketed and heated by thermostatic oil baths. The feed tanks FA-1 A and B are kept at 0.5 barg nitrogen pressure during the whole test run. The temperature of tanks in phosphorus test runs and in silicon test runs was 70 °C and 80 °C respectively. The temperature in the tanks was measured by a thermocouple placed in a pocket inside the tanks. The silicon test runs required higher temperature due to a different viscosity of the feed. The tanks were placed on scales to monitor their weight change during the experiment which enables calculation of the mass flow of the feed. The feed was filtered (filters HA-1 A and B) after the feed tank. 50 µm filters were used in phosphorus test runs and 230 µm in silicon test run. The purpose of the filters is to protect the pump from any insoluble particulates. The filters in the silicon test runs were larger than in phosphorus test runs because the feed contained so much particulates that the filters became plugged very quickly. The filters were in parallel so that, if a filter would have been blocked, the feed flow could be changed to pass through the other filter. The clogging of filters was monitored by the pressure difference before and after the filters. The pump GA-1 used in the experiments was an air powered Williams Milton Roy plunger pump. Its feed rate was adjusted manually by changing the stroke length and the frequency of pumping.

The reactor was a trickle bed reactor, where the liquid feed and gas feed moved through the reactor bed co-currently. Table 5 shows the dimensions of the reactor tubes used in the test runs. The reactor was heated by an oven which consisted of three heating element blocks. The heating set points of each block could be adjusted separately. The temperature inside the reactor was measured with six thermocouples which were placed inside a thermocouple pocket in the middle of the reactor tube. The temperature inside the reactor was adjusted with the oven set points. The gasses (hydrogen, nitrogen and helium) are mixed with the liquid feed at the top of the reactor. The hydrogen volume flow is controlled in both equipment by a Bronkhorst IN-FLOW mass flow controller. The same kind of controller was used in silicon test run equipment to control nitrogen and helium volume flow rate. In the test run with silicon rich feed, the pressures at the top and bottom of the reactor were measured using pressure gauges. Digital pressure gauges were used in the runs with the phosphorus rich feed.

Table 5. The dimensions of reactor tubes used in the test runs.

	Phosphorus rich feed	**Silicon rich feed**
Length / cm	54.5	50.5
Inner diameter / cm	1.5	1.5
Thermocouple pocket diameter / cm	0.64	0.64

The product stream from the reactor was filtered through HA-2 A and B which contained 15 µm filters in both systems. The pressure in the reactor was controlled by an adjustable relief valve located after the filters, which would release product to the jacket heated product tank FA-2 once the pressure would increase above the desired pressure. The products that evaporate in the product tank were caught by a cold trap FA-3 on top of the product tank. The non-condensed gasses continue from the trap to a gas clock which measured the exiting gas volume.

The phosphorus test runs were monitored and mostly controlled by a computer program provided by Protagon, which also logged data from the instruments. The data logger used in silicon test runs was DASYLab10.

3.3 Experimental procedures of the test runs

3.3.1 Reactor loading

The reactors were packed so that they contained four guard bed layers in the middle of the reactor. The guard bed layers were held in place with layers of SiC 30 on the top and bottom parts of the reactor tube. All packing layers were separated by a layer of quartz wool. Additionally, layers of quartz wool were placed on the top and at the bottom of the reactor bed. Figure 18 shows the ideal reactor loading.

Initially, the guard beds were planned to be positioned in the isothermal zone of the reactor. Unfortunately, the first bed in the phosphorus runs and the last bed in the silicon rich feed test runs were out of the isothermal zone. The same way of packing was continued to be used for all other test runs to ensure that the results were comparable. Additionally, this was thought to give more information about the effect of temperature gradient within one loading. Detailed description of the packing follows in Subsection 3.3.1.1.

The temperature inside the reactor was measured using six thermocouples located inside the thermocouple pocket of the reactor. Two thermocouples were placed 1 cm from the top and 1 cm from bottom of the first and the last guard bed layer, respectively. The other two thermocouples were placed into the middle of the guard bed layers 2 and 3. The ideal placements of the thermocouples are marked with red dots in Figure 18. The exact weights of each guard bed component, i.e., alumina and SiC, for each test run are presented in the Appendix 2.

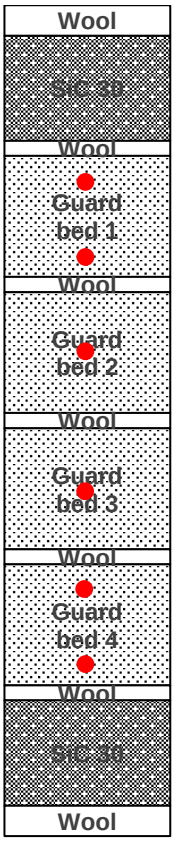

Figure 18. The ideal reactor loading of guard bed material for all test runs. The placement of the thermocouples in the thermocouple pocket inside the reactor is represented by the red dots.

3.3.1.1 Detailed method for reactor packing

The total amount of alumina loaded was 10 g. The total volume of this amount was measured with a measuring glass and then the material was divided into four equal portions. SiC 16 was added to each of the four alumina portions in the same volume as of guard material. Four portions (3 g) of SiC 100 were also weighted for the packing. The height of one guard bed was estimated using the volume of one alumina + SiC 16 portion and the diameter of the reactor tube. With the height of one guard material layer, the height of rest of the packing was calculated.

Packing of the reactor was started by closing the bottom flange of the reactor pipe with a layer of 2 cm quartz wool. SiC 30 was poured into the reactor until it reached the planned height which was decided so that the protective material was located in the middle of the reactor. To ensure the proper distribution of the material and as little void fraction as possible, the side of the reactor was struck with a recoilless

hammer a couple of times. A layer of 1 cm quartz wool was placed on top the SiC 30 bed. One alumina + SiC 16 portion was mixed and half of it was added to the reactor and then half of one SiC 100 portion was poured on top of it. After this, the rest of the alumina + SiC 16 portion and the remaining amount of SiC 100 was added. As with SiC 30, the side of the reactor was struck to avoid segregation of the alumina and the SiC diluent while loading. The other three guard beds were charged into the reactor similarly. Each bed was separated with a layer of 1 cm quartz wool. Once all four guard beds were placed in the reactor, 1 cm of quartz wool and the final SiC 30 layer was placed on top of them. The reactor was filled up with SiC 30 until 2 cm from the top of the reactor were reached. The last 2 cm were filled with quartz wool and the top flange of the reactor was closed.

3.3.2 Start-up procedure

Before every experiment a leak test was performed where the reactor was pressurized to 10 bar above the maximum pressure used in the test run afterwards. The pressures used in the test runs were 50 barg and 10 barg meaning the leak tests were carried out at 60 barg or 20 barg. The test run was started if the leakage overnight was below 0.1 bar/h.

All experiments had the same start-up procedure. First, the reactor was heated to 10 °C under the test run temperature with 50 °C/h. This was done to prevent heating overshoot. The lines of the equipment were also heated (70 °C for phosphorus rich feed and 80 °C for silicon rich feed). To reach the target temperature, the temperature of the heating blocks were slowly adjusted manually. Subsequently, the hydrogen gas flow was started and the reactor was pressurized to the test run pressure. The liquid feed flow was started thereafter.

3.3.3 Reference and condition change test runs

The impurity uptake of alumina from the both feeds at reference conditions was investigated in the reference test runs. The purpose of the reference test runs was also to study the capturing capacity of the guard material. In the condition change test runs, the conditions were similar to the reference runs but one condition was always altered in each test run. Table 6 lists the process conditions for the testing of the phosphorus rich feed and Table 7 for the silicon rich feed. The reactor packing was done as described in Subsection 3.3.1. The packing was renewed after each test run.

Table 6. The different reaction conditions applied for all test runs using the phosphorus rich feed.

Name of the test run	Temperature / °C	Pressure / barg	Feed rate / g/h	H_2 rate / l/h
Reference	325	50	102	92
Low temperature	**225**	50	102	92
Low pressure	325	**10**	102	92
Low feed rate	325	50	**51**	**46**

Table 7. The different reaction conditions applied for all test runs using the silicon rich feed.

Name of the test run	Temperature / °C	Pressure / barg	Feed rate / g/h	H_2 rate / l/h
Reference	230	50	26	21.6
Low temperature	**130**	50	26	21.6
Low pressure	230	**10**	26	21.6
Low feed rate	230	50	**13**	**10.8**

The runs were started by the method shown in Subsection 3.3.2. The reaction conditions were kept constant throughout the whole experiment. The reference test run lasted about three weeks whereas the condition change test runs lasted roughly two weeks each. After the test runs, shutdown is performed according to the instructions given in Subsection 3.3.4. The product tank emptying and sampling were done every weekday.

Analyses carried out from the liquid samples were:

- Density,
- total sulphur, nitrogen and chlorine,
- bromine number (only to the samples from phosphorus removal) and total acid number (TAN),
- Inductively coupled plasma (ICP) coupled with mass spectrometry (MS).

The spent alumina was characterized with the following methods:

- Semi-quantitative analysis of the elements by X-ray fluorescence (XRF),
- X-ray diffraction (XRD),
- elemental composition on the surface of extrudates by energy-dispersive X-ray spectroscopy (EDS),
- energy-dispersive X-ray spectroscopy (EDS) line scan and EDS map with scanning electron microscope (SEM),
- nitrogen physisorption including BET analysis.

3.3.4 Shutdown procedure

First, the temperature was decreased to 100 °C in the phosphorus rich feed runs and to 120 °C in the silicon rich feed runs. The temperature was higher in silicon rich feed test runs because of the viscosity of the feed. The feed rate was also halved. After that, the pressure was released and the hydrogen gas flow was switched to nitrogen. Sequentially, the feed was changed to an aromatic gas oil and the feed rate was increased to 100 - 250 g/h.

After flushing the equipment, pumping of the feed and heating were stopped and the reactor bed was dried in nitrogen (40 l/h) overnight. After that the nitrogen flow was switched off and the reactor was disconnected and replaced with a mannequin reactor. The system was then flushed with xylene to clean the lines further. The reactor was opened and the different layers of the bed were taken out separately and analysed.

3.3.4.1 Changes to the reactor bed washing

During the test run it was discovered that the alumina collected hydrocarbons into its pores that were difficult to remove during time on stream. These hydrocarbons would have affected the BET and TGA analysis of the spent alumina which is why their removal was important. The issue is discussed further in Subsection 4.1.1.2.4. To mitigate the amount of hydrocarbons in the pores, changes were made to the washing procedure described in the previous Subsection 3.3.4.

Table 8 shows the different washing procedures that were tested. The changes were made in the low pressure and low feed rate test runs. The washing solution was changed from an aromatic free gas oil to *n*-heptane. The reason for this was the high boiling point of the gas oil thus making it difficult to remove it from alumina by heating the samples. In the low pressure test runs the washing was done with

n-heptane at 70 °C and at atmospheric pressure. 2.5 l of *n*-heptane was used in the reactor bed cleaning of the low pressure test run using the phosphorus rich feed. The extrudates were visually darker than in the previous phosphorus removal test runs. This is why 5 l of *n*-heptane was used in the low pressure silicon removal test run to make sure the extrudates are properly washed. To see if the washing would improve at higher temperature, the temperature was increased to 140 °C which is over the boiling point of *n*-heptane at atmospheric pressure. To avoid boiling *n*-heptane, the pressure was increased to 5 barg. It was noticed that the extrudates had an even darker colour than in the low pressure test run of the phosphorus rich feed most likely because *n*-heptane evaporated despite the higher pressure. Due to this reason in the low feed rate test run of the silicon removal, cleaning was carried out at 70 °C and 5 barg pressure to decrease the evaporation of *n*-heptane. The extrudates had lighter colour than in the low pressure test run.

Table 8. The applied reactor bed washing procedures for low pressure and low feed rate test runs.

		Low Pressure	Low feedrate
Phophorus removal	Cleaning agent	*n*-heptane	*n*-heptane
	Temperature	70 °C	140 °C
	Pressure	0 barg	5 barg
Silicon removal	Cleaning agent	*n*-heptane	*n*-heptane
	Temperature	70 °C	70 °C
	Pressure	0 barg	5 barg

3.4 Analysis methods

In this section analysis methods and equipment are described. The author of this thesis did the density, the total sulphur and the bromine number measurements. The other analyses were done by an external analytics provider.

3.4.1 Product analysis methods

3.4.1.1 Density of the liquid products

The density measurements were conducted using a digital density meter ANTON PAAR DMA 38 using the method ASTM D 4052. The measurements were carried

out at 50 °C. For the analysis, the sample was injected into an oscillating sample tube. The equipment measures the change to frequency caused by the change to mass of the tube and then translates the result to density using calibration data. Repeatability of the results for phosphorus rich feed was +/- 0.2 kg/m^3 and for silicon rich feed +/- 0.4 kg/m^3.

3.4.1.2 Total sulphur content of the liquid products

A monochromatic wavelength-dispersive X-ray fluorescence spectrometer Sindie 7039 XR was used to measure the total sulphur content of the products according to the ASTM D 7039-15a method. The equipment measured the sample two times and reported their average. Repeatability of the measurements for samples with 10 ppm, 15 ppm, 25 ppm and 1000 ppm of sulphur were 1.7 ppm, 2.2 ppm, 2.8 ppm and 21 ppm, respectively.

3.4.1.3 Total nitrogen content of the liquid products

The total nitrogen content is determined by method ASTM D 4629. The sample was placed into a combustion tube where the nitrogen in the sample is oxidized into nitric oxide which is then converted into excited nitrogen oxide. The released signal is detected by a photomultiplier and the nitrogen amount is calculated. The repeatability of samples with 150 ppm nitrogen were 13.3 ppm and 530 ppm were 46.1 ppm.

3.4.1.4 Total chloride content of the liquid products

The chloride content was determined by burning the sample in a furnace which produces hydrogen chloride gas which is then microcoulometrically titrated. The method used for this was ASTM D 4929-15A.

3.4.1.5 Bromine number of the liquid products

Potentiometric titration was utilized to measure the bromine number which describes the amount of double and triple bonded hydrocarbons by the method ISO 3839-96. A known amount of sample was dissolved in the titration solvent which contained glacial acetic acid, 1,1,1-trichloroethane, methanol and sulfuric acid. Subsequently, the solution was titrated with bromide bromate solution. The titration was stopped when the free bromine caused the conductivity to plummet.

3.4.1.6 Total acid number (TAN) of the liquid products

The content of free fatty acids and the total acid number of the products was measured by titration (ISO 660). The sample was titrated with potassium hydroxide dissolved in toluene-isopropanol.

3.4.1.7 Inductively coupled plasma (ICP) coupled with mass spectrometry (MS) of the liquid products

ICP-MS was used to measure the content of small concentrations of elements. The elements analysed in this work were: P, Si, Na, K, Ca, Mg, Fe and Al. Prior to the analysis, the sample was dissolved in xylene which was then released to plasma as aerosol. The sample was atomized and ionized and then separated and also analysed by the mass spectrometer. Table 9 lists the repeatability of each impurity which were measured by performing five measurements from the same sample and calculating the standard error. In this work, the ICP-MS results have been used to calculate the conversion of each impurity by comparing the detected amount in the feed to the detected amount in the products (Equation 2):

$$X_i = \frac{x_{if} - x_{ip}}{x_{if}} \quad (2)$$

where, X_i is the conversion of the species i,
x_{if} is the concentration of the species i in the feed,
x_{ip} is the concentration of the species i in the products.

Table 9. Reproducibility of the ICP-MS analysis for the different impurities in both feeds.

Element	**Phosphorus rich feed / +/- mg/kg**	**Silicon rich feed / +/- mg/kg**
Phosphorus	0.020	0.082
Silicon	0.029	0.466
Sodium	0.295	0.052
Potassium	0.010	0.031
Calcium	0.004	0.082
Iron	0.002	0.170

3.4.2 Characterization of the guard material

3.4.2.1 Semi-quantitative analysis of the elements in the extrudates by X-ray fluorescence (XRF)

A wavelengthdispersive X-ray fluorescence spectrometer was used to determine the content of elements between Fluorine – Uranium of the guard material. The analysis was carried out with a Rigaku ZSX Primus II. The material was milled to a fine powder before the analysis. The powdered sample was pressed into a pellet and then added to the machine which made the measurements with an EZ-scan program. The results were then processed with SQX program. The analysis results were normalized by the aluminium content to make the analysis results comparable to each other. The amount of aluminium in the spent alumina was divided by its amount in the fresh alumina to gain a ratio between them. The other impurity results were multiplied with this ratio. An assumption is made in this thesis that the increased content of different elements on the alumina is due to chemisorption.

3.4.2.2 X-ray diffraction (XRD)

Wide angle X-ray diffraction is mostly used for crystalline samples to identify their components, crystal size and crystallinity. In this work it was used to see possibly formed alumina-phosphorus species. Analyses were done with Panalytical empyrean 3. The samples were grinded to a fine powder before they were analysed.

The identification was done by comparing the measured reflections to PDF-2 data base.

3.4.2.3 Elemental composition of the surface of extrudates by energy-dispersive X-ray spectroscopy (EDS)

The composition of the surface of the extrudates was measured with EDS. The EDS used in the analysis of the extrudates was XFlash Detector 4010 (Bruker). Three extrudates per test run were fixed on a sample holder on a carbon tape. The samples were placed into the machine which made the measurements. The content of elements was determined using the average spectrum derived from the measured extrudates. The quantification of the results was done by software (Esprit). After this, the average results of the three extrudates were calculated in Excel. The results are only indicative as the method has not yet been verified.

3.4.2.4 Energydispersive X-ray spectroscopy (EDS) line scan and map with Scanning electron microscope (SEM)

EDS line scan was done to see how the content of different elements changes on the extrudates according to the depth of the extrudates. The EDS map showed the presence of different elements in the extrudates by colouring them in the SEM image. The SEM used in the analysis of the extrudates was JSM 6610LV (JEOL) and the EDS was XFlash Detector 4010 (Bruker). The extrudates were mounted in an epoxy resin. The surface was flattened by a Tegramin-30 (Struers) to grind and polish the prepared cross-section of the extrudates. The measurements were performed from cross sections of the extrudates. The subsequent measurements were done in vacuum. The indicative concentrations of the elements were calculated by the EDS's Esprit software.

3.4.2.5 Nitrogen physisorption

Nitrogen physisorption was used to measure the porosity, pore volume, pore size distribution and the surface area of the guard materials. The analysis were conducted with Micromeritics TriStar II plus 3030 l. Nitrogen was physisorbed on the surface of the solid forming a monolayer. This was continued until the pores got filled under an atmospheric pressure. The surface area was calculated from increasing adsorption isotherm which was initially growing linearly using Brunauer-Emmett-Teller (BET) theory. Once the sample was saturated the pore volume was calculated. Pore size distribution was calculated applying Barrett-Joyner-Halenda (BJH) method. BET analysis was planned to be performed for the spent alumina

extrudates but due to problems the analysis could not be performed. The pores of the extrudates had collected too much hydrocarbons and impurities so that the compounds would have evaporated and contaminated the analysis equipment. See Subsection 4.1.1.2.4 for more detailed information on this issue.

4 RESULTS AND DISCUSSION

4.1 Phosphorus removal test runs

The purpose of this section is to discuss the results of the test run done to study the influence of process conditions on the uptake of phosphorus by utilizing a guard bed consisting of alumina. The effects are investigated by conducting a reference test run to which the results of the test runs with different conditions are compared. The impact of the process conditions investigated are lower temperature, lower pressure and lower feed rate than the reference conditions. More information on the experiments are outlined in the Experimental part (Section 3). This section has been split into three parts. The first one discusses the phosphorus removal at the reference conditions and draws conclusions how the impurities are removed using alumina guard beds. The second part evaluates the effects of the changes of the reaction condition on the impurity removal. The third section draws conclusions for further test runs. The results of each liquid sample from the reference test run is listed in Appendix 3 and all condition change test run results are in Appendix 4.

4.1.1 Phosphorus removal reference run

4.1.1.1 Liquid sample results

4.1.1.1.1 ICP-MS results

The elemental content of impurities in the product samples was determined by ICP-MS. The phosphorus removal was high over the whole time on stream in the reference conditions (T = 325 °C, P = 50 bar and LHSV = 5.1 h^{-1}) as can be seen from Figure 19, where the removal of phosphorus is described as conversion of phosphorus among the introduced feed amount normalized to the weight of alumina. Initially, it was expected that the phosphorus removal would be high at the beginning of the test run and decline after the maximum capacity of the phosphorus on the guard material has been reached. However, the progress of the phosphorus content (Figure 19) along with time on stream shows that this did not occur which indicates that the capacity of the alumina for the phosphorus uptake was not reached. The phosphorus conversion seems to improve slowly, nearly linear, over the time on stream from 0.85 to 0.92. During the run it was also noticed that the

pressure difference in the reactor increased (0.1 → 0.5 barg). The enhanced phosphorus conversion and the built up of a pressure drop could hint that the phosphorus removal is occurring mostly by physical means. This observed phenomenon is similar to a filter as the filtration efficiency improves as more material is captured on the filter surface which enables capturing of even smaller particulates [20,61]. The phosphorus containing compounds in the feed are most likely phospholipids which can thermally decompose to phosphates under the applied reaction conditions [45]. The adsorption of a phosphate group on the surface of alumina increases the acidity of the alumina surface as two acid sites are created by the phosphate group. It could be possible that these acid sites act as active sites for the adsorption or ion-exchange with other impurities. Another way how the phosphorus is removed, is that the phosphates in the feed form phosphate salts by reacting with counter cations, such as potassium, from the feed [45]. Both of these removal pathways could occur simultaneously however it would seem that the thermal reaction could be the primary phosphorus removal pathway. It could be that the presence of the alumina is not required for the phosphorus removal. A small amount of white powder was seen in the product sampling container when the container was washed with xylene and acetone after it was used to collect the product from the product tank. This might indicate the formation of phosphate salts. The white material could also have been polyethylene which is known to be present in the feed in some amounts [62].

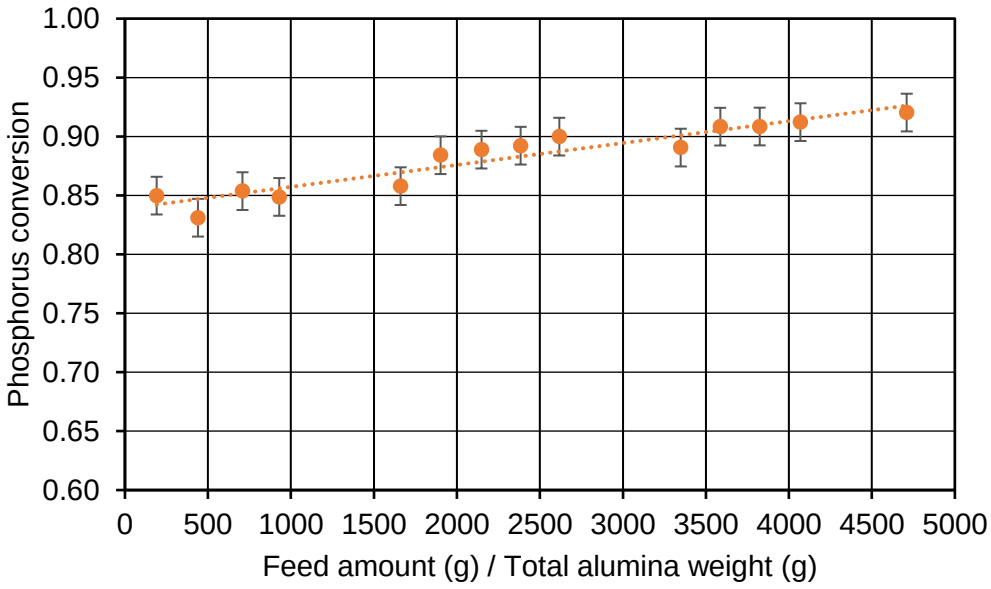

Figure 19. Conversion of phosphorus in the test run where the reference conditions (T = 325 °C, P = 50 bar and LHSV = 5.1 h^{-1}) have been used. The black marks around the points indicate the repeatability of the analysis.

The test run results for alkali and earth alkaline metal removal (Figure 20) show that potassium is nearly completely removed in all of the samples taken through the test run. It could be that that potassium removals happens by phosphate salt formation or the potassium cations are captured by alumina via an ion-exchange with the acid sites on the alumina surface.

Sodium conversion (Figure 20) is negative in the first product sample taken. This implies that the liquid product contains more sodium than the feed. After the initially high sodium content in the products, the conversion increases quickly and seems to stabilize after the second sample. The conversion seems to stabilize around 0.5. The high sodium content in the first sample indicates that leaching of sodium from the reactor bed occurs during the test run. Sodium could be leached from the alumina containing < 220 mg/kg of sodium. Sodium could also be leached from SiC The reason, why the sodium content is initially high, could be that the most easily leached sodium is first removed from the system. Thus, the sodium removed by alumina or a thermal reaction becomes higher as the sodium leached from the equipment. Leaching is most likely favoured by acid components in the feed, most likely free fatty acids. The decomposition of phospholipids could also produce

phosphate acids [45]. The removal of sodium occurs most likely by phosphate salt formation or by ion-exchange with surface acid sites of alumina.

The calcium content in the liquid products (Figure 20) is heavily fluctuating making the analysis results unreliable as it is difficult to separate the fluctuation from the actual changes in calcium content. The fluctuation could be caused by a measurement error or contamination of sample. The concentration is also close to detection limit of the ICP-MS method which is why the measurement is less accurate. Despite the fluctuation, a trend can be seen in the results. The conversion of calcium seems to be low at the beginning of the test run. The conversion increases after the first sample to alternate around 0.5 after the second sample. The reason for the initially higher concentration of calcium could be that, similar to sodium, calcium has been leached from the system. Possible sources of calcium are alumina (calcium content: 98 mg/kg) or SiC (calcium content: 360 mg/kg). As with potassium and sodium, the removal may further occur by ion-exchange or phosphate salt formation.

The content of magnesium in the feed is so small that the results are excluded from this discussion.

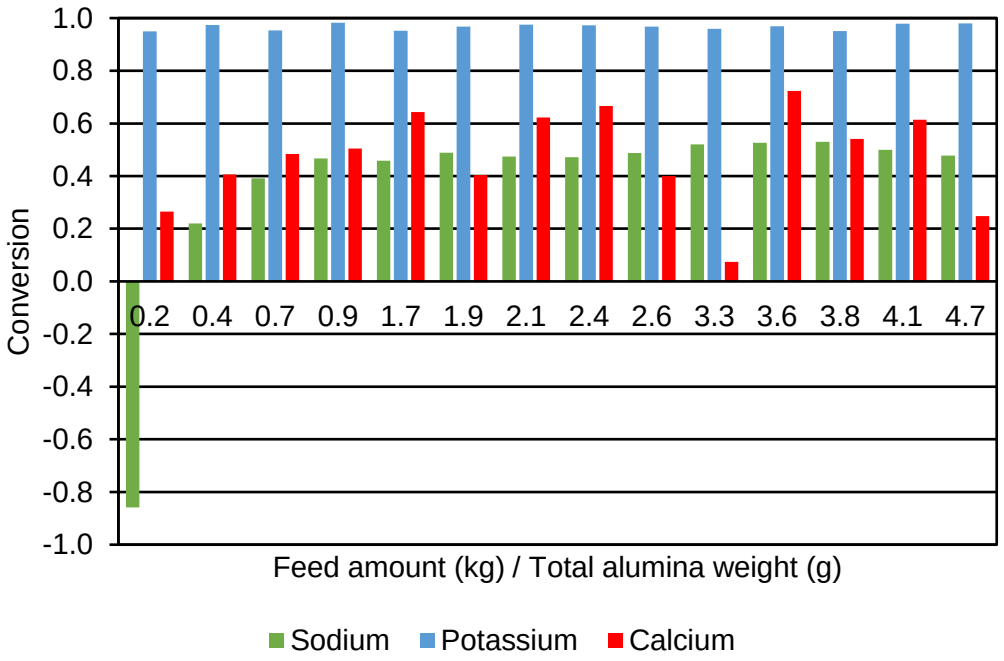

Figure 20. Conversion of sodium, potassium and calcium along with time on stream in the reference conditions (T = 325 °C, P = 50 bar and LHSV = 5.1 h^{-1}).

The iron conversion (Figure 21) is negative for nearly all sample of the test run. This means that the product samples contain a higher amount of iron than the feed. The first product sample has an approximately 13 times higher iron content than the feed. This indicates that leaching has occurred as observed in the case of sodium. The most probable origin for the leached iron is the equipment or the alumina (iron content of alumina: 89 mg/kg). The leaching could also occur from SiC. The iron content decreases after the first sample and then seems stabilizes between 0.1 – 0.2 after eight samples. Once stable, the iron content is a bit higher compared to the level of iron in the feed. Leaching of iron occurs throughout the test run because the conversion of iron is constantly negative which not the case for the other metals.

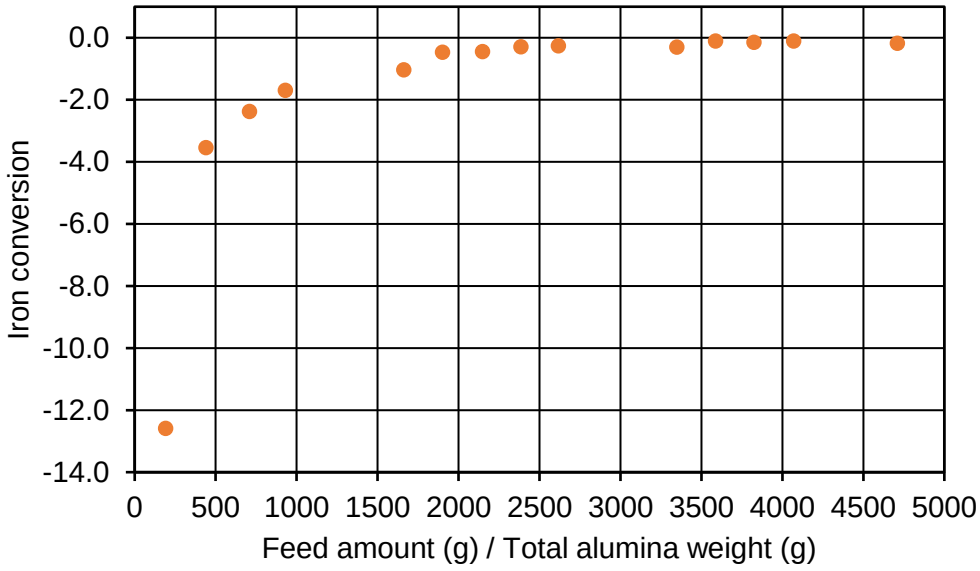

Figure 21. Conversion of iron along with time on stream in the reference conditions (T = 325 °C, P = 50 bar and LHSV = 5.1 h^{-1}). The black marks at the data points indicate the repeatability of the analysis.

As the amount of silicon in the feed is low, it is sensitive to a measurement error or contamination or unstable reaction conditions. However, in the following it has still been tried to draw conclusions about the silicon removal in this test run. The silicon conversion is highest at the beginning of the test run (0.45) as can be seen in Figure 22. The conversion after the first sample begins to decrease nearly linear to about 0.2 with time on stream. It is known that the silicon containing compounds

in the feed could be polydimethylsiloxanes (PDMS) itself or its decomposition products. These could potentially thermally decompose to volatile siloxanes by thermal reactions [51] and exit the reactor with the gas flow. In this test run, if the majority of silicon would have been removed by the evaporation, the silicon removal should be stable and not have declining trend. Due to these reasons, the results hint that silicon is mainly removed from the feed by adsorption on the acid sites of alumina. The decreasing conversion could be caused by the poisoning of the acid sites of the alumina or decreasing accessibility of the pores by other impurities captured on the alumina with time on stream. The acid sites are able to adsorb silicon containing compounds by condensation reaction [51] by lowering the concentration and accessibility of these acid sites capturing of silicon is thus inhibited causing declining conversion. In the last liquid sample, the silicon removal increased to same level as the first sample.

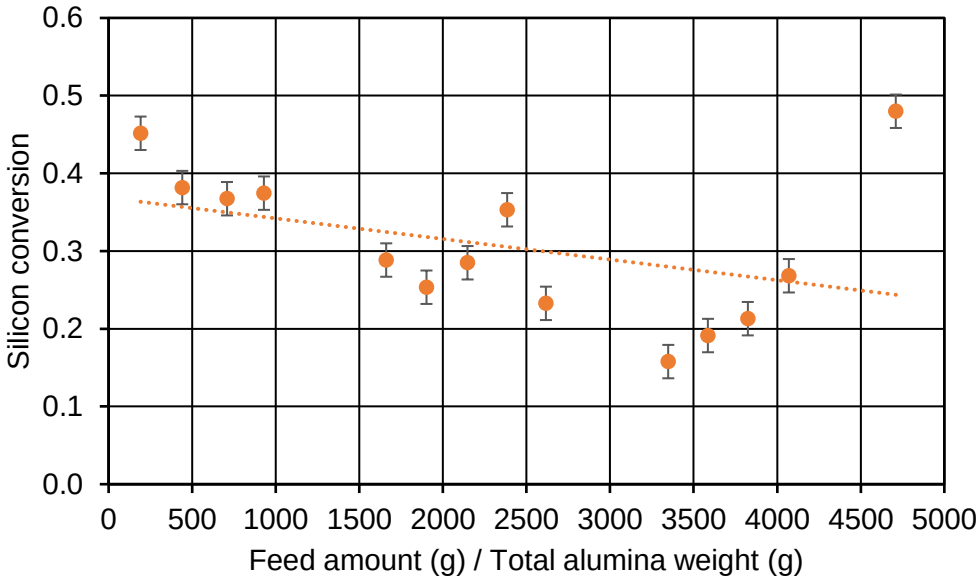

Figure 22. Conversion of silicon along with time on stream in the reference conditions (T = 325 °C, P = 50 bar and LHSV = 5.1 h^{-1}). The black marks around the points indicate the repeatability of the analysis.

4.1.1.1.2 Density results

The density of the liquid products is overall a little bit lower than the feed density (891.5 kg/m^3). However, the density of the liquid products increases logarithmically with time on stream (Figure 23). The density increase at the beginning of the run

is thought to be related to the phosphorus removal, however the trend of the phosphorus conversion is linear which suggests that there is no relationship between the density and phosphorus removal. The change of the density could be caused by an alumina catalysed reaction as if it was thermal reaction the density would stay constant. The density difference between feed and product is largest at the beginning where the most active sites on the alumina are available for catalysis. As the catalytically active sites deactivate with time on stream due to the adsorption of impurities on alumina, the density of the products increases towards the feed level.

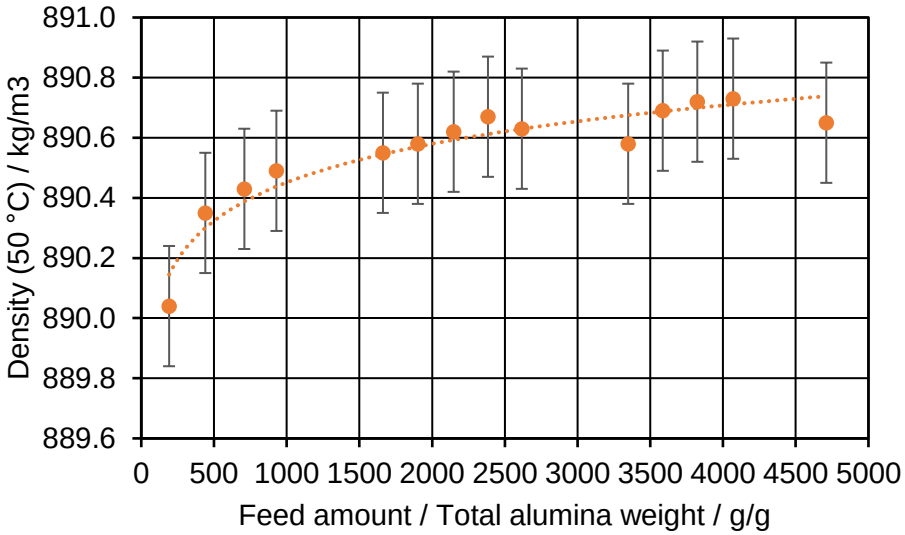

Figure 23. Density of products increases logarithmically during the reference run.

4.1.1.1.3 Other liquid sample results

The total acid number and the bromine number of the liquid products did not change compared to the feed during the test run. This means that the reaction has no impact on the amount of double bonds or the acidity or the changes are too small to be detected with these methods.

4.1.1.2 Spent alumina characterization results

4.1.1.2.1 XRF results

For XRF analysis of the guard beds 1 and 2 as well as 3 and 4 have been combined because it was noticed that the amount in one bed is not enough for all analyses. The results of the XRF analysis of the impurities have been normalized by the aluminium content as described in detail in Subsection 3.4.2.2. Table 10 shows the content of impurities on the spent alumina for the combined layers.

The results reveal that the ratio of phosphorus trapped by alumina between upper and lower guard beds is 0.93 meaning the lower guard bed layers collected much less phosphorus. As it has been discussed in a previous section (Subsection 4.1.1.1.1), phosphorus seems to be removed by phosphate salt formation which proceeds by the thermal reaction of the phospholipids. The upper beds have been closer to the top of the reactor and the first bed has not been completely in the isothermal zone which is why the thermal removal of phosphorus was small in this reactor part as higher temperature favours thermal reaction. Due to this more phosphorous species could adsorb on the surface of alumina in the upper guard beds. Most of the phosphates probably form salts before reaching the lower beds thus causing the lower beds to capture less phosphorus.

Nearly all potassium has also been collected in the upper beds (0.97). It is known that potassium tends to be the counter cation of phosphates to form salts [46]. The reason why the upper beds contain more potassium is most likely similar to phosphorus meaning most of the potassium form salts before reaching the lower beds.

The sodium uptake is almost the same in both upper and lower beds. This could be because sodium prefers to undergo an ion-exchange with acid sites of the alumina surface than to react with phosphates to salts. Sodium has been known to be highly poisonous to catalysts in general meaning it adsorbs to the surface of catalyst easily [46]. This is why the removal seems unaffected by the availability of phosphates to react to salts as it is captured by the alumina. The lower beds also contain a little bit larger amount of sodium (ratio upper to lower beds: 0.45) which could be because of the adsorption of phosphors or other impurities on the first bed impeding the adsorption of sodium. Sodium might be leached at the beginning of the test run (Section 4.2.1.1.1). If sodium has been leached from alumina, the actual removal of sodium by alumina from the feed might be higher than the XRF results show.

The amount of calcium on the alumina seems to decrease during the test run, which could mean that calcium leaching occurred. The leaching was already discussed to be a possibility in the previous section. The calcium content declines so little that it may fall under the detection limit of the XRF analysis meaning alumina might not have captured any calcium at all. It could also be that the alumina is removing calcium by ion-exchange while the feed leaches calcium from alumina. Calcium may also partake in the salt formation with the phosphates. This could

explain why the calcium content of the lower beds is lower than in the upper beds, as the upper beds could have captured more calcium because more calcium cations were available.

The amount of silicon in the upper beds is higher than in the lower beds. This is surprising as the ICP-MS results seem to indicate that the silicon removal decreased along the time on stream due to the deactivation of alumina. Which is why the silicon content should be similar in both beds as both beds are reaching the maximum of the possible Si uptake. After the test run it was noticed that SiC particles were stuck on the surface of the alumina. The extrudates of the first guard bed had the highest amount of SiC on their surface compared to the other beds. The SiC could have affected the silicon amount detected by XRF.

The iron content increased by a small amount in both upper and lower beds compared to fresh sample. In the previous section, it was noticed that iron has been leached during the whole test run. Because the iron content increased on alumina, it could be that iron is leached from other sources than alumina. The lower beds have a higher content of iron. This could mean that iron has been leached from the reactor bed so that more iron could have been collected on the lower beds. The increase of the iron content is quite small so it is possible that the accuracy of the analysis method caused the fluctuating results.

Table 10. Impurity amounts of the spent alumina in the upper and lower guard beds after the test run and calculated ratio of each impurity between upper and lower beds. The ratio was calculated by dividing the amount on the upper beds with the total amount in both beds.

	Upper guard beds / mg	Lower guard beds / mg	Upper / lower guard bed
Sodium	10.37	12.65	0.45
Silicon	17.33	2.34	0.88
Phosphorus	13.10	0.97	0.93
Potassium	6.07	0.20	0.97
Calcium	-0.08	-0.12	0.38
Iron	0.02	0.16	0.11

4.1.1.2.2 XRD results

All XRD diffractograms of the guard beds show by comparison with the database (PDF-2) that the beds consist mainly of aluminium oxide. The diffractograms of the two upper beds show small aluminium-phosphates reflections. These reflections do not appear in the diffractograms of the fourth guard bed thus they confirm the XRF analysis meaning the most of the phosphorus adsorption occurred on the upper guard beds. The third guard bed was not analysed with XRD. XRD diffractograms are depicted in Appendix 5.

4.1.1.2.3 EDS and SEM-EDS linescan

SEM-EDS analysis was conducted for all guard bed layers except the third layer and can be seen in Figure 24. All SEM-EDS results are listed in Appendix 6. The EDS analysis results are considered as indicative because the accuracy of the method has not yet been validated. The results show that a high amount of phosphorus is present on the surface of the alumina extrudates. The phosphorus amount decreases in subsequent beds. The potassium, sodium, calcium and iron content on the surface decreases towards the lower beds in the same way as the amount of phosphorus.

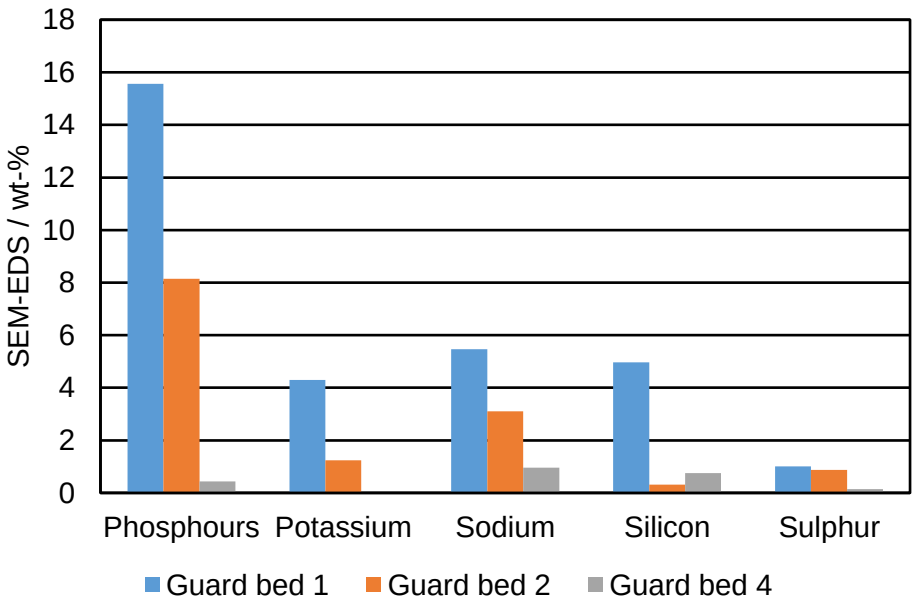

Figure 24. Indicative weight-based concentration of sodium, silicon, sulphur and potassium of the spent alumina from the guard beds 1, 2, and 4 determined by SEM-EDS of the surface.

Even though the XRF results show that sodium is captured by the lower and upper beds to approximately the same extent, SEM-EDS results show that the first bed captured most of the sodium of the guard beds. The explanation for this could be that the first bed has the highest amount of phosphates on its surface resulting in acid sites where the sodium could ion-exchange. The phosphate may also limit the accessibility to the pores which is why more sodium is captured on the surface. In the lower beds sodium can access the pores of alumina better due to the lower amount of phosphorus adsorbed and thus the sodium appears less on the surface of alumina.

Similar to the XRF results, the amount of iron and calcium on the surface of alumina is not high compared to the other impurities. SEM-EDS analysis of the fresh sample showed that there were barely any on the fresh alumina thus their amount may have increased.

The amount of silicon is the highest in the first bed and lowest in the second bed. The reason why the fourth bed has more silicon than the second is that the silicon containing compounds need to thermally decompose to smaller molecules which then are able to be adsorbed. A higher amount of decomposed silicon containing compounds have been available for adsorption in the lower guard beds than in the upper beds.

Some sulphur has also been identified on the surface meaning some of the sulphur is removed from the feed by adsorption on the alumina. The amount of sulphur adsorbed on the alumina is so small that it is not seen in the results of the sulphur content. However, the sulphur content measured from the liquid products should be the more accurate method compared to SEM-EDS.

SEM-EDS linescan MAP was performed only for the alumina extrudates from the first guard bed. The linescans show that phosphorus forms an impurity layer around the alumina extrudates which can be seen in Figure 25, marked with green. The impurity layer also contains a high amount of sodium and potassium. This suggests that the phosphate groups on the surface could provide the acid sites for ion-exchange which is why cation impurities appear more on the surface of the alumina. Calcium can also be seen on the impurity layer, however its amount is very small. Sulphur is additionally present in the impurity layer meaning it is adsorbed on the alumina surface itself or on phosphates adsorbed on alumina. Sodium, potassium, calcium and sulphur figures of the linescan MAPs are included

in the Appendix 7. The impurity layer around the particle could be the cause for the pressure drop increase in the reactor.

From the linescan image (Figure 26), particles containing a large amount of silicon can be seen on the surface of alumina. These are most likely SiC particles.

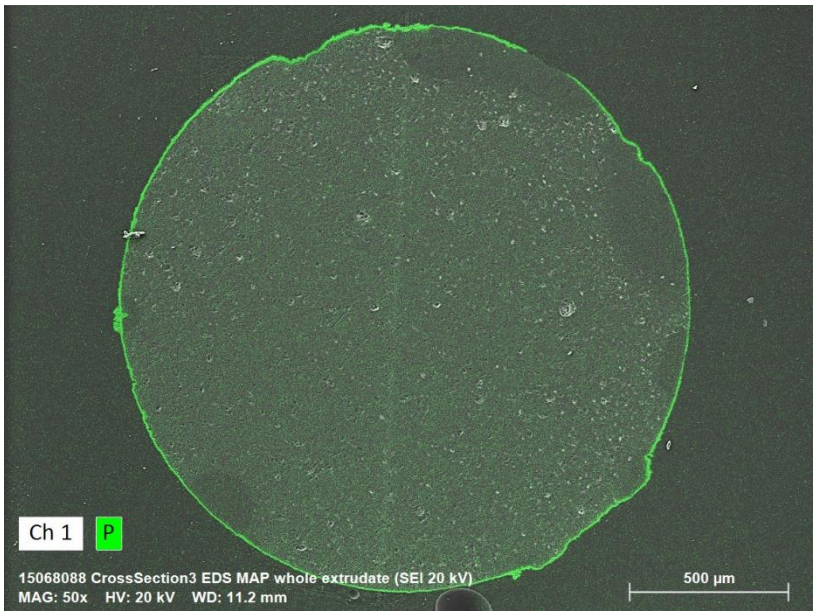

Figure 25. Phosphorus layer (marked with green) surrounding the alumina extrudate from the first guard bed.

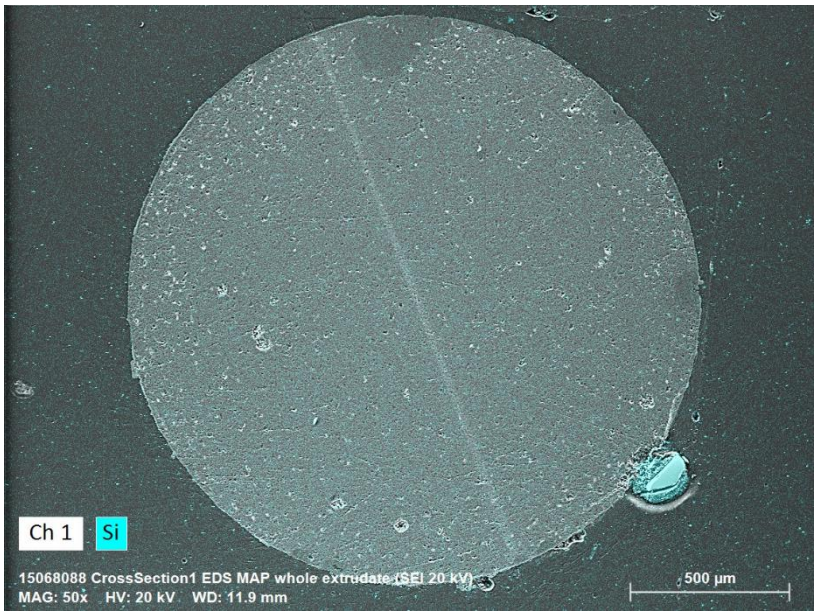

Figure 26. SiC particle (marked with teal) on the alumina extrudate (grey).

The profile of the linescan (Appendix 8) of the extrudates shows a high content of phosphorus, sodium and potassium on the rim of the extrudate. The phosphorus seems to have the higher concentration inside the extrudates than the other impurities. The linescan profile further shows some silicon spikes inside the extrudate. It is known that the silicon tends to adsorb on the all available active sites [46,50]. The phosphorus seems to form an impurity layer around the particle which may inhibit the silicon adsorption. Therefore the silicon content is high at some points inside the extrudates that correlate with the highest diameter pores. Thus silicon preferably adsorbs inside the pores. The presence of silicon within the cross-sectional area of the extrudates may also be a contamination from the equipment that was used during sample preparation to polish the surface.

4.1.1.2.4 N_2 physisorption and TGA analyses

Information about the pore distribution and the surface area by N_2 physisorption and following BET and BJH analysis could not be acquired from both phosphorus and silicon removal test runs in this thesis. The reason for this was that the hydrocarbons were stuck inside the pores of the alumina. Removal of the hydrocarbons is required before N_2 physisorption because the hydrocarbons would affect the analysis results and also contaminate the analysis equipment. TGA would also be influenced by these hydrocarbons causing the detected carbon amount of alumina to be very high. Therefore, no information about possible coke formation during test runs has been generated.

The removal of hydrocarbons from the pores of the spent alumina was tried by degassing the samples meaning heating up the material to 300 °C in vacuum. This turned out to be not an efficient way to remove the hydrocarbons as the samples still contained too much hydrocarbons even after a month of degassing. Dissolving of the hydrocarbons was tried next which had the risk of removing some of the impurities from the surface of alumina. The solvents used for dissolving were toluene and *n*-heptane. The washing procedure is outlined in the FT-IR analysis section (Subsection 3.4.2.2). The washing removed some of the hydrocarbons and in addition some insoluble powders from the alumina of both test runs. Unfortunately, the washing with both solvents did not remove the hydrocarbons from the pores of alumina sufficiently. The powders have been identified using FT-IR spectroscopy.

They consist of aluminium oxides and carboxylic acid. The aluminium oxide has most likely been formed by attrition or leaching of alumina. In the test run, carboxylic acids may have been formed, thus it could be that the free fatty acids in the feed have reacted with counter cations. Some traces of sulphur salts are additionally detected in the insoluble solid.

After washing of alumina, the solvents were evaporated from the liquid products of washing. According to FT-IR analysis, mostly paraffinic hydrocarbons, probably the once used for reactor cleaning, remained after evaporation. To prevent the collection of the oil in the pores, the reactor cleaning method was changed to use *n*-heptane instead which has shown to be a good solvent for the hydrocarbons according to dissolving tests. These methods are explained in Subsection 3.3.5.1. In the end, all methods failed to sufficiently remove the hydrocarbons from the spent alumina as also *n*-heptane did not manage to remove the feed components from the pores.

Due to these reasons N_2 physisorption and TGA are not discussed further which limits the knowledge about the impurity coverage on alumina.

4.1.1.3 Mass balance calculations

The calculations of the mass balance of this test run were performed using the results of ICP-MS analysis of the liquid samples and XRF analysis of the solid samples (Table 11).

Table 11. Calculated mass balance for each impurity in the reference run.

Elements	Total amount feed / mg	Total amount products / mg	Mass balance / mg	Increase on alumina / mg	Overall removal / mg/mg	Removed by alumina / mg/mg
Sodium	300.7	178.2	122.4	23.0	0.41	0.19
Silicon	25.3	17.6	7.7	19.7	0.30	2.56
Phosphorus	364.9	42.5	322.4	14.1	0.88	0.04
Potassium	169.8	5.8	164.0	6.3	0.97	0.04
Calcium	21.0	12.0	9.0	-0.2	0.43	-0.02
Iron	5.4	11.8	-6.4	0.2	-1.17	-0.03

The overall removal of phosphorus from the feed is relatively high (0.88). However, the amount of phosphorus collected on the alumina was only 0.04 from the total removal quantity. The low content of phosphorus on the spent alumina confirms that the removal occurred mostly by the thermal formation of phosphate salts with

counter cations such as potassium and collecting to the reactor bed, as already discussed in the previously (Subsection 4.2.1.1.1).

The mass balance for potassium is similar to phosphorus as the most of potassium is removed during the test run (0.97). Again, only a small amount of potassium has been collected by the alumina (0.04) which suggests that the potassium removal happens mostly via the salt formation with phosphates.

0.41 from the total amount of sodium fed into the reactor is removed according to mass balance. The calculation is affected by the apparent leaching, meaning the total removal would be higher if leaching would not have occurred. In the discussion of the XRF results (Subsection 4.2.1.2.1) it was suggested that sodium is mainly removed by reaction with alumina. According to the mass balance calculations, however, only 0.19 of the removed sodium was captured by alumina. Thus, it seems that a high portion of sodium is removed differently, meaning most likely by the salt formation.

Because the calcium content in the feed and products has been very small and the product content of calcium is fluctuating, the mass balance results of calcium are somewhat unreliable. Despite this some suggestions can be drawn from the results. Roughly half of the calcium is removed during the test run (0.43). Further, the content of calcium in the spent alumina is smaller than in the fresh sample, which is why it seems that calcium is leached from the alumina. Another source for the calcium could also be SiC. The alumina also does not seem to adsorb calcium or its calcium uptake is not enough to outnumber the impact of calcium removal. The ICP-MS results of the calcium content also exhibit a trend, where the conversion increases by time on stream, that hints that calcium leaching occurs at the beginning of the test run. The amount that the calcium content decreased in the alumina by only a small amount (-0.2). This could fall under the repeatability of XRF which semi-quantitative analysis method thus it could mean that the content did not actually change during the test run. Due to these reasons, there is a possibility that no leaching of calcium was actually occurring.

Some of the silicon is removed during the test run (0.30). After the run, SiC particles stuck on the surface of the alumina extrudates. These silicon containing particles can be also seen in SEM-EDS on the surface of alumina (Figure 26). The SiC particles distort the XRF results suggesting a much higher amount of Si present, which explains the unrealistically high fraction of silicon uptake by alumina from

the total silicon removal (2.56). Because of this, it is unknown how much of silicon is captured by alumina or removed in a different manner. The ICP-MS results of silicon hint that adsorption could be the primary removal method.

Similarly to sodium and calcium, iron seems to be leached during the test run. The total iron removal is negative, meaning that the products contained more iron than was fed into the reactor. The iron amount in alumina increased during test run which shows that iron most likely is not leached from the alumina. Thus the leaching occurred from the SiC and/or the test run equipment.

4.1.2 Impact of process conditions

The effects of different process conditions on the impurity removal are evaluated with ICP-MS, normalized XRF and SEM-EDS results as well as mass balance calculations. The density change of the product samples is also discussed.

4.1.2.1 Phosphorus removal

Figure 27 shows ICP-MS results for the phosphorus removal in each test run. In all of the test conditions phosphorus removal is relatively high. The lowest phosphorus removal is detected in the low temperature test run (T = 225 °C, P = 50 bar and LHSV = 5.1 h^{-1}) where the overall phosphorus conversion was 0.74 (Table 12). The conversion is smaller than at the start of the reference test run. In the final two samples, the conversion seems to decrease. In the preceding section (Section 4.2.1.1.1) it has been concluded that the phosphorus removal happens mainly by a thermal reaction. Consequently, the reason for the worse conversion than in the reference run is most likely that less phospholipids manage to decompose to phosphates due to the lower temperature. The decrease of the conversion in the last two samples is difficult to explain. It could be that the some of the collected phosphate groups were released from the reactor bed to the products. Another possibility is that the guard material reached its maximum phosphorus uptake under these test run conditions. However, the conversion decrease is quite large (0.78 → 0.67) and it has been confirmed that the majority of phosphorus removal happens via thermal reaction meaning that it is not very likely that the material has reached its maximum uptake. Analysis of the spent guard bed materials revealed that the division of the increased phosphorus content in the guard beds is more equal than in the reference run where the majority of the phosphorus is present in the upper beds. The thermal decomposition of phospholipids has decreased due to the lower temperature. Thus the decomposition occurred more at the reactor

bottom where more phosphates were available to be adsorbed on the lower guard beds. The uptake of phosphorus in the low temperature run by alumina (0.08) is a little bit higher than in the reference run. This is because of the lower thermal removal of phosphorus compared to alumina adsorption caused be the higher amount non salt phosphates.

The overall phosphorus removal when a lower pressure (T = 325 °C, P = 10 bar and LHSV = 5.1 h^{-1}) was applied is nearly the same as with the reference run, which indicates that the removal is independent of the pressure. The conversion is a little bit smaller but this can be explained by the pumping issues during the test run. These issues caused a higher feed flow rate in some parts of the test run which then decreased the phosphorus conversion. Even though the overall removal is nearly the same as in the reference run, the distribution of the alumina removed phosphorus between the top and the bottom guard beds is more even. The low pressure run also has the highest phosphorus uptake by the alumina compared to the other runs. This suggests that the lower pressure enhances the phosphorus uptake on the alumina instead of salt formation. The reason for this could be that the lower pressure affects the liquid-gas balance of some components (for example siloxanes) causing the evaporation of these components from the liquid. Thus, the alumina has more available active sites for phosphorus adsorption in both beds.

The results during the flow rate issues in the low pressure run hints that increasing the flow rate decreases the conversion. The lower flow rate, in turn, increases the conversion as the overall phosphorus removal is 0.91. The progress of the conversion of phosphorus during the test run (Figure 27) shows that, in the beginning, the removal level is the same as in the reference run. After the first sample, the conversion increases with a higher rate than in the reference run. Using a lower feed rate (T = 325 °C, P = 50 bar and LHSV = 2.55 h^{-1}), the phospholipids have more time to decompose to phosphates and either react to salts or adsorb on the alumina resulting in a higher overall conversion than in the reference run. The reason for a higher rate of conversion could be that the pressure of the incoming feed is less able to push the formed phosphate salts out of the reactor due lower feed rate. Thus, more phosphate salts remain in the reactor bed. The ratio between the phosphors capture by the alumina in the upper and lower beds is 0.76 which is higher than in the low temperature and the low pressure test runs. The alumina captures

0.06 from the total removal amount. The lower feed rate allows a higher phosphorus adsorption as the phosphates have more time to react with the alumina surface.

From XRD results it can be seen that the diffractograms of all test run, except the low temperature test run, contain aluminiumphosphate reflections in first guard bed alumina samples. XRD diffractiongram for low temperature test run can be seen in Appendix 9. This is interesting because the low temperature run has a higher phosphorus uptake than the reference run according to the mass balance and XRF results. SEM-EDS results of the condition change test runs show a similar trend compared to the reference test run. This means that the content of phosphorus is higher in the extrudates at the reactor top and the content decreases in the subsequent guard beds. It could be that the adsorbed phosphate is not in crystalline form in the low temperature test run which is why it is not detected. The weight fraction of phosphorus on the alumina determined by the SEM-EDS is in a similar scale. Due to indicative accuracy of the results, the difference between the different phosphorus results are considered to be negligible. SEM-EDS linescans for the low temperature and low pressure test runs show that, as in the case of the reference run, the phosphorus collects as a layer around the extrudates.

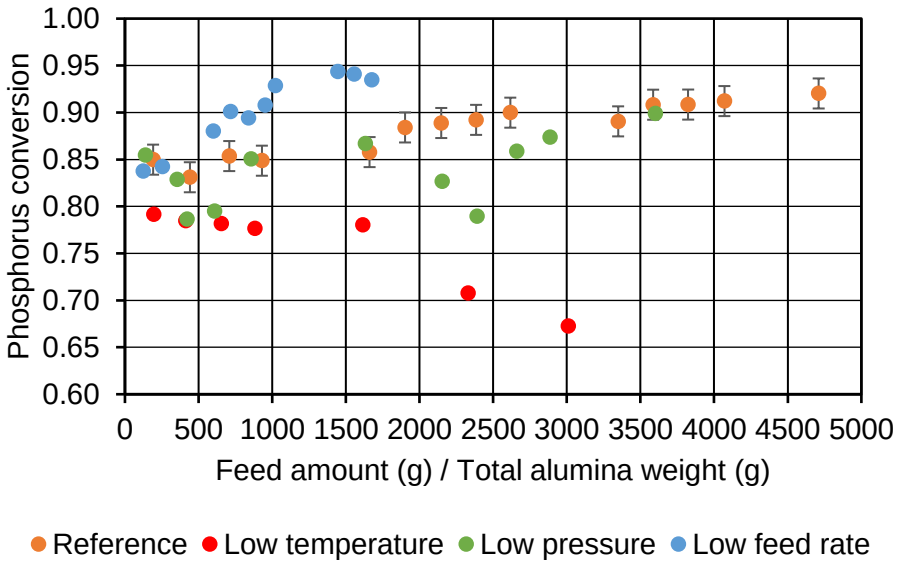

Figure 27. Conversion of phosphorus in the reference test run (T = 325 °C, P = 50 bar and LHSV = 5.1 h^{-1}), low temperature test run (T = 225 °C, P = 50 bar and LHSV = 5.1 h^{-1}), low pressure test run (T = 325 °C, P = 10 bar and LHSV = 5.1 h^{-1}) and low feed rate test run (T = 325 °C, P = 50 bar and LHSV = 2.55 h^{-1}). The black marks at the orange data points indicate the repeatability of the analysis.

Table 12. Mass balance calculations and the ratio between the amounts of phosphorus captured by the alumina and mass balance for phosphorus in all of the phosphorus removal test runs.

Test run	Total amount in / mg	Total amount in products / mg	Mass balance / mg	Increase on alumina / mg	Overall removal / mg/mg	Removed by alumina / mg/mg
Reference	364.9	42.5	322.4	14.1	0.88	0.04
Low temperature	229.2	59.8	169.4	13.0	0.74	0.08
Low pressure	271.6	40.0	231.7	23.0	0.85	0.10
Low feed rate	126.7	11.9	114.7	7.0	0.91	0.06

4.1.2.2 Potassium removal

As can be seen from the ICP-MS results, the potassium removal is quite high in each test run (Figure 28). The overall phosphorus conversion (Table 13) in all condition change test runs is nearly the same as in the reference run, except in the

lower temperature. As discussed in the reference run discussion part, the potassium is mostly removed by the reaction with phosphates produced by the thermal decomposition of phospholipids which is why the overall removal decreases in lower temperature. Similar to the phosphorus removal in the low temperature run, the potassium content decreases in the final three samples which then reduces the overall removal. This could be caused by same reasons as explained above for the removal of phosphorus implying that some deposits in the reactor bed came off the reactor. The low temperature leads to the highest amount of potassium captured on alumina. As at the lower temperature has a lower amount of phosphate available for salt formation, a higher fraction of potassium is able to be captured by alumina. This is also why the ratio of the potassium content between the upper and lower beds is closer to equal than in the other runs.

The potassium removal seems to be independent of the pressure and the feed flow rate as the conversion seems unaffected by their change. The amount of potassium captured by the alumina is low from the removal amount because the removal happened by the salt formation in both test runs. According to EDS of the spent alumina of both test runs and the reference test run, the fast majority of potassium is adsorbed on the alumina of the upper beds as the potassium reacted with phosphates.

In the low pressure test run, due to pumping issues, the feed rate increased higher than the reference feed rate. This caused a small decrease in the potassium conversion which can be seen in the third sample from the ICP-MS results. Thus, the potassium removal is also affected by the flow rate.

SEM-EDS results of potassium behave in the same way as in the reference test run, meaning the potassium amount in the guard beds decreases in the axial direction. SEM-EDS linescan shows in all of the test runs, most of the potassium is in the impurity layer surrounding the alumina extrudate. As suggested in the reference run discussion, potassium may perform an ion exchange with the acid sites created by the adsorbed phosphate. The linescan of extrudates of the low temperature test run seems to contain a lower amount of potassium on the surface than the other runs despite it having the highest potassium amount increase on alumina. This could hint that the potassium is not collected by the phosphorus impurity layer but the surface of the alumina.

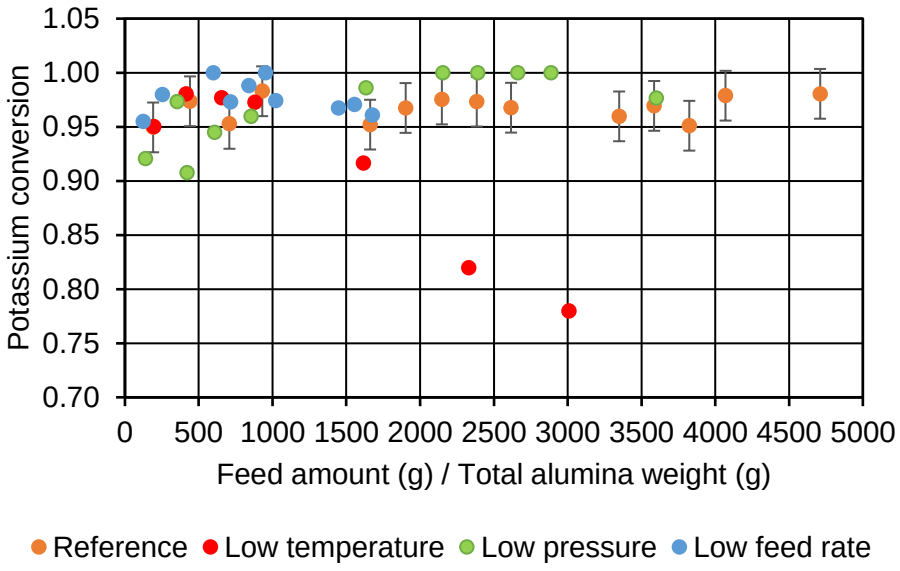

Figure 28. Conversion of potassium in the reference test run (T = 325 °C, P = 50 bar and LHSV = 5.1 h^{-1}), low temperature test run (T = 225 °C, P = 50 bar and LHSV = 5.1 h^{-1}), low pressure test run (T = 325 °C, P = 10 bar and LHSV = 5.1 h^{-1}) and low feed rate test run (T = 325 °C, P = 50 bar and LHSV = 2.55 h^{-1}). The black marks around the points indicate the repeatability of the analysis.

Table 13. Mass balance calculations and the ratio between the amounts of potassium captured by the alumina and mass balance for potassium of all the phosphorus removal test runs.

Test run	Total amount in / mg	Total amount in products / mg	Mass balance / mg	Increase on alumina / mg	Overall removal / mg/mg	Removed by alumina / mg/mg
Reference	169.8	5.8	164.0	6.3	0.97	0.04
Low temperature	110.6	13.2	97.4	7.8	0.88	0.08
Low pressure	131.6	2.5	129.1	0.4	0.98	0.00
Low feed rate	64.4	1.4	63.0	0.0	0.98	0.00

4.1.2.3 Sodium removal

As noticed in the reference test run, the apparent sodium leaching can be seen in the beginning of each condition change test run (Figure 29). The conversion trends

in all of the test runs are nearly the same as in the reference run. The overall removal of sodium (Table 14) is similar in nearly all runs except the lower feed flow rate run in which the conversion is lower compared to the other test runs. The first sample of the low feed flow rate test run has the largest sodium content compared to the other test runs. The conversion of sodium takes more time on stream to reach the stable level while using the low feed flow rate than at the other test run conditions. The reasons for this could be that due to the low feed flow rate the feed could have leached more alumina. It also might be that due to the longer space time, thermal decomposition of the feed is enhanced which may produce free fatty acids. This can be seen from the TAN results which decreases from roughly 15 mg KOH/g in the reference and low pressure test runs to about 19 mg KOH/g in the low feed rate test run. The sodium conversion of the low temperature test run seems to increase with the highest conversion rate. The average TAN in the liquid products of the low temperature run was 13 mg KOH/g, which is lower than in the reference test run due to lower amount of decomposition product free fatty acids.

According to SEM-EDS, the progress of sodium content in the different test run conditions behaves similar to the sodium content in the reference run. The linescans of the extrudates from the first guard beds also have the same shape as in the reference run. As potassium, the sodium amount on the surface seems to be smaller at lower temperature.

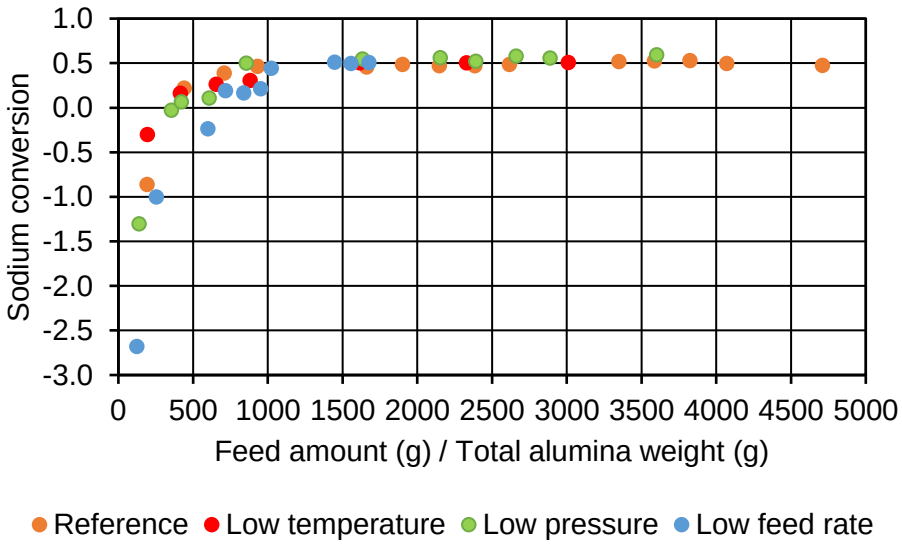

Figure 29. Conversion of sodium in the reference test run (T = 325 °C, P = 50 bar and LHSV = 5.1 h^{-1}), low temperature test run (T = 225 °C, P = 50 bar

and LHSV = 5.1 h^{-1}), low pressure test run (T = 325 °C, P = 10 bar and LHSV = 5.1 h^{-1}) and low feed rate test run (T = 325 °C, P = 50 bar and LHSV = 2.55 h^{-1}). The black marks around the points indicate the repeatability of the analysis.

Table 14. Mass balance calculations and the ratio between the amounts of sodium captured by the alumina and mass balance for sodium in all of the phosphorus removal test runs.

Test run	Total amount in / mg	Total amount in products / mg	Mass balance / mg	Increase on alumina / mg	Overall removal / mg/mg	Removed by alumina / mg/mg
Reference	300.7	178.2	122.4	23.0	0.41	0.19
Low temperature	187.2	111.2	76.0	15.7	0.41	0.21
Low pressure	222.4	122.5	99.9	23.9	0.45	0.24
Low feed rate	104.1	103.7	0.4	19.2	0.00	51.79

4.1.2.4 Calcium removal

The ICP-MS results of calcium in each test run have the same trend as in the reference run (Figure 30). This means that leaching occurs in all runs. The amount of calcium in the alumina particles is negative (Table 15). Thus, it seems that negative calcium content in the spent alumina is not a measurement error as it has been suggested in the reference discussion part (Section 4.2.1.1.1). This means that the most easily removable calcium was leached from the alumina at the start of the test runs. From the ICP-MS results of calcium, it is difficult to say if lower temperature or lower pressure have an impact on the calcium conversion because the results are fluctuating.

The low temperature test run seems to have a lower calcium conversion. Calcium removal occurs most likely by salt formation with counter anions such as phosphate. As already discussed in previous sections, phosphates are produced by decomposition of phospholipids which is why the temperature can affect the removal of calcium. Despite the fluctuation of the calcium amount in the low feed rate test run, the conversion is clearly higher than in other test runs. The lower feed rate allows a higher amount of phosphates to be present as the phospholipids have more space time to decompose to phosphates.

SEM-EDS results show a low amount of calcium on the surface of the alumina extrudate. The calcium amount in the linescan is very small. As the content of calcium on the fresh sample was undetectable this means, some calcium was captured.

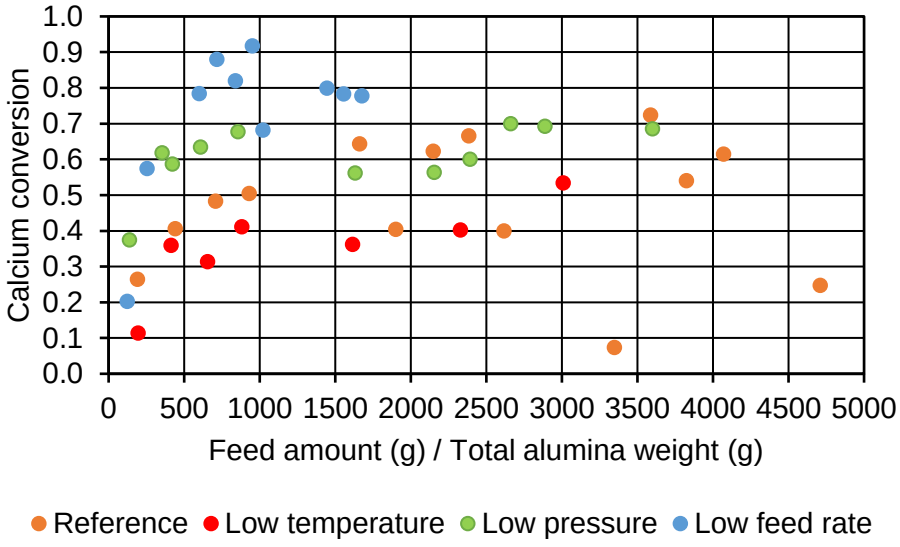

Figure 30. Conversion of calcium in the reference test run (T = 325 °C, P = 50 bar and LHSV = 5.1 h^{-1}), low temperature test run (T = 225 °C, P = 50 bar and LHSV = 5.1 h^{-1}), low pressure test run (T = 325 °C, P = 10 bar and LHSV = 5.1 h^{-1}) and low feed rate test run (T = 325 °C, P = 50 bar and LHSV = 2.55 h^{-1}). The black marks around the points indicate the repeatability of the analysis.

Table 15. Mass balance calculations and the ratio between the amounts of calcium captured by the alumina and mass balance for calcium in all of the phosphorus removal test runs.

Test run	Total amount in / mg	Total amount in products / mg	Mass balance / mg	Increase on alumina / mg	Overall removal / mg/mg	Removed by alumina / mg/mg
Reference	21.0	12.0	9.0	-0.2	0.43	-0.02
Low Temperature	14.5	8.7	5.8	-0.2	0.40	-0.03
Low Pressure	15.5	5.9	9.5	-0.1	0.62	-0.01
Low Feed rate	8.1	1.9	6.1	-0.2	0.76	-0.03

4.1.2.5 Silicon removal

Figure 31 shows ICP-MS results of the different test runs. In the reference test run, the conversion of silicon decreases linearly during the test run. It has been suggested previously that this decrease is caused by other impurities deactivating the alumina (Subsection 4.2.1.1.1) This declining conversion phenomenon also occurs in the low pressure and low feed rate, where the silicon conversion in the first samples are nearly the same as in the reference run. The conversion of silicon becomes negative in the low pressure test run implying that the silicon content in the product samples are higher than in the feed. The mass balance of the low pressure run (Table 16) is also negative because of this. The silicon content in the feed is small which is why the conversion is sensitive to small changes of the silicon content. The pump issues during the low pressure test run are most likely the reason for the increased silicon content in the products. The issues caused a higher feed flow rate at one point of the test run which could have pushed some physically removed silicon containing compounds from the reactor. After the silicon removal returns from the negative value, the silicon content seems to fluctuate around the feed content meaning the alumina has most likely been deactivated. A similar conversion increase as seen in the reference run is not observed in the results of the low pressure test run. The low feed flow rate leads to a higher silicon removal compared to the reference run as the shown by the mass balance. The silicon containing compounds had more time to decompose and also to adsorb on the alumina using the low feed rate. The silicon content in the liquid products seems to fluctuate around the silicon content in the feed in the low temperature run. This is most likely because the temperature has not been high enough for silicon containing compounds to decompose so that they could be adsorbed. Other studies on the adsorption of silicon on the surface of alumina have found that the adsorption capacity of alumina increases with temperature, which could be why the removal is lower than in the reference test run [49,50].

Different methods for reactor bed washing after the test runs compared to the low pressure and low feed rate test runs have been applied in the reference and the low temperature run (Section 3.3.5.1). After the guard materials were unloaded from the reactor, it was visible that SiC 100 particles stuck on the surface of the alumina extrudates. These contaminated the samples which in turn caused the silicon content in the spent alumina measured by XRF to be higher than the silicon amount that was removed during the test run. The mass balance calculation results

for the silicon fraction removed by alumina in the reference and low temperature test runs is very high, thus the XRF results of silicon are not further discussed. Moreover, it is possible that the SiC contamination affects other XRF results such as sodium, calcium and iron. The extent of this is unknown but the effect is assumed to be very small as the volume of SiC on the extrudate surface was not high compared to the volume of the extrudate. Due to the negative mass balance of silicon in the low pressure test run, caused by the pumping issues, the fraction of silicon captured on the alumina cannot be determined. The low feed flow rate test run is the only one from which the amount removed by alumina can be discussed. Its mass balance shows that the silicon is mostly removed by adsorption as a high fraction of the removed silicon is collected by the alumina (0.87). The rest of the silicon is most likely removed by the fore mentioned evaporation of decomposition products and maybe through formation of silicon containing solids (Subsection 4.2.1.1.1).

The low pressure run is the only one test run in which the silicon content on the surface of alumina differed from the reference as guard bed 4 of the low pressure run contains the lowest amount of silicon compared to the other beds. It might be that due to the lower pressure more silicon containing compounds evaporated from the liquid phase before the guard bed 4.

SEM-EDS linescan exhibits the same issue as the reference run meaning the equipment used to smooth the alumina extrudate before the SEM-EDS analysis contain silicon which likely falsifies the results. The silicon “spots” appearing on the extrudate and also outside of the extrudates, thus could be caused by the sample preparation leading to no reliable results of the linescan.

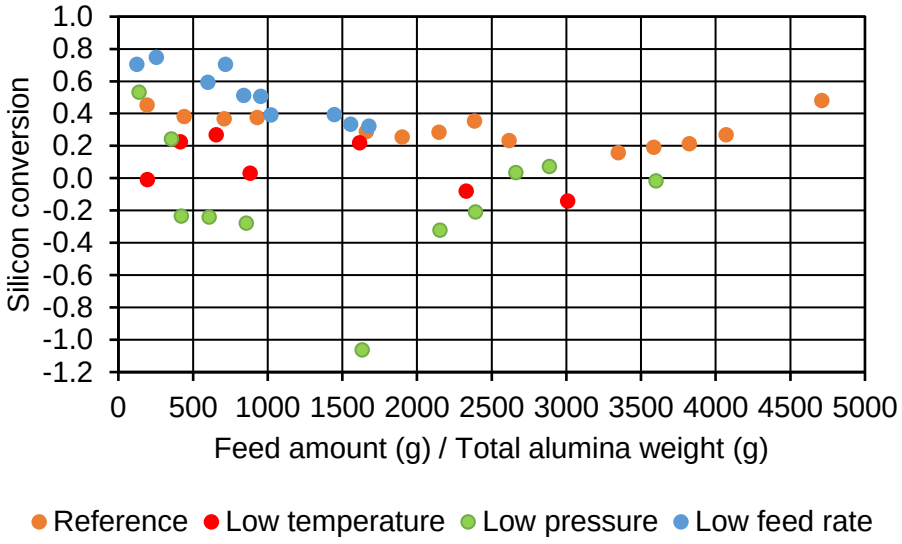

Figure 31. Conversion of silicon in the reference test run (T = 325 °C, P = 50 bar and LHSV = 5.1 h^{-1}), low temperature test run (T = 225 °C, P = 50 bar and LHSV = 5.1 h^{-1}), low pressure test run (T= 325 °C, P = 10 bar and LHSV = 5.1 h^{-1}) and low feed rate test run (T = 325 °C, P = 50 bar and LHSV = 2.55 h^{-1}). The black marks around the points indicate the repeatability of the analysis.

Table 16. Mass balance calculations and the ratio between the amounts of silicon captured by the alumina and mass balance for silicon in all of the phosphorus removal test runs.

Test run	Total amount in / mg	Total amount in products / mg	Mass balance / mg	Increase on alumina / mg	Overall removal / mg/mg	Removed by alumina / mg/mg
Reference	25.3	17.6	7.7	19.7	0.30	2.56
Low temperature	15.8	15.2	0.6	29.4	0.04	45.88
Low pressure	18.3	24.1	-5.7	28.8	-0.31	-5.02
Low feed rate	8.6	4.2	4.4	3.8	0.51	0.87

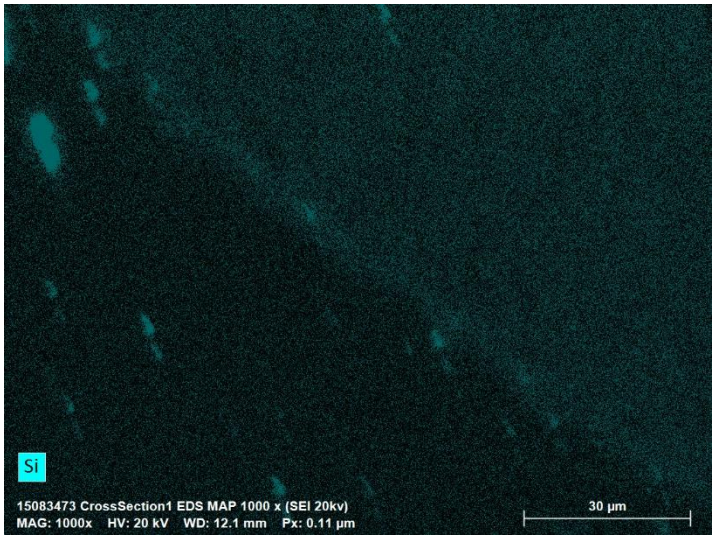

Figure 32. “Silicon spots” (marked with teal) inside and outside of the cross-section of alumina. The extrudates was from the low temperature test run.

4.1.2.6 Iron removal

As with the reference test run, all of the condition change test runs have a negative overall iron removal, meaning the product samples contain more iron than the feed (Table 17). This has been discussed in Subsection 4.2.1.1.1 and it has been surmised that this phenomena is likely caused by the leaching either from the guard bed materials and/or the reactor system. The low feed rate run seems to have a little bit smaller increase of the conversion rate than the other test runs. This is similar to the behaviour of the sodium conversion in the low feed rate (Figure 33), which is most likely caused by the enhanced leaching with the lower feed flow rate.

The SEM-EDS results do not differ from the reference run. Iron is not detected in any SEM-EDS linescans. This could be because the iron content in the feed is so small that its collection is too small to be detected by the linescan.

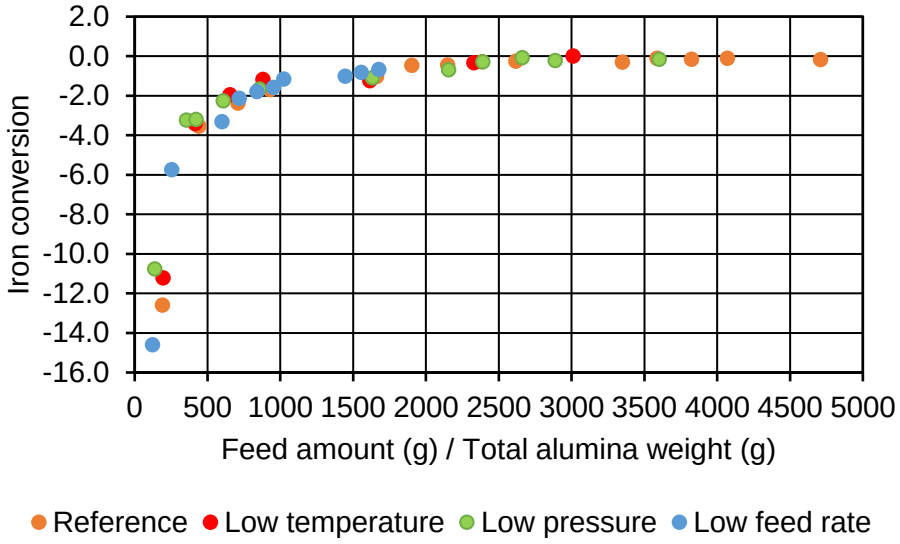

Figure 33. Conversion of iron in the reference test run (T = 325 °C, P = 50 bar and LHSV = 5.1 h^{-1}), low temperature test run (T = 225 °C, P = 50 bar and LHSV = 5.1 h^{-1}), low pressure test run (T = 325 °C, P = 10 bar and LHSV = 5.1 h^{-1}) and low feed rate test run (T = 325 °C, P = 50 bar and LHSV = 2.55 h^{-1}). The black marks around the points indicate the repeatability of the analysis.

Table 17. Mass balance calculations and the ratio between the amounts of iron captured by the alumina and mass balance for iron in all of the phosphorus removal test runs.

Test run	Total amount in / mg	Total amount in products / mg	Mass balance / mg	Increase on alumina / mg	Overall removal / mg/mg	Removed by alumina / mg/mg
Reference	5.4	11.8	-6.4	0.2	-1.17	-0.03
Low temperature	3.5	9.0	-5.5	0.2	-1.55	-0.03
Low pressure	4.1	9.0	-4.9	0.4	-1.20	-0.09
Low feed rate	1.8	7.1	-5.3	0.6	-2.85	-0.11

4.1.2.7 Density differences between runs

The density results (Figure 34) show that the low pressure and low feed rate runs have similar density development as the reference run. As discussed in Subsection 4.2.1.1.1, the density change could be caused by an unknown catalysed reaction. The density in low temperature run is at feed level which means that the reaction

requires higher temperature than 225 °C to occur. The results show that the reaction seems to be independent of the pressure decrease. This confirms that the alumina is not able to disassociate the hydrogen molecules for reactions or the gas-liquid balance does not affect the density. The density increase, in the middle of low pressure run, is caused by the unstable feed flow rate. The high feed flow rate decreases the reaction conversion which is why the density rises towards feed level. Decreasing the feed rate does not have a major impact on the density. The density of low feed rate samples seems to be lower than of the samples from the reference run but this falls under the repeatability of the density results in the reference run.

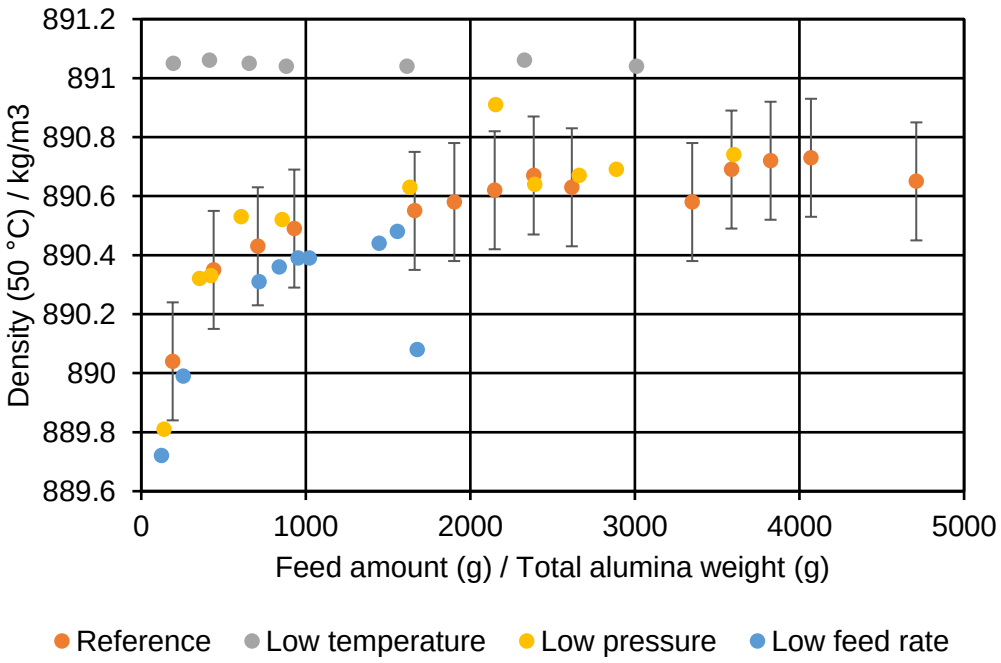

Figure 34. Density of the liquid samples from the phosphorus removal test runs along the time on stream.

4.1.3 Suggestions for further test runs

The suggestions for continuation test runs are provided in this section. A pre-washing procedure is suggested to decrease the impact of the leaching on the mass balance calculations. Two recommendations for the reactor packing are given. The choice of the packing depends on the purpose of future studies. Suggestions for suitable reaction conditions are based on the phosphorus removal test runs. One additional washing method to the ones already used in the test runs is also provided.

4.1.3.1 Pre-washing of the reactor bed

The ICP-MS results of sodium, calcium, and iron show that they are leached from the reactor bed by the organic acids of the feed. It could possible to pre-wash the reactor bed before starting the actual test run. The benefit of this would be that the effect on the mass balance would be mitigated and the evaluation of the results would be more reliable. The beds could be washed using either an aromatic free gas oil or a less impure phosphorus rich feed. If the gas oil is used, the washing could be carried out at the test run temperature. Using the cleaner version of the feed at elevated temperatures has the risk of coking or causing other thermal reactions. This feed also contains some amounts of impurities which deactivate alumina. Thus the aromatic free gas oil would be the better option for initial washing.

4.1.3.2 Suggested reactor packing

From the results of the phosphorus removal test runs, two suggested changes to the reactor bed packing can be derived. The choice which of these two packing methods should be used depends on the focus of future test runs.

If the different guard materials have to be studied and compare to the previous runs, only small changes should be done to the reactor bed. Figure 35 shows projection of option 1. Here, the reactor beds should be placed in the isothermal zone. Due to this, the reactor will also have less guard material for each bed. The number of guard beds should be decreased to three as with the four beds would not provide enough material for all solid analyses without combining some of the beds.

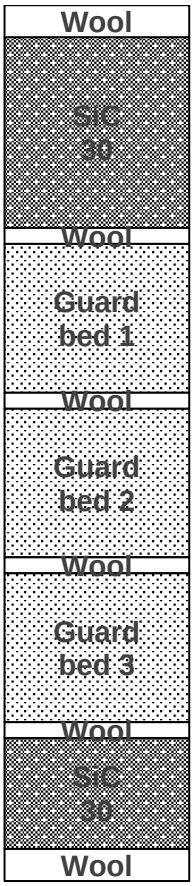

Figure 35. Suggestion for the reaction packing in case of guard material studies (option 1).

In the case that the maximum removal capacity of the impurities is more interesting to study, utilizing the filtering effect of the reactor bed could allow higher removal. The phosphorus removal test runs showed that the phosphorus and other metals are mainly removed by phosphate salt formation. A higher amount of these could be captured by the reactor bed if the void fraction of the bed would be smaller which could be possible utilizing SiC beds instead of guard material. The reactor bed could use size grading thus allowing a more controlled uptake of the precipitates to avoid spots in the reactor where the solids are primarily collected which could result in blocking of the reactor bed. Some guard material could be added to the bottom of the reactor because it could uptake silicon and metals that have not been thermally removed. The proposed reactor packing for the investigating the maximum removal (option 2) is shown in Figure 36.

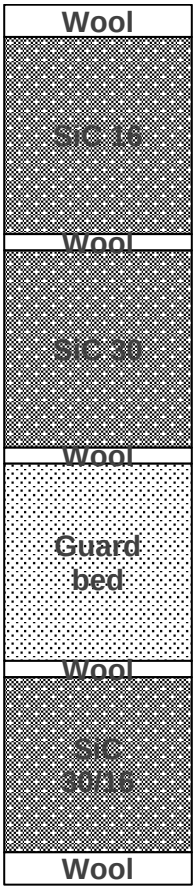

Figure 36. Suggestion for the reaction packing in case of phosphorus removal studies (option 2).

4.1.3.3 Suggested test run conditions

The phosphorus removal is strongly affected by the temperature according to the test runs. This also is especially evident in the lower temperature test run as the conversion of phosphorus is smaller compared to the reference. In the further test runs, the temperature could be increased higher for enhanced phosphorus removal. The higher temperature could cause the phosphorus rich feed to decompose to greater extend. Increasing the temperature, however, can potentially lead to production of more free fatty acids which would increase feed acidity. This would increase the leaching of alumina and equipment. The thermal stability of the feed should be studied.

The products of the phosphorus removal test run have densities lower than the feed and the density increases slowly towards the feed level. This was not seen with the low temperature test run where the feed and product densities were the

same. It could be the acid sites of alumina act as a catalyst that could cause unknown reactions.

However, the acid sites of alumina could act as a catalyst that could cause reactions which have not been observed during the thermal stability run. The products of the phosphorus removal test run have densities lower than the feed and the density increases slowly towards the feed level while the liquid product of the thermal stability run at 325 °C had density at the feed level. This hints that some reactions are catalysed by the alumina. This is why if the temperature in the future runs is increased, the liquid products should be analysed by GPC.

The pressure does not seem to have much effect on the phosphorus removal compared to the other conditions. The lower pressure seems to enhance the alumina adsorption and also removal of silicon. Due to these reasons the pressure could be decreased in further test runs.

Even though the low feed rate possess a better silicon removal, its impact on the phosphorus removal has been very small. Utilizing the lower feed rate would be less time efficient than the reference feed rate. As less feed passes through the reactor, it would require longer test runs to see how the impurity uptake changes with time of stream. Moreover leaching of sodium, calcium and iron are increased with a lower feed flow rate which in turn affects the mass balance calculations negatively. Due to the pumping issues in the low pressure test run, the feed flow rate increased above the reference feed flow rate. This significantly decreased the removal of impurities. Thus the feed rate should not be increased.

4.1.3.4 Washing of the reactor bed after the test run

Due to the issues caused by the hydrocarbons stuck inside the pores, some washing methods have already been tried during the experiments. One that has not yet been tested, is the combination of the *n*-heptane and the aromatic free gas oil. The reactor bed could be washed first with the aromatic free gas oil and then washed with *n*-heptane mainly to remove the gas oil. The aromatic free gas oil is able to dissolve a higher fraction of hydrocarbons compared to *n*-heptane because it can be used at higher temperature without the risk of evaporation. The temperature in the reactor could be then lowered for n-heptane wash.

4.2 Silicon removal test runs

This section shows and evaluates the main results of the silicon removal test runs from the silicon rich feed. The purpose of these experimental runs was to investigate how the process conditions affect the removal of silicon containing compounds by means of alumina guard beds. The effects of the conditions were investigated by performing test runs at the decided reference conditions. The first reference run that was done failed due to several pump problems. The pump stopped pumping the feed for many hours many times during the test run. Therefore, it was decided that the subsequent test run, where the maximum capacity of the silicon separation is investigated, would be used as a reference for the other test runs. The results of the reference run are compared to three silicon removal test runs, where one process condition was changed in each compared to the reference run. The process condition was altered to lower temperature, lower pressure, and lower LHSV. The experimental procedures of the test runs are explained in more detail in Section 3. The first part of this section discusses the results of the silicon removal reference test run and draws conclusion about the removal of impurities. The second part of the following section compares the results of the process condition change test runs to the reference results. Finally, the third part makes suggestions for future test runs investigating the silicon removal using guard bed technology. All analysis results of the liquid products of reference test run are shown in Appendix 10 and condition change test runs in Appendix 11.

4.2.1 Silicon removal reference run

4.2.1.1 Liquid product sample results

4.2.1.1.1 ICP-MS results

The amount of silicon in the liquid product samples measured by ICP-MS analysis are shown in Figure 37. The conversion of silicon remains very stable during the run at the reference conditions (T = 230 °C, P = 50 bar and LHSV = 1.2 h^{-1}), which means that the maximum capacity of alumina for silicon capture was not reached during time of stream. The silicon results are above the calibration curve of the analysis method which is why they can have some inaccuracy. The specific types of the silicon containing compounds in the feed are not known but PDMS could one source for the silicon in the feed. The PDMS needs to decompose to smaller compounds before it can become adsorbed on the acid sites of alumina. Some

decomposition products can also be volatile and thus, are present in the off gas stream [51]. From the analysis of the liquid samples it is difficult to say which way is the dominate route for the removal of silicon containing products.

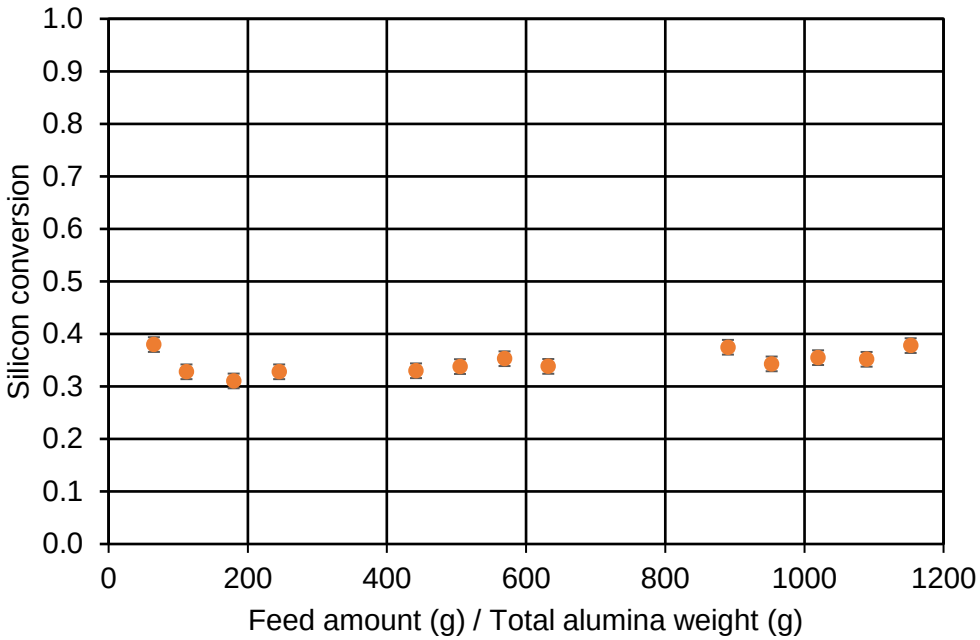

Figure 37. Conversion of silicon in the test run where reference conditions (T = 230 °C, P = 50 bar and LHSV = 1.2 h^{-1}) have been used. Black marks indicate the repeatability of the analysis.

The phosphorus conversion seems to increase during the time on stream (Figure 38). It is not known in which compounds the phosphorus is present in the feed. However, if the phosphorus containing compounds in the feed are phospholipids, they can thermally decompose to phosphates. The phosphorus may also be present already as phosphates in the feed. The alumina is able to capture phosphates by adsorption [43]. The phosphates may also form phosphates salts if counter cations are present [45]. The conversion of phosphorus is increasing during the test run similarly to the phosphorus removal test runs (Section 4.2.3.1), where it was concluded that the phosphorus is removed mainly by salt formation. The salt trapping by the reactor bed then increases as more salts are captured resulting in lower phosphors content in the subsequent samples. It could be that silicon removal happens here in a similar manner.

Potassium removal was high during the whole test run (Figure 38). The removal of alkali metals can happen by ion-exchange with the acid sites of alumina. It is also

known that the potassium has a high affinity to react with phosphates to form phosphate salts [45] which then are trapped in the reactor bed. The potassium cations also may act as the counter ions for other compounds in the feed such as free fatty acids.

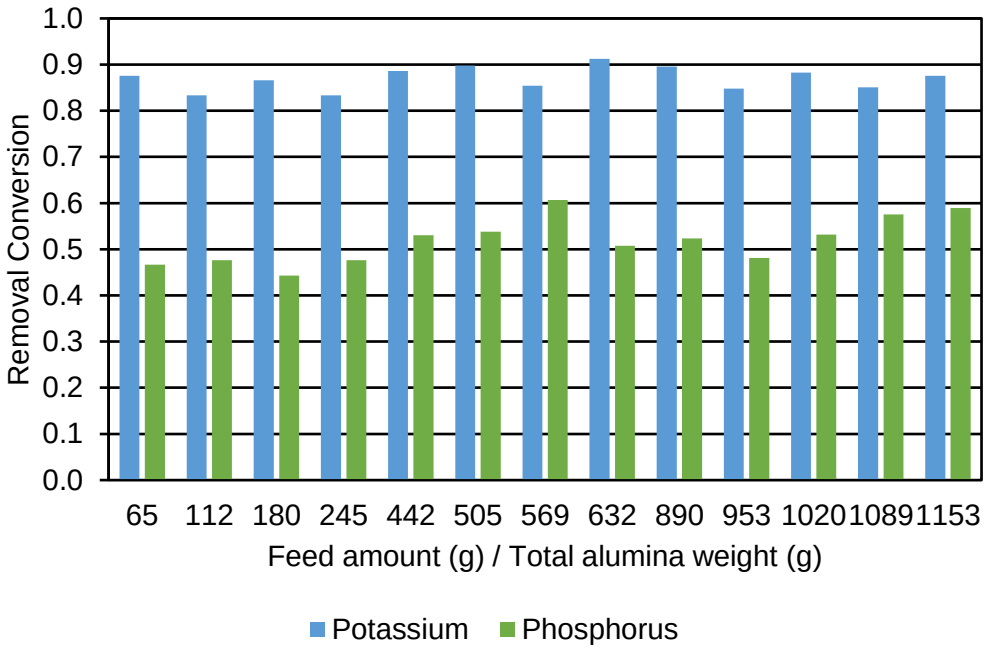

Figure 38. Conversion of potassium and phosphorus at the reference conditions (T = 230 °C, P = 50 bar and LHSV = 1.2 h^{-1}).

Sodium results show that the conversion is negative throughout the test run (Figure 39). This means that the sodium amount in the products is much higher than in the feed in the beginning of the run, which indicates that sodium was leached during the test run most likely from the alumina (sodium content:< 220 mg/kg) or/and the SiC (sodium content:< 200 mg/kg). The amount of sodium in the product decreases in the subsequent samples after the first sample. After that, the amount starts to decrease in the products to finally either becoming stable or continue increasing linearly. The amount can be high in the first samples because all the most easily removable sodium is leached from the reactor bed first after which the content decreases. In the test runs with the phosphorus rich feed, the trend of the sodium conversion is similar to this this run. However in those test runs, the sodium amount in the products eventually decreases below its content in the feed. The conversion here is constantly negative as the feed is much more acidic than the phosphorus rich feed. Sodium could also be removed during the test run. However, because

the leaching is affecting the results, the removal is most likely overlapped by it. The sodium removal could occur by ion-exchange with acid sites on the alumina. As with potassium, sodium could have formed salts with the phosphates or with other feed components such as carboxylates of free fatty acids. As the conversion seems to continue increasing similarly to the phosphorus, which could be caused by the leaching or possible formation of participates which are collected to the reactor bed. As in the case of silicon ICP-MS results, the sodium content in some of the products exceeds the limits of the analysis method. This is why it is difficult to say if the sodium conversion keeps increasing at the end of the test run.

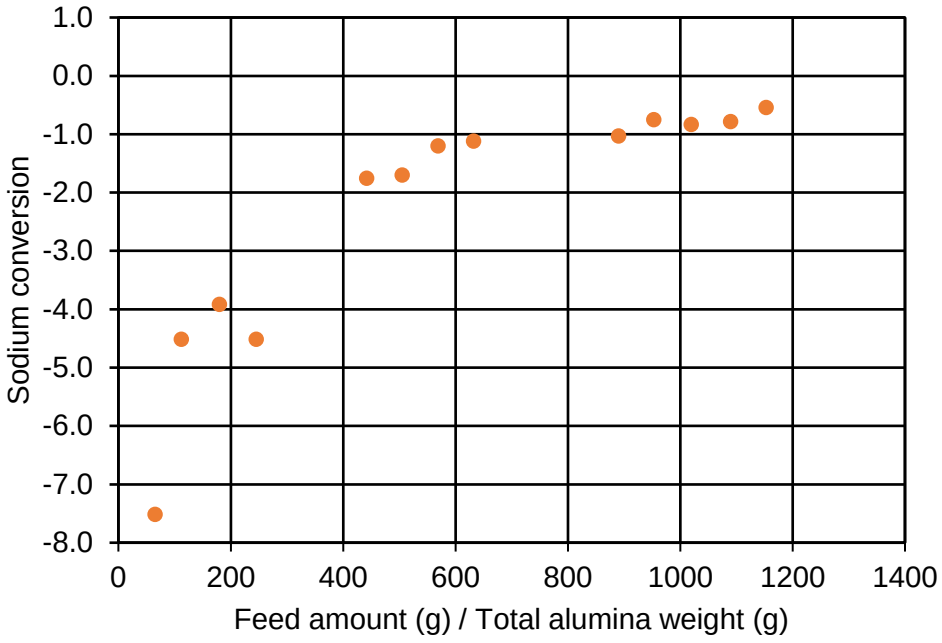

Figure 39. Conversion of sodium at reference conditions (T = 230 °C, P = 50 bar and LHSV = 1.2 h^{-1}).

Evaluation of the calcium analysis results (Figure 40) reveals that the conversion of calcium is fluctuating around 0.3 during time on stream. The reason for the fluctuation of the results is unknown. The first four samples taken seem to imply a trend where the calcium conversion increases compared to the feed level. This seems similar to the sodium thus indicating that most easily removable calcium is leached at the start of the test run. The calcium content in the alumina (calcium content: 98 mg/kg) or SiC (calcium content: 360 mg/kg) is also relatively high meaning in case of the leaching occurring it should affect the results.

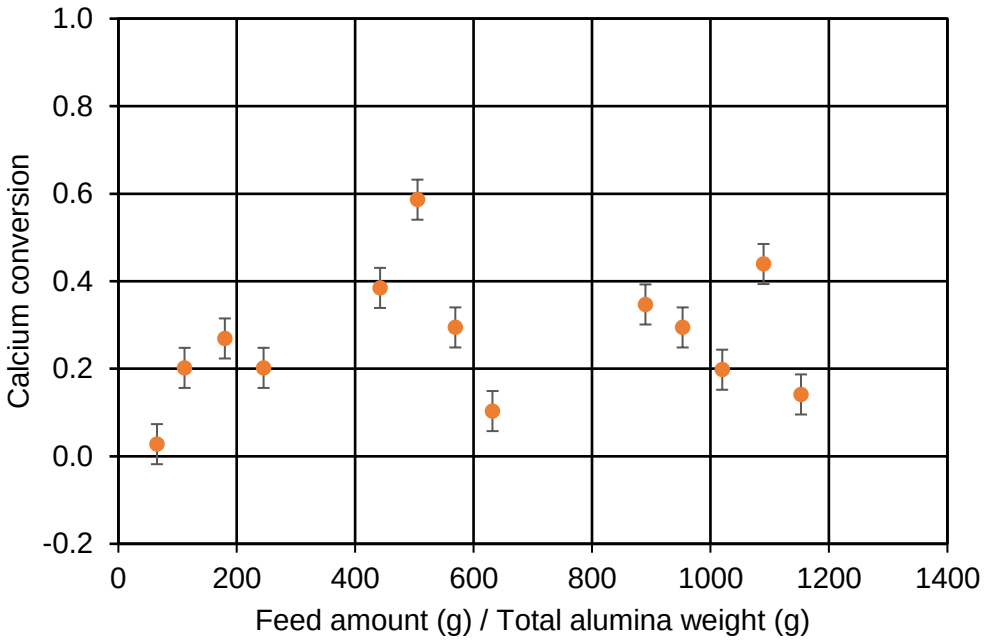

Figure 40. Conversion of calcium at reference conditions (T = 230 °C, P = 50 bar and LHSV = 1.2 h^{-1}). Black marks indicate repeatability of the analysis.

The iron conversion (Figure 41) at the beginning of the test run is negative meaning that the product samples contained more iron than the feed. This hints that iron is leached at the beginning similarly to sodium and calcium. As the run continued, the iron conversion begins to increase to 0.2. Suddenly, the conversion decreases rapidly to a negative conversion meaning the products have more iron than has been fed into the reactor. After this, the conversion started to increase once again to nearly 0.2. The trend of the last samples shows that the conversion could increase even higher. It could be that iron formed some kind of agglomerates, which could be salts, in the reactor. The agglomerates could have been released after a small pressure difference was built up in the reactor. This pressure difference cannot be confirmed from datalogger due the limitations of the unit as the system is only equipped with pressure gauges at the both ends of the reactor.

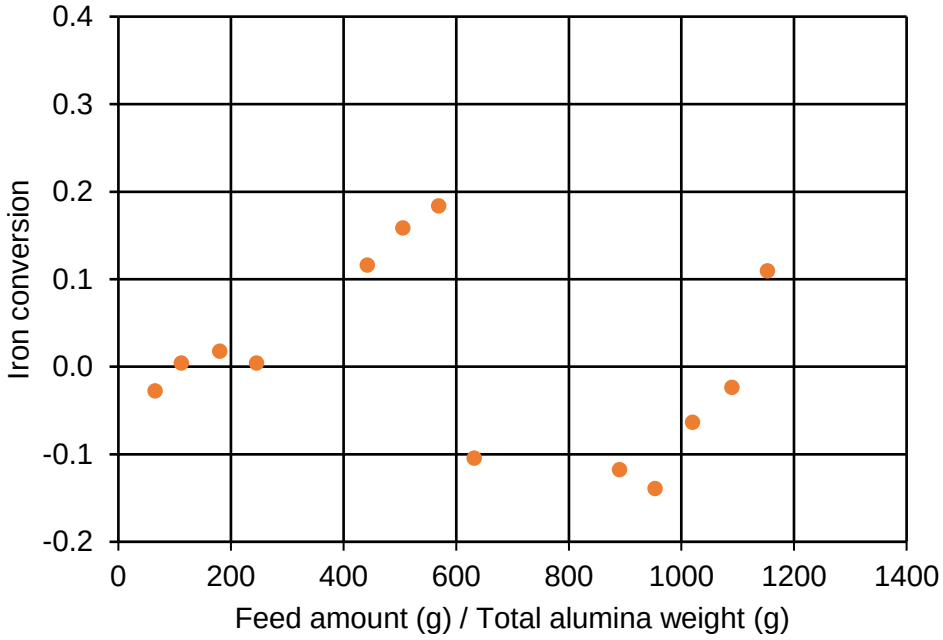

Figure 41. Conversion of iron at reference conditions (T = 230 °C, P = 50 bar and LHSV = 1.2 h^{-1}).

Because the feed has a high TAN value (76 mg KOH/g) and the ICP-MS results of sodium indicate that leaching has occurred during the test run, the amount of aluminium in the liquid product was additionally analysed. The content of aluminium in the feed was minimal (< 0.1 mg/kg), however its amount in the products was much higher as Figure 32 shows up to 208 ppm in the first sample. The aluminium behaves similar to sodium as its content in the products decreases with time on stream. The trend of calcium conversion seems to behave in similar manner. At the end of the test run, the aluminium amount in the products becomes stable at close to 50 mg/kg. This confirms that sodium and iron are leached from alumina, however the leaching from SiC cannot be excluded. The aluminium has been leached most likely due to the free fatty acids in the feed. As with sodium, the reason why the aluminium content in the products is initially higher is that the most easily leachable parts are leached first thus the leaching amount decreases with the time on stream.

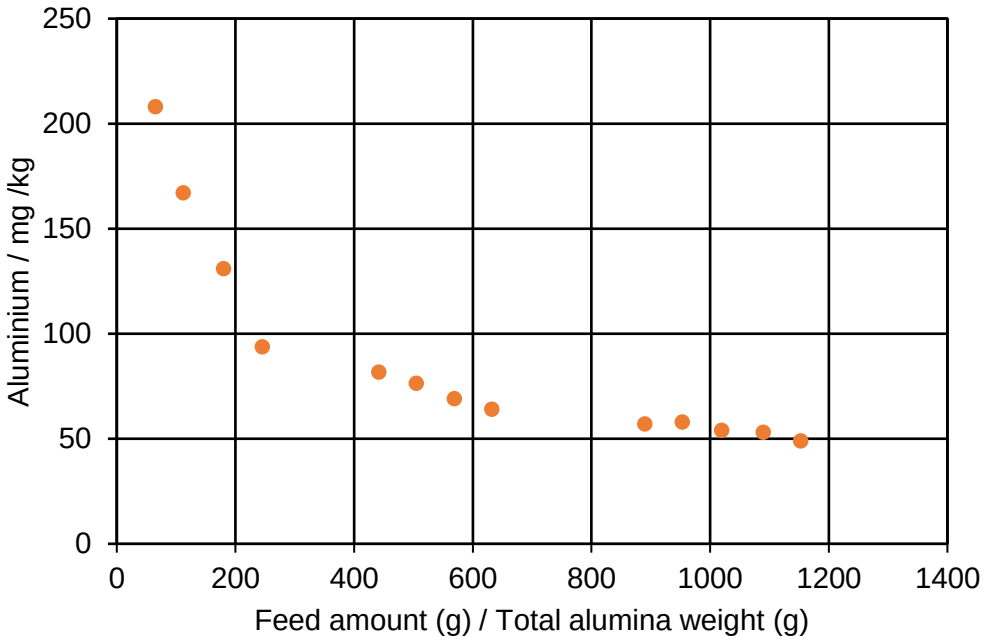

Figure 42. Aluminium content in the samples from the silicon removal test run (T = 230 °C, P = 50 bar and LHSV = 1.2 h^{-1}).

4.2.1.1.2 Density and total sulphur content results

The densities of the liquid product samples are fluctuating around the feed level (956.27 kg/m^3) (Figure 43). The fluctuation is within the repeatability of the analysis method. The total sulphur content of the product samples is also show in the figure. The amount of sulphur in the product samples is slightly lower than the amount in the feed (2162.3 mg/kg) which could mean that some of the sulphur is removed during the test run for example by formation of volatile compounds or adsorption on the alumina.

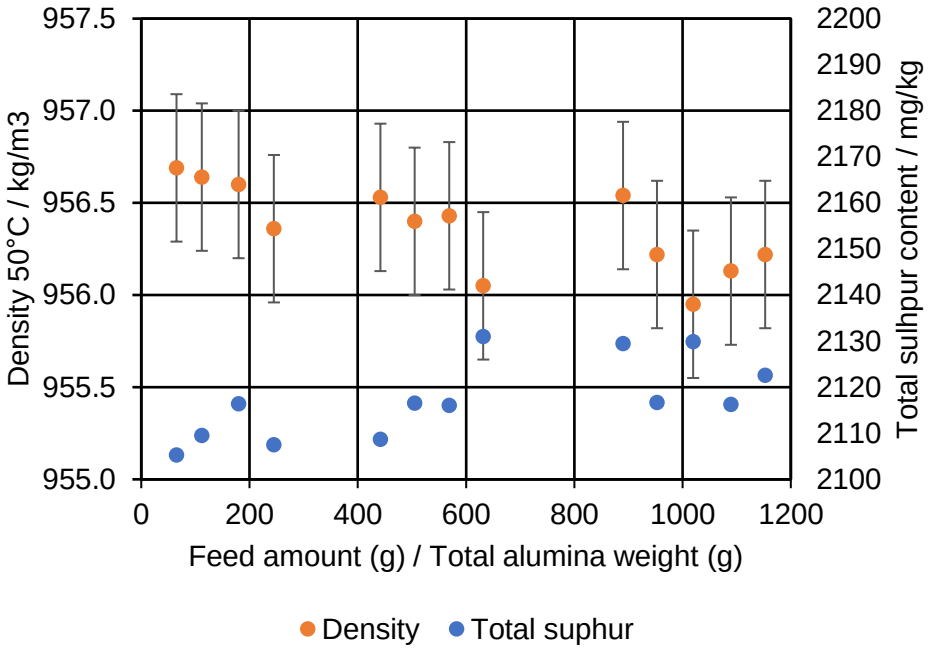

Figure 43. Density and the sulphur content in the samples from the silicon reference removal test run (T = 230 °C, P = 50 bar and LHSV = 1.2 h^{-1}). The black marks indicate the repeatability of the analysis.

4.2.1.2 Spent alumina characterization results

4.2.1.2.1 XRF results

The guard beds 1 and 2 as well as 3 and 4 had to be combined for XRF analysis to two samples as the material was not enough for all of the analyses. The XRF results were normalized to the content of aluminium in the fresh and spent alumina as explained in detail in Subsection 3.4.2.2. Because the ICP-MS results show that leaching of aluminium occurred in the test run, the increase of the content of impurities in the alumina appears most likely smaller in the XRF analysis than the alumina actually captured. Another normalization method was tested, where ICP-MS data of the product samples was used to determine the total amount of the leached aluminium. This total amount was subtracted from the aluminium content of the fresh to gain the aluminium content of the spent alumina to be used in the normalization calculation. The method was considered because the ICP-MS has higher accuracy than the semi-quantitative XRF. By this method the aluminium amount of the spent alumina was higher, however the difference between the results of XRF and ICP-MS normalized methods was not significant and the ICP-MS method also did not take in account the amount of aluminium in the waste emptying before the first sample. In Table 18, it can be seen how much the content of each impurity

increases compared to fresh alumina in the upper and lower beds and also the ratio between them.

Evaluation of the XRF analysis shows that the amount of silicon in the upper beds is lower than in the lower beds. If the silicon in the feed is in PDMS, its removal via both pathways, adsorption and evaporation, requires silicon compounds to decompose, it makes sense that the lower beds have a higher silicon content as the decomposition has more space time to occur [51]. It is also possible that the other impurities tend to adsorb or plug the pores of alumina faster than the silicon containing compounds can adsorb causing the first beds to have a smaller amount of silicon than the lower guard beds.

The majority of phosphorus and potassium is found in the upper guard beds. It is known that they tend to form phosphate salts precipitates [46,64]. The formation of precipitates most likely occurs quickly which is why their presence is smaller in the lower guard beds as more phosphorus and potassium containing compounds are available for adsorption at the upper guard beds before precipitate formation.

The content of sodium and calcium in both beds is negative after calculating how much their amount has increased in the spent alumina compared to the fresh alumina. This means that sodium and calcium were leached from the alumina which is supported by the ICP-MS results. The leaching of sodium seems to have occurred to a larger extent in the upper parts. Leaching of calcium seems to take place equally in both parts. The uptake of iron in the both lower and upper beds is nearly the same. The increasing iron content means that iron might have not been leached from the alumina or the uptake of iron by alumina was higher than the amount leached.

Table 18. Impurity amounts from the spent alumina in the upper and lower guard beds after the test run and calculated ratio between upper and lower beds. The ratio was calculated by dividing the amount on the upper beds with the total amount in both beds.

Elements	Upper guard beds / mg	Lower guard beds / mg	Upper / lower guard bed ratio
Sodium	-0.25	-0.12	0.67
Silicon	0.74	1.71	0.30
Phosphorus	4.35	1.23	0.78
Potassium	0.51	0.11	0.82
Calcium	-0.23	-0.24	0.49
Iron	0.83	0.94	0.47

4.2.1.2.2 XRD results

Alumina extrudates from the first, second and fourth alumina guard bed were analysed by XRD. The diffractograms do not differ from the fresh alumina and all of them match the diffractograms of aluminiumoxide. The third guard bed was not analysed with XRD. The XRD patterns are included in Appendix 12.

4.2.1.2.3 EDS and SEM-EDS linescan

EDS spectra for the impurities on the surface of alumina are shown in Figure 44. These results are indicative as the accuracy of the method has not been tested. Thus, the concentration differences between the extrudates may not actually be as significant as results show. Some trends can be seen with the results. The amount of phosphorus on the surface is higher than of other impurities. It may be that it forms a similar impurity layer around the alumina as it was seen in the phosphorus removal test runs. Figure 44 shows that the silicon amount increases along the reactor bed, which matches its XRF results. The amount of iron, sodium and potassium on the surface alumina is small. Similarly, to the phosphors, the content of iron and potassium decreases in the subsequent guard beds. The sodium content is nearly equal in all beds. Calcium was not detected by the analysis which could either mean that it was leached from the extrudates or its amount is so small that analysis cannot detect it. Unfortunately, SEM-EDS line scan was not carried out for the due to time constraints of this work.

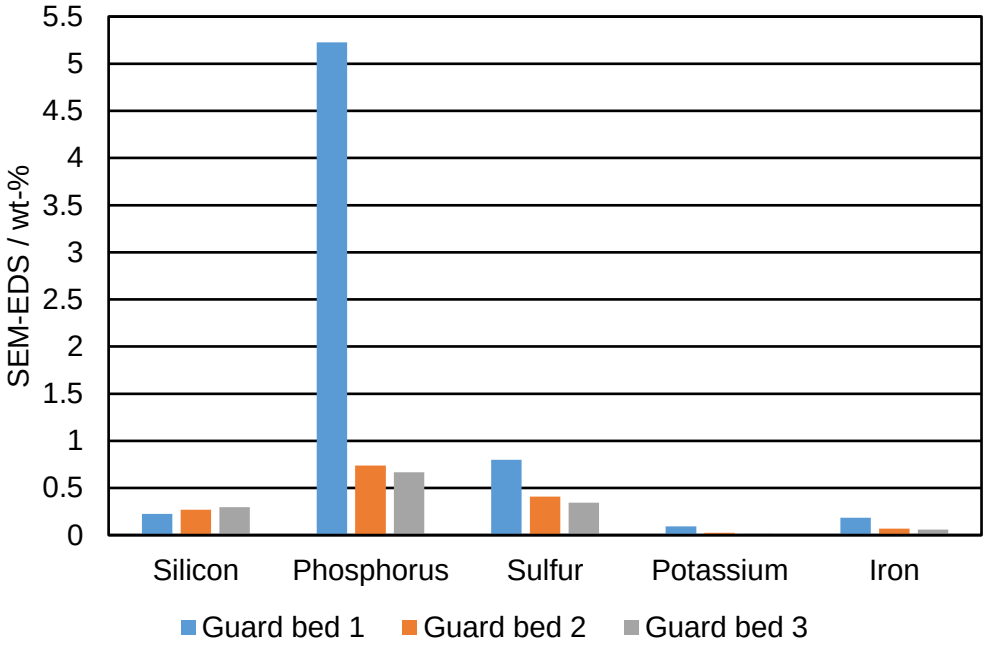

Figure 44. Indicative weight percentages of sodium, silicon, sulphur and potassium on the spent alumina from guard beds 1, 2, and 4 derived from SEM-EDS analysis of the surface.

4.2.1.2.4 N_2 physisorption and TGA analyses

Nitrogen physisorption and thus BET and BJH analysis as well as TGA analysis could not be performed for the spent alumina extrudates due to hydrocarbons stuck inside the alumina pores. The more detailed description of this issue is provided in Section 4.2.1.2.4.

4.2.1.3 Mass balance of the impurities

The ICP-MS results to estimate how much impurities were fed into the reactor and how much were in the liquid products. The mass balances for the impurities (Table 19) were calculated from these by subtracting the amount in the products from the feed. The content of impurities in the spent and fresh alumina was measured with XRF and the results were compared to receive the how much the amount increased on the alumina.

Table 19. Calculated mass balance for the impurities in the reference run.

Element	Total impurities in the feed / mg	Total impurities in the products / mg	Mass balance / mg	Impurity increase on alumina / mg	Overall impurity removal / mg/mg	Fraction removed by alumina mg/mg
Sodium	2.35	6.50	-4.15	-0.04	-1.77	0.01
Silicon	27.88	18.17	9.71	0.24	0.35	0.03
Phosphorus	3.54	1.69	1.86	0.56	0.52	0.30
Potassium	1.39	0.17	1.21	0.06	0.88	0.05
Calcium	0.53	0.36	0.16	-0.05	0.31	-0.29
Iron	6.51	6.50	0.01	0.18	0.00	26.92

The overall silicon conversion (0.35) is quite low. As already mentioned, in addition to adsorption, the removal of silicon from the feed can take place by forming volatile silicon containing compounds which are then present in the gas stream. The silicon mass balance hints that the removal of the silicon from the feed occurs mostly by the evaporation as the fraction captured on the alumina is small (0.03). The ICP-MS results indicate that the sodium and aluminium were leached from the reactor bed. This means that it is possible that the silicon was also leached from the alumina (silicon content: < 400 ppm) or SiC. Leaching would lower the apparent overall conversion of silicon and also the apparent the silicon uptake by the alumina. Thus the removal by the alumina could be actually higher.

Half of the total phosphorus was removed during the test run from which 0.4 was captured by the alumina. This shows the large portion of the removal occurs by the adsorption. The other removed phosphorus most likely formed into phosphate salts.

Most of the potassium (0.88) was removed during the test run. Only a small amount of potassium was captured by the alumina which would mean that it is removed by other means such as the formation of phosphate salts during the test run. A fraction of the potassium might have also reacted with the free fatty acids or other organic acids in the feed as carboxylic acid salts were detected by FT-IR analysis that was performed for the insoluble powder removed from the spent alumina extrudates while washing (Subsection 4.2.1.2.4). Potassium could act as counter ion to form these salts.

The overall removal of sodium is negative as its amount in the product samples was higher than in the feed due to the leaching (Subsection 4.3.1.1.1). As the sodium content decreases only slightly from the fresh alumina to the spent alumina, it is likely that the alumina captures some of the sodium or the sodium is mainly leached from SiC. Some of the sodium may also form carboxylic acid salts similar to potassium.

As already discussed, the conversion of calcium fluctuated around 0.3. It seems that calcium is leached from the reactor bed as its removal amount is negative. The total calcium removal is most likely higher but overlapped by the amount of calcium leached.

The overall iron conversion was extremely low according to the calculations. The reason for this is most likely the decrease in the iron conversion in the middle of the test run (Subsection 4.3.1.1.1). Due to calculation method for the fraction removed by alumina, the low iron amount removed by alumina caused the fraction to be extremely high. Thus the alumina removal fraction for the iron is not reliable.

4.2.2 Impact of process conditions on the impurities

4.2.2.1 Aluminium leaching from the reactor bed

Aluminium leaching occurs in all test runs. Different reaction conditions seem to have an effect on the leaching as ICP-MS results in Figure 45 show. Leaching of aluminium is by far lowest at low temperature (T = 130 °C, P = 50 bar and LHSV = 1.2 h^{-1}) because the temperature affects the leaching by increasing the reaction rate [13]. The pressure does not affect the corrosion according to the results. Lowering the LHSV causes the liquid products to have even higher amount of aluminium according to the ICP-MS than in the reference rest run. The reason for this is that leaching has more time to occur. The leaching impacts both ICP-MS and XRF results of the impurities in all of the test runs. Due to this, it is difficult to estimate if the difference between the results of the test run are caused by the leaching or by the condition change.

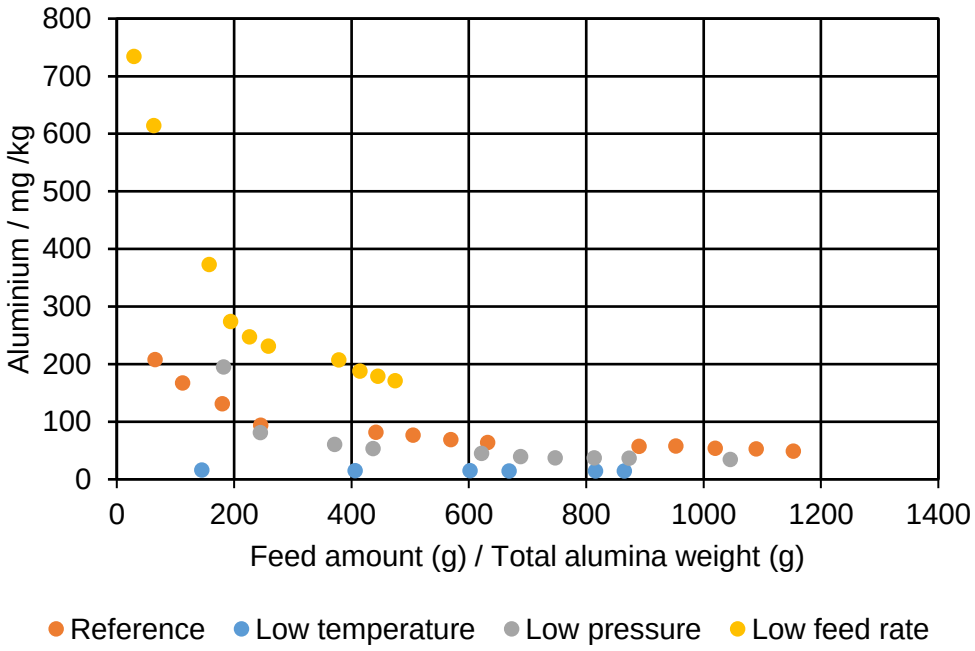

Figure 45. Aluminium content in the samples from the silicon removal test run.

4.2.2.2 Silicon removal

The mass balance calculation results of the removal of silicon are shown in Table 20 and the ICP-MS conversion results are depicted in Figure 46. The removal of silicon seems to occur mostly by the evaporation of volatile decomposition products of silicon containing compounds in the reference run. At lower reaction temperature, the silicon removal could be expected to be lower as the thermal decomposition is affected by the temperature and also the research preceding this thesis has shown that the adsorption of silicon increases with temperature [49,50]. However, the results show that silicon is removed more at low temperature than in the reference test run. The reason could be that the silicon containing compounds that can be removed by the evaporation already evaporate at low temperature. It could be that the removal of silicon containing compounds is the same in both, the reference and the low temperature test run, as the difference between their amounts of silicon removed is small. The reference test run results of sodium, calcium and iron indicate that leaching occurs during the test run. Leaching could affect the lower temperature run to a smaller extent thus the silicon conversion appears to be higher at low temperature. The other option is that the removal occurs more by other means at low temperature, such as adsorption on the surface of alumina or by formation of precipitates. The amount of silicon captured by alumina is less than in the reference run and also negative which could mean that silicon is leached

more than it is captured. The reason why the fraction removed by alumina is lower at the low temperature is that the lower temperature influences the adsorption rate. It might also be that there is no difference between silicon absorption in the reference and in the low temperature test runs as the XRF is a semi-quantitative method. In the low temperature run, the silicon conversion seems to have an increasing trend with time on stream, which could hint that the silicon containing compounds form precipitates which are trapped in the reactor bed. The aluminium results showed that the leaching decreases by the time on stream which might have caused the apparent conversion increase.

The pressure was expected to affect the gas-liquid equilibrium of the feed. If the silicon is removed by the evaporation, lowering the pressure (T = 230 °C, P = 10 bar and LHSV = 1.2 h^{-1}) should allow the evaporation of more generated volatile silicon containing compounds. However, the conversion of silicon in the lower pressure test seems to fluctuate in the same region as in the reference test runs. The overall silicon removal is nearly the same in both test runs showing that lowering the pressure does not have significant impact on the silicon conversion. If the removal mostly happens by the evaporation, the high pressure is not enough to inhibit it. This could also support that nearly all of the silicon that can evaporate is removed from the feed. As the silicon amount change in the alumina was negative compared to the fresh alumina, the removal unlikely occurs by adsorption. The silicon amount of the extrudates in the reference test run was higher than in the low per pressure test run. This indicates that the pressure has some effect on the removal by the adsorption. The low temperature and the low pressure both contain most of the adsorbed silicon in the upper beds (0.6) which larger amount than in the reference run.

In the low feed rate run (T = 230 °C, P = 50 bar and LHSV = 0.6 h^{-1}) the silicon conversion was at the same level as at the beginning of the reference run. With time on stream, however, the silicon amount in the products increases nearly linearly which is why the total silicon removal is lower than in the reference test run. The low feed rate test run shows the highest uptake of silicon by alumina. This suggests that the removal of silicon happens by adsorption which is contradicting to the results of other test runs. The uptake by the alumina is high at the beginning and then the conversion begins to decrease as the acid sites of alumina become

poisoned or the pores of the alumina get more plugged. It might be that the decomposition of the silicon containing compounds happens by formation of intermediate compounds which then decompose further to volatile compounds. Maybe these intermediates are able to be adsorb on the alumina in a higher amount due to lower feed rate. The intermediates might also react to other silicon containing compounds instead decomposition to volatile ones due to the feed rate. The ratio between the silicon captured by the upper and lower beds is at same level as in the reference (0.3)

The XRD analysis was made from the alumina extrudates of the first guard bed in all of the runs. The diffractograms of all test runs show no difference compared to the fresh alumina. The surface of the first, second and fourth guard bed layers of the low temperature and low pressure test runs were analysed with EDS. The weight fraction of silicon is nearly same in all of the test runs. It seems that the silicon amount on the alumina layers increases in an axial direction in the low temperature and reference run. The low pressure test run collected a large amount of silicon in the second guard bed. SEM-EDS line scan was done for the extrudates from the first beds of low temperature and low pressure test runs. According to EDS line scans (Appendix 13), the extrudates of the low pressure test run have a large silicon concentration areas inside the extrudate which have not been observed in the extrudates of the low temperature run. This is also reflected in the mass balance where the silicon amount captured by alumina in the low pressure is higher than in the low temperature test run. The EDS analysis is unfortunately not that reliable as the extrudates are milled before the analysis with an equipment that can leave silicon contaminations on the extrudate. EDS mapping was performed for the extrudates of the low temperature test run. They show small amounts of adsorbed silicon on the surface. The fore mentioned traces of the silicon contaminations can be seen in Figure 47.

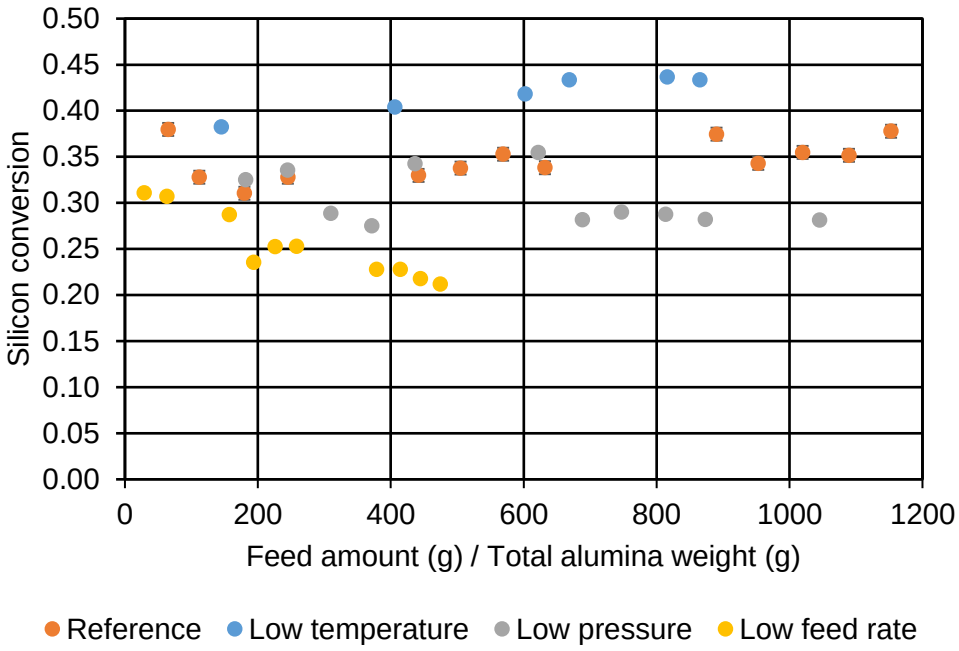

Figure 46. Conversion of silicon in the reference test run (T = 230 °C, P = 50 bar and LHSV = 1.2 h^{-1}), low temperature test run (T = 130 °C, P = 50 bar and LHSV = 1.2 h^{-1}), low pressure test run (T = 230 °C, P = 10 bar and LHSV = 1.2 h^{-1}) and low feed rate test run (T = 230 °C, P = 50 bar and LHSV = 0.6 h^{-1}).

Table 20. Mass balance calculations and the ratio between the amounts of silicon captured by the alumina and mass balance for silicon in all of the phosphorus removal test runs.

Test run	Total amount in / mg	Total amount in products / mg	Mass balance / mg	Increase on alumina / mg	Overall removal / mg/mg	Removed by alumina / mg/mg
Reference	27.88	18.17	9.71	0.24	0.35	0.03
Low temperature	21.84	12.82	9.02	-0.17	0.41	-0.02
Low pressure	25.93	17.90	8.03	-0.05	0.31	-0.01
Low LHSV	11.98	8.86	3.11	1.09	0.26	0.35

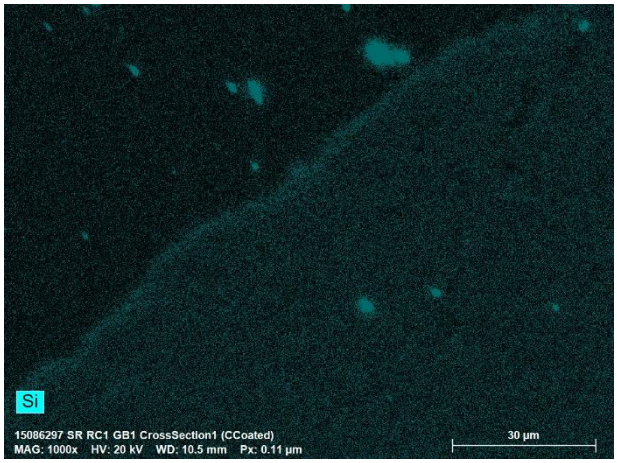

Figure 47. EDS image of an alumina extrudate close to the edge of the extrudate. The detected silicon is marked with teal.

4.2.2.3 Phosphorus removal

The phosphorus conversion for the test runs are shown in Figure 48 and the mass balances in the Table 21.

An interesting phenomenon can be seen in the ICP-MS results of the low temperature and low pressure test runs. After the start-up, the phosphorous conversion seems to increase similarly to the reference test run. After the total feed amount fed into the system reaches roughly 600 g/g, the conversion drops and increases subsequently again. This behaviour is also seen in the progress of ICP-MS results of iron in the reference run. The *sudden conversion decrease* seems to happen in smaller magnitude for phosphorus in the reference and the low temperature run compared to the low pressure test runs. As the decrease occurs always nearly after same total feed amount, it could be that it is caused by a collection of particulates to the reactor bed. Maybe phosphorus precipitates form agglomerates that are stuck in the reactor bed. After enough material has been collected in the bed, some of these are then released. When comparing the test run diaries to each other, it was noticed that, in the low temperature and low pressure runs, the sudden decrease occurred after the feed addition to the feed tank. During the feed addition the tank was depressurised which could have affected the pumping thus lowering the feed rate. This suddenly lower feed rate could have allowed some of the collected phosphorus salts to dissolve into the feed thus increasing the phosphorus amount in the products. Another option is that once the tank was pressurized again this suddenly increased the pumping speed which then pushed some of the col-

lected phosphorus containing agglomerates from the reactor beds which then dissolved into the products. The phenomenon will be referred as "*sudden conversion decrease*" in subsequent mentions.

The evaluation of the results of reference test run showed that the removal of phosphorus mostly occurred by the salt formation (Section 4.3.1.1.1). Lowering the temperature does not seem to have large impact on the total conversion as it only decreased by 0.05 compared to the reference. This suggests that most of the phosphorus is present in compounds that are able to form salts or absorb without requiring the thermal reaction to be removed chemically as the phospholipids would. The amount of phosphorus removed by the alumina was smaller than in the reference run most likely the temperature decreased lowered the adsorption reaction.

As stated above, the low pressure test run is most affected by the *sudden conversion decrease* as the conversion drops roughly by 0.3. Despite this, the overall removal of phosphorus is higher than in the reference run. The uptake of phosphorus by the alumina via adsorption is a little bit lower than in the reference run but this could be because of the accuracy of the XRF measurement. The reason why the change of the feed rate could have the highest impact on the phosphorous conversion during the low pressure run might be because the system at a lower pressure is more sensitive to a sudden pressure alteration than a system at higher pressure. It is also possible that the larger decrease is caused by some other test run specific parameter besides the sudden pressure changes but none has been identified.

The low feed rate run has the highest phosphorus removal (0.74) compared to the others. As a lower residence time enables the phosphorus containing compounds to react with the surface of alumina and/or to form phosphate salts with counter cations. The fraction that has been adsorbed on alumina is equal to the amount adsorbed in the low pressure run which could imply that the feed rate does not affect the overall phosphorus removal but the fraction of phosphorous captured on alumina.

In all of the test runs the phosphorus has been collected to a higher extent in the upper guard beds than the lower beds. From the EDS results of the first guard beds of low temperature and the pressure test runs, it can be seen that similar to the reference run, the phosphorus content on the surface decreases along the reactor bed. This matches the XRF results and suggests that phosphorus reacts very

quickly with the alumina or the counter cations. However, the second bed of the low pressure test run has captured the highest amount of phosphorus compared to the other beds. It could be that this somehow related to the *sudden conversion decrease*. Maybe the agglomerates are formed in the first bed and during the time on stream they or parts of the agglomerates migrate from the first bed some of them become trapped in the second bed. From the results it is difficult to say if the agglomerate migration occurs by desorption of captured components from the alumina or by independent formation without alumina. EDS mapping was only measured from the extrudates of the first bed of the low temperature run. They show a very thin layer of phosphorus around the analysed extrudate (Figure 49). The uptake of phosphorus by alumina is lowest at the low temperature according to the mass balance. So most likely the other runs contain a larger amount of phosphorus on the surface.

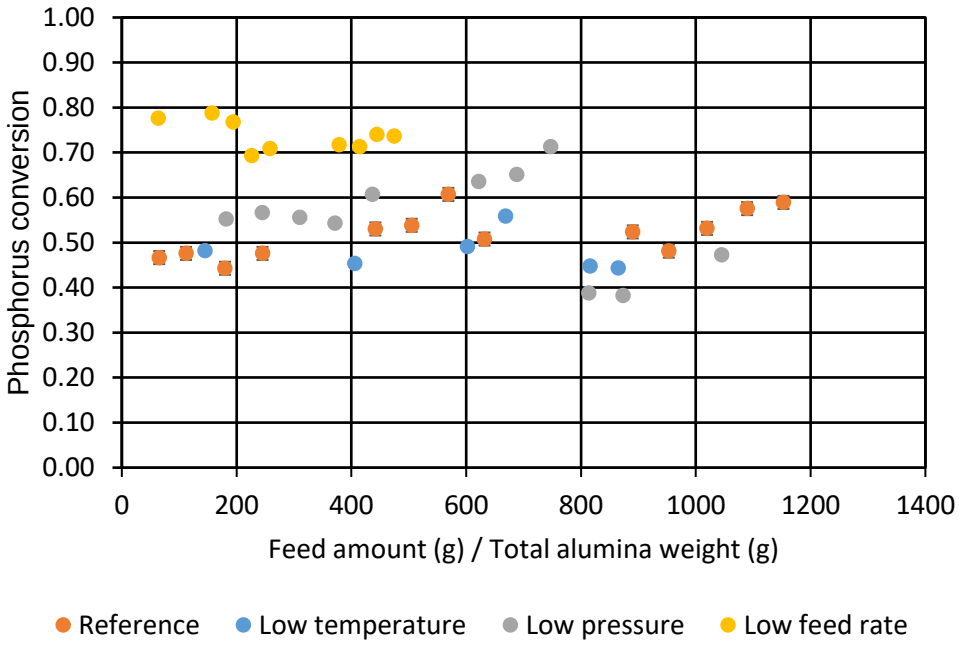

Figure 48. Conversion of phosphorus in the reference test run (T = 230 °C, P = 50 bar and LHSV = 1.2 h^{-1}), low temperature test run (T = 130 °C, P = 50 bar and LHSV = 1.2 h^{-1}), low pressure test run (T = 230 °C, P = 10 bar and LHSV = 1.2 h^{-1}) and low feed rate test run (T = 230 °C, P = 50 bar and LHSV = 0.6 h^{-1}). Black marks indicated the repeatability of the analysis.

Table 21. Mass balance calculations and the ratio between the amounts of phosphorus captured by the alumina and mass balance for iron in all of the phosphorus removal test runs.

Test run	Total amount in / mg	Total amount in products / mg	Mass balance / mg	Increase on alumina / mg	Overall removal / mg/mg	Removed by alumina / mg/mg
Reference	3.54	1.69	1.86	0.56	0.52	0.30
Low temperature	2.77	1.46	1.31	0.05	0.47	0.04
Low pressure	3.29	1.47	1.82	0.36	0.55	0.20
Low LHSV	1.52	0.39	1.13	0.24	0.74	0.21

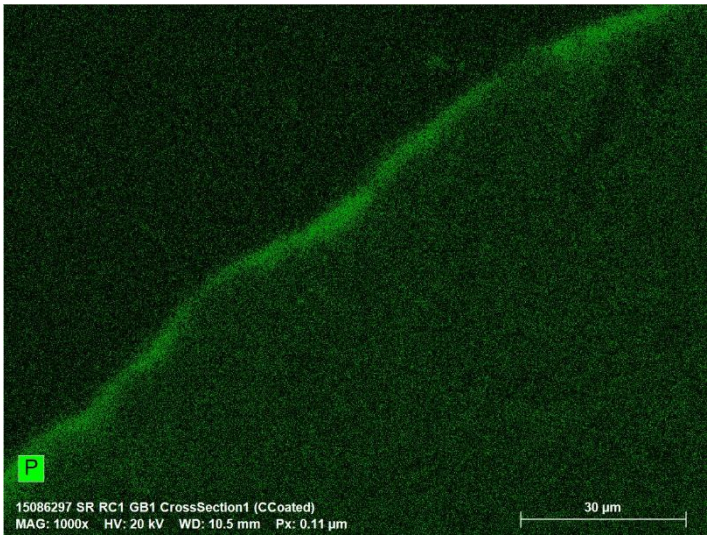

Figure 49. Thin phosphorus layer (marked green) surrounding the alumina extrudates from the low temperature test run.

4.2.2.4 Potassium removal

Nearly all of the potassium has been completely removed in all of the test runs except the low temperature run (Figure 50), where the total potassium removal is 0.74. As the potassium fraction adsorbed on the alumina is very small in all of the test runs (Table 22), the potassium is probably removed from the feed by salt formation. It most likely forms salts with phosphates or other compounds such carboxylates derived from free fatty acids or other organic acids. If the phosphorus in the feed are as phospholipids, it requires thermal decomposition to form phosphates. In the low temperature run, the phosphorus conversion to phosphates is lower than in the reference test run. This could be the reason why the potassium conversion is lower than in the other test runs as less phosphate are available to

form salts. The residence time in the reactor has been too short to reach an equal conversion to the reference. The content of potassium in the feed is low which could mean that even small decrease in availability of counter anion decreases the potassium conversion. To see if the decrease in phosphorus conversion caused the smaller potassium conversion, the mole difference between how much was removed in the reference and low temperature test runs for phosphorus and potassium was calculated. It was assumed that the potassium is the counter cation of phosphates (PO_4^{3-}). After these calculations the molar ratio between phosphate and potassium was calculated. One phosphate molecule should be able to form potassium phosphate salt (K_3PO_4) with three potassium ions thus the amount of potassium moles should be three times higher. However, according to the ratio, the mole amounts were nearly equal. Thus, the salt formation of potassium most likely also occurs with other compounds in the feed and the formation is limited by the temperature in the low temperature test run. The potassium content decreases in the final two samples after first increasing linearly in the low temperature test run. This is also reflected in the ICP-MS results of the low temperature run of the phosphorus, sodium, calcium and iron. All of these elements have nearly the same conversion decrease by roughly 0.1 in the last two samples. This might again be related to the *sudden conversion decrease* which has been discussed in the previous section. The reason why this decrease is only observable at the low temperature with potassium could be caused by the potassium removal occurring lower in the reactor bed than in the other conditions. It could have occurred low enough in the reactor bed so that some of the agglomerates manage to leave the reactor causing the conversion of potassium to decrease. The XRF results show that potassium is evenly distributed over the upper and lower beds while most of it has been collected in the upper beds in the reference run. This means that the lower beds have more free potassium to partake in agglomeration formation compared to the reference run.

The potassium content in the liquid products and the potassium uptake of the alumina of the low pressure test run are nearly the same as in the reference test run. This means that the potassium removal seems to be independent of the pressure.

The first three samples of the low feed rate run show signs of leaching of potassium occurring at the beginning of the test run, as the conversion in the beginning is small and then increases to become stable after two samples. This shape has been

noticed to be an indication of leaching with the other impurities in the silicon removal test run. The conversion remains slightly below the conversion level in the reference run most likely because of the more pronounced leaching with the lower feed flow rate. The fraction of potassium removed by the alumina is also negative meaning potassium has been removed from the alumina. It is difficult to say how the feed rate affects the conversion of potassium as the effect of process conditions cannot be separated from the effect of leaching.

EDS results of the first guard bed of the low temperature test run are similar to the reference test run, however the difference of the weight fraction of potassium between the first and the second bed is smaller than in the reference run. In the low pressure test run the second bed again contains a higher amount than the other beds. As discussed in the previous section, this could be related to the *sudden conversion decrease* phenomenon. The phenomenon also affects the removal of potassium in the low temperature run which could be why the difference between the first and the second be is smaller than in the reference. EDS mapping of extrudates from the low temperature test run shows that a small amount of potassium is present on the surface which could be either the adsorbed potassium.

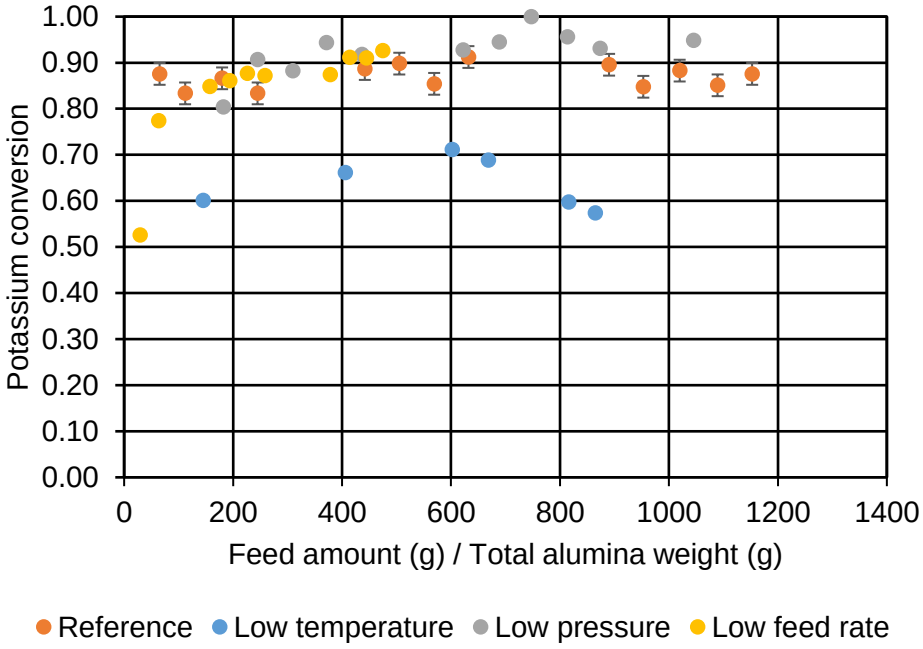

Figure 50. Conversion of potassium in the reference test run (T = 230 °C, P = 50 bar and LHSV = 1.2 h^{-1}), low temperature test run (T = 130 °C, P = 50 bar and LHSV = 1.2 h^{-1}), low pressure test run (T = 230 °C, P = 10 bar and LHSV = 1.2 h^{-1}) and low feed rate test run (T = 230 °C, P = 50 bar and LHSV = 0.6 h^{-1}). Black marks indicate the repeatability of the analysis.

Table 22. Mass balance calculations and the ratio between the amounts of potassium captured by the alumina and mass balance for potassium in all of the phosphorus removal test runs.

Test run	Total amount in / mg	Total amount in products / mg	Mass balance / mg	Increase on alumina / mg	Overall removal / mg/mg	Removed by alumina / mg/mg
Reference	1.39	0.17	1.21	0.06	0.88	0.05
Low temperature	1.08	0.38	0.70	0.01	0.65	0.02
Low pressure	1.29	0.11	1.18	0.01	0.91	0.01
Low feed rate	0.60	0.09	0.51	0.00	0.85	0.00

4.2.2.5 Sodium removal

The sodium conversion is very similar in all of the test runs (Figure 51). Like with the reference test run, the conversion is lowest in the first samples after which the conversion increases. The conversion is negative in every test run which is why the mass balances are also negative (Table 23). The negative conversion means that the sodium content of the products is higher than the content in the feed. The leaching of sodium significantly affected the results thus it is difficult to say if the sodium is removed in the test runs and also how the removal of sodium primarily occurs.

Leaching of sodium seems to occur to a lower extent in the low temperature test run as the conversion seems to be a bit higher than in the reference run. From the mass balance calculations it can be seen that the low temperature and low feed rate test run are the only ones where the sodium amount on alumina has increased meaning some amount of sodium has been removed by adsorption of sodium on the alumina even while sodium is leached from the alumina. These results are in agreement with the aluminium results meaning less leaching occurred at lower temperature. The upper guard beds captured less sodium than the than the lower ones, which could because they were leached more than the lower ones. The sodium conversion decreases at the end of the test run similar to other impurities at low temperature. This could be related to the *sudden conversion decrease* meaning some parts of sodium have been also removed as agglomerates.

A similar phenomenon can be observed in the low pressure run as seen with phosphorus in the same test run. At first the conversion has increased rapidly to nearly complete removal (0.81), then it has decreased to a little bit lower level (-1.39) than the conversion in the reference test run (about -1.12). This is very similar to the phosphorus conversion results in the same test run. The reason for this could be the same *sudden conversion decrease* meaning formation of agglomerates and also lower pump setting allowing collection of more of these agglomerates.

Lowering the feed rate causes a slower conversion increase rate towards uptake stability than in the other runs most likely due to increased leaching. It is interesting that the sodium content on the alumina increases even though the amount of sodium leaching is also highest in this run. Thus, lowering the feed rate could allow sodium to be adsorbed on alumina to an even larger amount than which was leached from the alumina. However, this contradicts the results of ICP-MS.

According to the EDS, the sodium content is nearly equal in guard beds 1, 2 and 4 from the low temperature test run. The XRF results show that the sodium content is higher in lower beds. This could be because XRF analysis was done for the milled sample while the EDS analysis was performed for the surface layer of the extrudates. This means that the sodium was more on the surface in the upper beds as the upper guard beds had smaller accessibility due to presence of other impurities. EDS analysis from the extrudates of the low pressure run shows that guard bed 2 has collected significantly more sodium compared to the other runs. This most likely reason is that impurity agglomerates are released from the first bed and thus collecting to the second bed. The EDS mapping done from the extrudates of first guard bed of the low temperature run shows that the extrudates have sodium all over the surface of the extrudate.

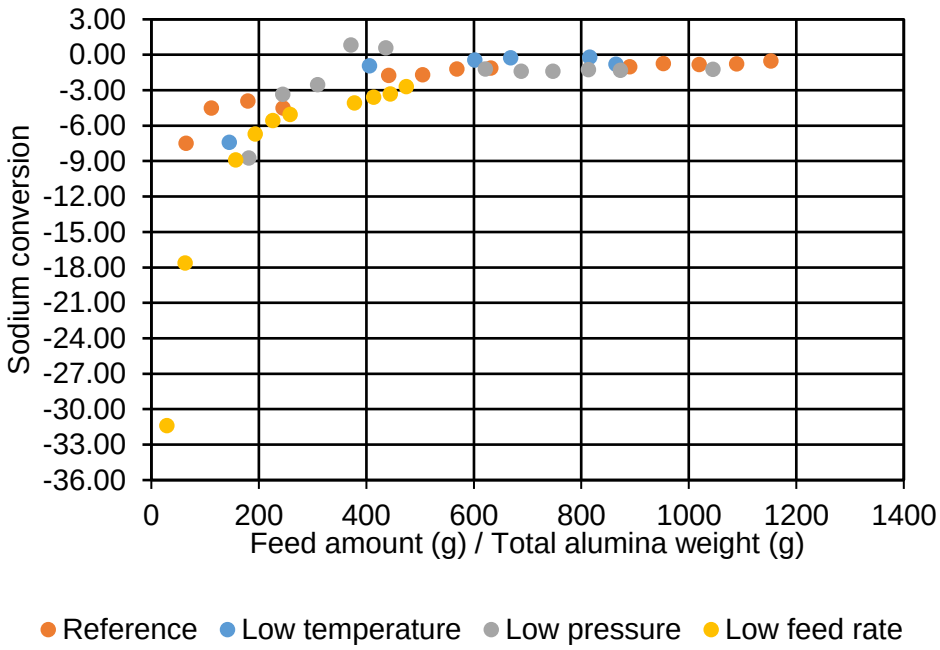

Figure 51. Conversion of sodium in the reference test run (T = 230 °C, P = 50 bar and LHSV = 1.2 h^{-1}), low temperature test run (T = 130 °C, P = 50 bar and LHSV = 1.2 h^{-1}), low pressure test run (T = 230 °C, P = 10 bar and LHSV = 1.2 h^{-1}) and low feed rate test run (T = 230 °C, P = 50 bar and LHSV = 0.6 h^{-1}).

Table 23. Mass balance calculations and the ratio between the amounts of sodium captured by the alumina and mass balance for sodium in all of the phosphorus removal test runs.

Test run	Total amount in / mg	Total amount in products / mg	Mass balance / mg	Increase on alumina / mg	Overall removal / mg/mg	Removed by alumina / mg/mg
Reference	2.35	6.50	-4.15	-0.04	-1.77	0.01
Low temperature	1.84	5.01	-3.17	0.13	-1.73	-0.04
Low pressure	2.18	7.49	-5.30	-0.03	-2.43	0.01
Low LHSV	1.01	8.61	-7.61	0.16	-7.54	-0.02

4.2.2.6 Calcium removal

Figure 52 shows the ICP-MS results of the calcium content in the liquid product samples and Table 25 lists the calculated mass balances. As the conversion is in the first samples close to zero and negative in the low feed rate samples, leaching could have occurred during all test runs. The calcium content on the spent alumina extrudates is in all test runs negative meaning the products contained more calcium than the feed. The calcium might be leached similar to aluminium, sodium and iron by the organic acids in the feed. The *sudden conversion decrease* can be observed in all test runs except in the low feed rate test run. As the phenomenon affects the calcium content, it could be that the calcium is mostly removed by the formation of agglomerates.

The low temperature test run seemingly has the highest calcium removal (0.84). The *sudden conversion decrease* has the least impact in the low temperature test run which is seen in the last two samples where the conversion decreases about 0.1 (Figure 52). This phenomena has also been observed with other impurities in the same test run. The reason for this could be that leaching occurs less at lower temperature as the aluminium ICP-MS results indicate.

The alumina uptake of calcium in the low temperature run is negative for all product samples. Despite the leaching some amount of calcium could be removed by ion-exchange with the acid sites of alumina.

The trend of the calcium conversion in the low pressure test run is similar as in the other test runs the *sudden conversion decrease* affects. After the typical conversion increase from negative to positive caused by the decreasing leaching, the

conversion increases as the calcium particulates are collected to the reactor bed. Then the *sudden conversion decrease* occurs. The calcium has been leached from the alumina nearly to the same extent as in the reference test run, according to the fraction removed by the alumina results.

The lower feed rate enhanced leaching of calcium from the reactor bed which causes the mass balance to be negative. At the end of the low feed rate test run the conversion progression seems to reach the same level as in the reference. It could be that feed rate has no impact on the calcium removal from the feed or the effect is overlapped by the leaching.

According to the EDS analysis of the surface of the spent alumina extrudates from the low temperature and low pressure test runs the content of calcium is very small on the surface of alumina. EDS mapping identifies a small amount of calcium on the extrudates.

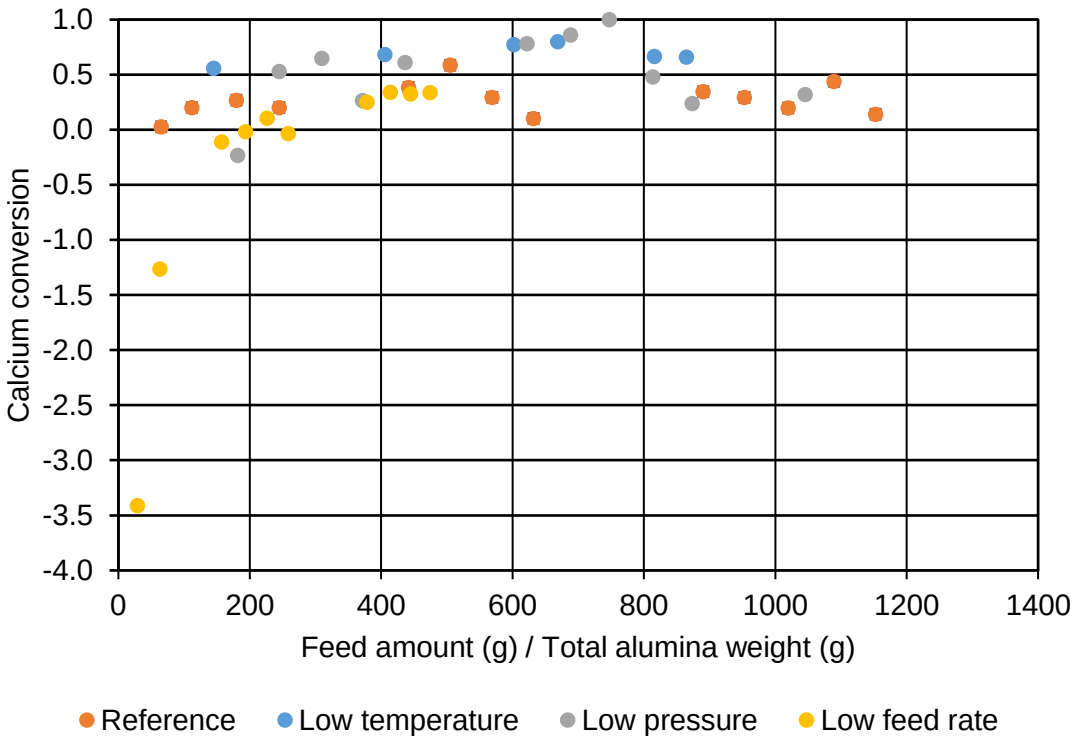

Figure 52. Conversion of calcium in the reference test run (T = 230 °C, P = 50 bar and LHSV = 1.2 h^{-1}), low temperature test run (T = 130 °C, P = 50 bar and LHSV = 1.2 h^{-1}), low pressure test run (T = 230 °C, P = 10 bar and LHSV = 1.2 h^{-1}) and low feed rate test run (T = 230 °C, P = 50 bar and LHSV = 0.6 h^{-1}).

Table 24. Mass balance calculations and the ratio between the amounts of calcium captured by the alumina and mass balance for iron in all of the phosphorus removal test runs.

Test run	Total amount in / mg	Total amount in products / mg	Mass balance / mg	Increase on alumina / mg	Overall removal / mg/mg	Removed by alumina / mg/mg
Reference	0.53	0.36	0.16	-0.05	0.31	-0.29
Low temperature	0.41	0.07	0.34	-0.05	0.84	-0.15
Low pressure	0.49	0.27	0.22	-0.06	0.44	-0.26
Low LHSV	0.23	0.26	-0.03	-0.03	-0.14	0.80

4.2.2.7 Iron removal

The conversion of iron calculated from the ICP-MS results (Figure 53) has progressed in a similar manner as in the reference run, meaning first the conversion increases and then it drops in the middle of the test run. This behaviour causes the mass balances of the reference and the low pressure test run to be very small (Table 25). The *sudden the conversion* decrease is the most probable explanation for this. Additionally, leaching of iron seems to occur during the test run. This has been already discussed in the mass balance section. The increasing conversion at the beginning of reference, low pressure and low feed rate test runs is typically seen with leaching of other impurities in silicon removal test runs (Section 4.3.1.1.1). The iron content in the feed is quite high compared to other impurities except the silicon and sodium which is why the effect of leaching on the liquid sample results is quite small.

The highest iron removal has been achieved in the low temperature test run (0.84). The reason for this could be that the lower temperature has decreased the solubility of the iron containing compounds in the feed which have subsequently been captured by the reactor bed. The other reason for the higher conversion of iron could be that iron has been leached less at lower temperature which has also been shown in the ICP-MS aluminium results. The iron collection by alumina is not remarkable at lower temperature implying a negative impact of the lower temperature on the adsorption of iron on alumina. This could be because leaching occurs mostly in the upper guard beds as the ratio between upper and lower beds was 0.07.

As in the case of phosphorus in the low pressure test run, the ICP-MS results of iron at lower pressure are the most affected by the *sudden conversion decrease* compared to the other reaction conditions. At first, the iron conversion follows a similar trend than in the reference run. The conversion of iron has increased to a higher level than the reference before the *sudden conversion decrease* occurs most likely initiated by same reasons as with phosphorus meaning decreasing void fraction increased the removal of even smaller particulates. The *sudden conversion decrease* seems to occur quicker in the reference test run than in the lower pressure test run. After this decrease, the conversion appears to increase once again. Despite the *sudden conversion decrease,* it might be that the pressure does not affect the calcium removal as they follow very similar trend.

The low feed rate results show a higher initial leaching of iron compared to the other test runs. Despite this, the smaller feed rate has increased the amount of iron captured on alumina compared to the reference run. Otherwise the iron removal seems to have a similar trend as in the case of the reference run. The slower feed rate might favour precipitation followed by a collection of iron containing precipitates in the reactor bed. Thus, the amount of iron increased in the alumina like in the low temperature.

The EDS analysis of the surface of the first, second and fourth guard beds of extrudates of the low temperature and the low pressure test runs suggest that the iron content is nearly equal in all of the guard beds layers. This iron content is similar to the alumina found on the reference test run. In the low pressure test run, guard bed 2 contains much more iron compared to the other beds. This is similar with the behaviour of other impurities in the low pressure test run. The reason could be that the collected precipitates in the first bed have been released and large portions of them have been captured by the second bed. EDS mapping shows that the alumina contains a small amount of iron that is distributed all around the cross-section of the extrudates.

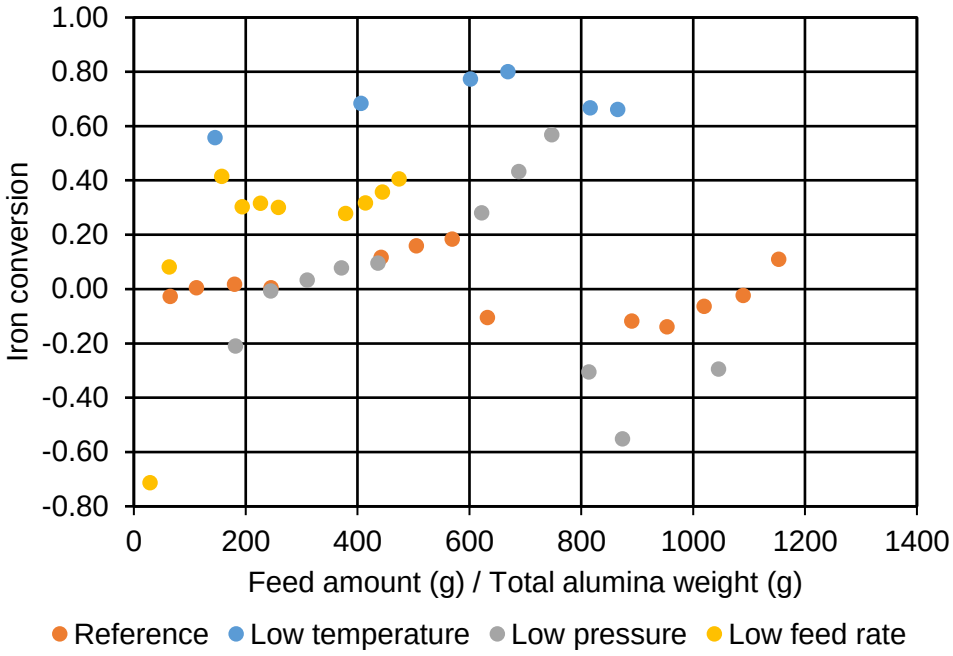

Figure 53. Conversion of iron in the reference test run (T = 230 °C, P = 50 bar and LHSV = 1.2 h^{-1}), low temperature test run (T = 130 °C, P = 50 bar and LHSV = 1.2 h^{-1}), low pressure test run (T = 230 °C, P = 10 bar and LHSV = 1.2 h^{-1}) and low feed rate test run (T = 230 °C, P = 50 bar and LHSV = 0.6 h^{-1}).

Table 25. Mass balance calculations and the ratio between the amounts of iron captured by the alumina and mass balance for iron in all of the phosphorus removal test runs.

Test run	Total amount in / mg	Total amount in products / mg	Mass balance / mg	Increase on alumina / mg	Overall removal / mg/mg	Removed by alumina / mg/mg
Reference	6.51	6.50	0.01	0.18	0.00	26.92
Low temperature	5.10	1.59	3.51	0.01	0.69	0.00
Low pressure	6.05	6.12	-0.07	0.14	-0.01	-2.16
Low LHSV	2.80	2.04	0.76	0.14	0.27	0.19

4.2.3 Suggestions for further silicon removal test runs

In this section suggestions for the future silicon removal test runs are presented. As it was observed during the silicon removal test runs, a large amount of impurities were leached from alumina and possibly SiC. This affected both results of ICP-MS

and XRF of sodium, iron and calcium. Leaching not only increased the amount of these impurities in the products, it also hides some of the behaviour of the impurity removal in the test runs. This makes it difficult to interpret which process effects are condition based and which are caused by the leaching. Due to the leaching, future test runs should be conducted using more leaching resistant materials such as alumina-silica because pure alumina seems unfit to handle the high TAN value of the feeds. In the following subsections, additional suggestions are provided.

4.2.3.1 Pre-washing of the reactor bed and the pre-treatment of the feed

Pre-washing the reactor bed before the start of the test run with hydrocarbon feed, such as non-paraffinic oil, might mitigate some initial leaching in the first products. This could be tested before starting the continuation test runs. As the acidity of the feed is high, a pre-wash might also be non-effective. In this case, the feed could be pre-treated by dilution which would decrease its acidity. An unfortunate effect of this is the decreased impurity content in the feed. The silicon content could be increased in the diluted feed by adding polydimethylsiloxane (PDMS) as model compounds, however it is not certain what kind of silicon containing compounds are finally present in the feed. Consequently, the results of the experiments might not be that comparable to the results in this thesis or to the behaviour of the real feed without the spiking agent.

4.2.3.2 Suggested reactor packing

As stated above, more leaching resistant guard material should be used in the continuation test runs. This why it is suggested that future test runs should focus on the study of different guard materials. The reactor packing could be the same as used in this thesis. However some small changes could be made to improve the packing. The amount of beds could be decreased to three as the beds in the silicon removal test run did not contain enough material for the XRF without combining the beds. More guard material could be then be added to each bed. The reactor bed has not been in the isothermal zone in the silicon removal test runs. Thus using the three beds would enable the placement of all guard beds in the isothermal region. The suggested reactor packing can be seen in Figure 54.

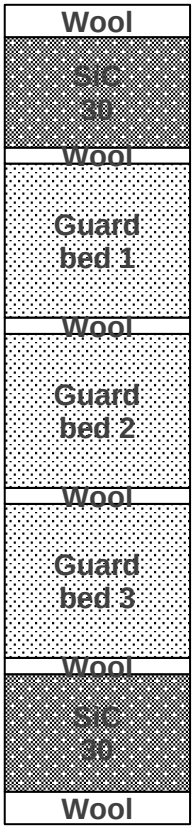

Figure 54. Suggestion for the reactor packing.

4.2.3.3 Suggested test run conditions

Lowering the temperature increases the apparent removal of silicon but lowers the removal of the phosphorus. Form the ICP-MS results for the alumina it could be seen that the leaching occurred less in low temperature (130 °C), which is why it would be recommended to use this temperature in future test runs. Pressure did not seem to have a high impact on the removal of impurities or the leaching when compared to the reference. The lower pressure, however, has the highest impact regarding the *sudden conversion decrease* phenomenon. This might have been caused by pressure or by some other run specific issues. Therefore the lower pressure could be used in following runs to clarify which one it was. A lower pressure would also be more attractive for industrial applications. Low LHSV increased the leaching of the reactor bed, which is why using this feed flow rate runs is not recommended for future testing. The lower feed rate would also require longer time on stream to see the effect on the impurity removal which is why it is not time efficient. Once the sufficient guard material has been determined, test run with

higher LHSV could be done to see how the silicon removal improves versus the leaching.

5 CONCLUSIONS

The purpose of this thesis was to acquire new information of the utilization of guard beds to remove phosphorus, silicon and metal impurities from renewable feedstocks and also to give recommendations for the further research on the subject. This section induces conclusions for the test runs with the phosphorus rich and silicon rich feed.

5.1 Phosphorus rich feed test runs

The majority of phosphorus is removed by formation of phosphate salts with counter cations meaning the alkali and alkaline earth metals in the feed. The formed salt precipitate was collected in the reactor bed. In line with that the conversion of phosphorus is highest if only SiC is loaded into the reactor and only small amounts of phosphorus have been detected on the spent alumina of the various test runs. It was further found that a lower temperature (325 °C) decreases the phosphorus conversion (0.88 → 0.74). Decreasing the feed flow rate, enhances the thermal removal of the phosphorus by a small amount. Potassium has a high affinity to form salts with phosphorus as most of it is removed from the feed in all test runs and conditions. However, the dependence on the reaction conditions is the same as for phosphorus. Sodium, iron and calcium are leached from the reactor bed by the free fatty acids in the feed. Their content in the liquid products at the start of test runs is high before it decreases and gets stable with the time of stream. The leaching increases as feed flow rate decreases. Volatile silicon containing compounds are formed above 325 °C by the decomposition of PDMS. Moreover, silicon is probably also leached from SiC.

Lowering the pressure does not have any significant impact on the removal of the impurities compared to the reference however it seemed that adsorption of the phosphorus on alumina increased by a small amount.

In future test runs, passivation of the alumina and SiC should be carried out prior to the test run by pre-washing of the reactor beds to avoid or at least mitigate leaching. If the goal of continuation run is the research of the maximal removal of phosphorus of certain materials a reactor packing with layers of size graded SiC

and a single alumina layer could be used. Moreover, it should be ensured that all guard layers are placed within the isothermal zone of the reactor.

5.2 Silicon rich feed test runs

Leaching of alumina occurred with the silicon rich feed by acid compounds in all test runs. Silicon seems to be removed by decomposition of silicon containing compounds into volatile compounds as the content of silicon on the spent alumina is low. However, adsorption of silicon on alumina cannot be excluded as silicon is already present in the fresh alumina and the semi-quantitative XRF analysis might not be able to reveal that. Sodium, calcium and iron are leached from the reactor bed whereas phosphorus and potassium are again removed via salt formation. The alkaline and alkaline earth metal cations may have also formed salts with the carboxylates derived from the feed acids besides the phosphates.

The phenomenon *sudden conversion decrease* is observed in all silicon removal test runs. This phenomenon describes a sudden drop of the conversion of impurities in the middle of the test run after a linear increase of the conversion. The reasons for this might be related to the feed rate as the phenomenon occurred close to the feed addition. Another reasons could be the migration of collected agglomerates from the reactor bed to the liquid.

The removal of silicon is favoured at lower temperature (130 °C). Decreased leaching of silicon from the reactor bed might be an explanation for this. This could also explain the higher conversion of the other impurities. Pressure does not seem to have a significant impact, however it seems to affect the *sudden conversion decrease* phenomenon more than the other reaction conditions. A lower feed rate increases leaching of silicon and the metals resulting in lower conversion. Despite the increased leaching a higher amount of silicon was detected on the spent alumina indicating removal of silicon via adsorption.

As the alumina used in the test runs could not withstand the acidity of the feed, the further research should be about the testing of other guard materials. The guard beds should be placed in the isothermal zone. Leaching of the reactor bed could be mitigated by pre-washing of the reactor bed and dilution of the feed to decrease its acidity. A lower temperature (130 °C) should be used in future test runs for a

minor effect of leaching. But the feed rate should not be lowered as it would increase leaching and be less time efficient. Higher feed rate could be studied after guard material test runs.

6 REFERENCES

[1] Jering A., Günther J., Raschka A., Carus M., Piotrowski S., Scholz L. Use of renewable raw materials with special emphasis on chemical industry. Copenhagen: European Topic Centre on Sustainable Consumption and Production; 2010. Report no.: ETC/SCP report 1/ 2010.

[2] Verdier S., Alkilde OF., Gabrielsen J., Grubb M. Hydroprocessing of renewable feedstocks - challenges and solutions. Copenhagen: Haldor Topsoe A/S; 2019.

[3] Perez M., Cenni R., Maroun Z., Myntman K. Avoiding unplanned reactor shutdowns. Copenhagen: Haldor Topsoe A/S; 2019.

[4] Ancheyta J. Deactivation of Heavy Oil Hydroprocessing Catalysts: Fundamentals and Modeling. New Jersey: John Wiley & Sons; 2016.

[5] Bartholomew C.H., Farrauto R.J. Fundamentals of industrial catalytic processes. New Jersey: John Wiley & Sons; 2006.

[6] Schmidt F. The Importance of Catalysis in the Chemical and Non-Chemical Industries. In: Baerns M., Castleman A.W., Schafer F.P., Toennies J.P., Zinth W. Basic Principles in Applied Catalysis. New York: Springer-Verlag Berlin Heidelberg; 2004. p. 5–15

[7] Chorkendorffand I., Niemantsverdriet J.W. Concepts of modern catalysis and kinetics. 3rd ed. Weinheim: Wiley-VCH; 2017.

[8] Hagen J. Industrial Catalysis: A Practical Approach. 3rd ed. Weinheim: Wiley-VCH; 2015.

[9] Rothenberg G. Catalysis: Concepts and Green Applications. 2nd ed. Weinheim: Wiley-VCH; 2008.

[10] Ertl G., Knözinger H., Weitkamp J. Handbook of Heterogeneous Catalysis, Volume 1. Weinheim: Wiley-VCH; 1997.

[11] Kakaei K., Esrafili M.D., Ehsani A. Introduction to Catalysis [Internet]. Interface Science and Technology. 2019; 27: p. 1 – 21. DOI: 10.1016/B978-0-12-814523-4.00001-0.

[12] Dutta B.K. Principles of mass transfer and separation processes. New Delhi: PHI Learning; 2007.

[13] Fogler H.S. Elements of chemical reaction engineering. 5th ed. Boston: Prentice Hall; 2016.

[14] Foo K.Y., Hameed B.H. Insights into the modeling of adsorption isotherm systems [Internet]. Chemical Engineering Journal. 2010; 156(1): p. 2 – 10 DOI: 10.1016/j.cej.2009.09.013.

[15] Ertl G., Knözinger H., Weitkamp J. Handbook of Heterogeneous Catalysis, Volume 3. Weinheim: Wiley-VCH; 1997.

[16] Forzatti P., Lietti L. Catalyst deactivation [Internet]. Catalysis Today. 1999; 52(2): p. 165 – 181. DOI: 10.3390/catal5010145.

[17] Argyle M., Bartholomew C. Heterogeneous Catalyst Deactivation and Regeneration: A Review [Internet]. Catalysts. 2015; 5(1): p. 145 – 269. DOI: 10.3390/catal5010145.

[18] Lange J.P. Renewable feedstocks: the problem of catalyst deactivation and its mitigation [internet]. Angewandte Chemie (international edition). 2015; 54(45); p. 13186 – 13197. DOI: 10.1002/anie.201503595.

[19] Rase H.F. Fixed-Bed Reactor Design and Diagnostics: Gas-Phase Reactions. Stoneham: Butterworth Publishers; 1990.

[20] Mayo S. Maximize hydrotreating cycle length with guard-bed and liquid distribution technology. Hart's Fuel Technology & Management. 1998; 8(8): p. 51 – 56.

[21] Ancheyta J., Speight J.G. Hydroprocessing of Heavy Oils and Residua. Boca Raton: CRC Press; 2007.

[22] Speight J.G. Fouling in Refineries. 1st ed. Waltham: Gulf Professional Publishing; 2015.

[23] Minderhoud J.K., van Veen J.A.R., Hagan A.P. Hydrocracking in the Year 2000: A strong interaction between technology development and market requirements. Studies in Surface Science and Catalysis. 1999; 127: p. 3 – 20.

[24] Bartholdy J. Haldor Topsoe A/S. Void grading. US Patent. 5368722. 1994-11-29.

[25] Trueba M., Trasatti S.P. γ-Alumina as a Support for Catalysts: A Review of Fundamental Aspects [Internet]. European Journal of Inorganic Chemistry. 2005; 2005(17): p. 3393 – 3403. DOI: 10.1002/0471238961.0103200916050118.a01.

[26] Pearson, A. Aluminum Oxide (Alumina), Activated [Internet]. In Kirk-Othmer Encyclopedia of Chemical Technology. 2003. DOI: 10.1002/0471238961.0103200916050118.a01.pub2.

[27] Busca G. The surface acidity of solid oxides and its characterization by IR spectroscopic methods. An attempt at systematization. Physical Chemistry Chemical Physics. 1999; 1(5): p. 723 – 736. DOI: 10.1039/a808366e.

[28] Mukherjee S., Ghosh B. The Science of Clays Applications in Industry, Engineering and Environment. New Delhi: Capital Publishing Company; 2013.

[29] Lagaly G., Bergaya F. Handbook of Clay Science. Volume 5. London: Elsevier; 2013.

[30] O'Brien R.D., Farr W.E., Wan P.J. Introduction to fats and oils technology. 2nd ed. Champaign: AOCS Press; 2000.

[31] Siegel J., Olsen C. Feed Contaminants in Hydroprocessing Units. Colmbia: Catalagram. 2012: 112; 2008.

[32] Takahashi T., Higashi H., Kai T. Development of a new hydrodemetallization catalyst for deep desulfurization of atmospheric residue and the effect of reaction temperature on catalyst de-activation. Catalysis Today 2005: 104(1): p. 76 – 85. DOI: 10.1016/j.cattod.2005.03.025.

[33] Cash D., Trimble H. Chevron USA. Fixed bed reactor assembly having a guard catalyst bed. US Patent. 5879642A. 1996-4-24

[34] Pérez M.J.R. Grading is great – overgrading is not [Internet]. 2019. Available at: https://blog.topsoe.com/grading-is-great-overgrading-is-not. Accessed: 24.1.2020.

[35] Furimsky E., Massoth FE. Deactivation of hydroprocessing catalysts. Catalysis Today. 1999; 52(4): p. 381 – 495. DOI: 10.1016/S0920-5861(99)00096-6.

[36] Shaban HI., Khan AR. Pressure-related operational problems and their remedies in hydrotreating reactors in petroleum refineries. Journal of Petroleum Science and Engineering. 1995; 14(1): p. 79 – 88. DOI: 10.1016/0920-4105(95)00030-5.

[37] Hung C., Reynolds B. Chevron Research and Technology. Graded catalyst system for removal of calcium and sodium from a hydrocarbon feedstock. US Patent. 4830736. 1989-5-16.

[38] Morel F., Kressmann S., Harlé V., Kasztelan S. Processes and catalysts for hydrocracking of heavy oil and residues. Studies in Surface Science

and Catalysis. 1997; 106: p. 1 – 16. DOI: 10.1016/S0167-2991(97)80003-1.

[39] Afandizadeh S., Foumeny E.A. Design of packed bed reactors: guides to catalyst shape, size, and loading selection. Applied Thermal Engineering. 2001; 21(6): p. 669 – 682. DOI: 10.1016/S1359-4311(00)00072-7.

[40] Haldor Topsoe A/S. Grading - your weapon against pressure drop build-up and catalyst poisons [Brochure]. Copenhagen: Haldor Topsoe A/S; 2018.

[41] Armstrong J., Hamrin J. The Renewable Energy Policy Manual. Washington, D.C.: United States Export Council for Renewable Energy; 1999.

[42] Hassan M.H., Kalam M.A. An Overview of Biofuel as a Renewable Energy Source. Procedia Engineering. 2013; 56: p. 39 – 53. DOI: 10.1016/j.proeng.2013.03.087.

[43] Morales A., de Agudelo MMR., Hernández F. Adsorption mechanism of phosphorus on alumina. Applied Catalysis. 1988; 41: p. 261 – 271. DOI: 10.1016/S0166-9834(00)80397-8.

[44] Kubička D., Horáček J. Deactivation of HDS catalysts in deoxygenation of vegetable oils. Applied Catalysis A, General. 2011; 394(1): p. 9 – 17. DOI: 10.1016/j.apcata.2010.10.034.

[45] Al-Sabawi M., Chen J. Hydroprocessing of Biomass-Derived Oils and Their Blends with Petroleum Feedstocks: A Review. Energy & Fuels. 2012; 26(9): p. 5373 – 5399. DOI: 10.1021/ef3006405.

[46] Catia Duarter Catalyst Deactivation. Amsterdam: Albemarle Hydroprocessing Course; 18.2.2020.

[47] Kanakraj S., Dixit S. A comprehensive review on degummed biodiesel. Biofuels 2016; 7(5): p. 537 – 548. DOI: 10.1080/17597269.2016.1168021.

[48] Dubreuil AC., Chainet F., Miguelde R., Bartolomeu S., Mota F.M.M., Janvier J., Lienemann CP. Understanding the impact of silicon compounds on metallic catalysts through experiments and multitechnical analysis. Comptes Rendus Chimie. 2017; 20(1): p. 55 – 66. DOI: 10.1016/j.crci.2016.05.020.

[49] Charles Olsen. The ART of Trapping Silicon and Arsenic. Chicago: Advanced refining technologies; 2012.

[50] Pérez-Romo P., Navarrete-Bolaños J., Aguilar-Barrera C., Angeles-Chavez C., Laredo G.C. Morphological and structural study of the Si deposition on the sulfided NiMo/γ-Al2O3 catalyst: Effect on the support. Applied Catalysis A, General. 2014; 485: p. 84 – 90. DOI: 10.1016/j.apcata.2014.07.038

[51] Chainet F., Meur L.L., Lienemann C., Ponthus J., Courtiade M., Donard O.F.X. Characterization of silicon species issued from PDMS degradation under thermal cracking of hydrocarbons: Part 1 – Gas samples analysis by gas chromatography-time of flight mass spectrometry. Fuel. 2013;111: p. 519 – 527. DOI: 10.1016/j.fuel.2013.03.046.

[52] Nadeina K.A., Kazakov M.O., Kovalskaya A.A., Danilevich V.V., Klimov O.V., Danilova I.G., et al. Guard bed catalysts for silicon removal during hydrotreating of middle distillates. Catalysis Today. 2019; 329: p. 53 – 62. DOI: 10.1016/j.cattod.2018.11.075.

[53] Koval'skaya A., Kazakov M., Nadeina K., Klimov O., Deliy I., Noskov A. Effect of Composition and Texture Characteristics of NiMo/Al2O3 Guard-Bed Catalysts on Silicon Removal from Diesel Fractions. Petroleum Chemistry. 2017; 57(12): p. 1165 – 1168. DOI: 10.1134/S0965544117060196.

[54] Iglesias J., Melero J.A., Bautista L.F., Morales G., Sánchez-Vázquez R. Continuous production of biodiesel from low grade feedstock in presence of Zr-SBA-15: Catalyst performance and resistance against deactivation. Catalysis Today. 2014; 234: p. 174 – 181. DOI: 10.1016/j.cattod.2014.01.004.

[55] Kokayeff P., Zink S., Roxas P. Hydrotreating in Petroleum Processing. In: Treese S., Jones D., Pujado P. Handbook of Petroleum Processing: 2nd ed. Dordrecht: Springer International Publishing; 2015. p. 361 – 434.

[56] Seader J.D., Henley E.J., Roper D.K. Separation process principles. 3rd ed. Hoboken: John Wiley & Sons; 2011.

[57] Harri Hallinen. Phenomena and mechanisms in purification of animal fat [Master's Thesis]. Lappeenranta: Lappeenranta University of Technology; 2014.

[58] Haas M.J. Improving the economics of biodiesel production through the use of low value lipids as feedstocks: vegetable oil soapstock. Fuel processing technology. 2005; 86(10): p. 1087 – 1096. DOI: 10.1016/j.fuproc.2004.11.004.

[59] Al-Sabawi M., Chen J. Hydroprocessing of Biomass-Derived Oils and Their Blends with Petroleum Feedstocks: A Review. Energy & Fuels. 2012; 26(9): p. 5373 – 5399. DOI: 10.1021/ef3006405.

Appendix 1: Characterization of the fresh γ-alumina

Table 1. XRF results of the fresh γ-alumina.

Sample name		γ-Alumina
Sodium, (XRF)	mg/kg	<220
Magnesium, (XRF)	mg/kg	<200
Aluminium, (XRF)	mg/kg	500000
Silicon, (XRF)	mg/kg	400
Phosphorus, (XRF)	mg/kg	88
Chlorine, (XRF)	mg/kg	210
Potassium, (XRF)	mg/kg	<50
Calcium, (XRF)	mg/kg	98
Titanium, (XRF)	mg/kg	<120
Vanadium, (XRF)	mg/kg	<90
Chromium, (XRF)	mg/kg	<30
Manganese, (XRF)	mg/kg	<50
Iron, (XRF)	mg/kg	89
Cobolt, (XRF)	mg/kg	<50
Nickel, (XRF)	mg/kg	28
Copper, (XRF)	mg/kg	<20
Zinc, (XRF)	mg/kg	79
Gallium, (XRF)	mg/kg	55
Arsenic, (XRF)	mg/kg	<20
Selenium, (XRF)	mg/kg	<20
Bromine, (XRF)	mg/kg	<100
Molybdenum, (XRF)	mg/kg	<450
Tungsten, (XRF)	mg/kg	<120

Appendix 1: Characterization of the fresh γ-alumina

Table 2. Characterization results of the fresh γ-alumina.

Sample name		γ-Alumina
BET-surface area	m2/g	252.50
Micropore area	m2/g	5.94
External surface area	m2/g	242.30
BJH desorption surface area of pores (Cumul.)	m2/g	359.40
Pore voulume	cm3/g	0.85
Micropore volume	cm3/g	0.00
Average pore diameter 4 V/A	Å	133.92
BJH average pore diameter	Å	99.44
Aluminum (EDS)	wt-%	43.00
Silicon (EDS)	wt-%	0.14
Phosphorus (EDS)	wt-%	0.36
Carbon	wt-%	0.05
Sulphur	wt-%	0.02
Apparent bulk density of catalysts	g/cm3	0.44

Appendix 2: Guard bed contents in the test runs

Table 1. Content of the guard beds in test runs with the phosphorus rich feed.

		Reference	Reaction condition 1	Reaction condition 2	Reaction condition 3
Total	Alumina / g	10.0255	10.0494	10.004	10.0058
	SiC16 / g	34.3903	35.0263	34.1511	34.1572
Bed 1	Alumina / g	2.5051	2.5004	2.5021	2.5074
	SiC16 / g	8.5969	8.7597	8.5378	8.5372
	SiC100 / g	3.0266	3.0003	3.0073	3.0050
Bed 2	Alumina / g	2.5065	2.5054	2.5064	2.5034
	SiC16 / g	8.5969	8.7579	8.5366	8.5355
	SiC100 / g	3.0588	3.0011	3.0063	3.0015
Bed 3	Alumina / g	2.4922	2.5067	2.5035	2.5080
	SiC16 / g	8.6041	8.7599	8.5391	8.5362
	SiC100 / g	3.009	3.0072	3.0097	3.0069
Bed 4	Alumina / g	2.495	2.5697	2.4974	2.5001
	SiC16 / g	8.5788	8.745	8.5322	8.5204
	SiC100 / g	3.0167	3.0075	3.0167	3.0041

Table 2. Content of the guard bed in test runs with the silicon rich feed.

		Reference	Reaction condition 1	Reaction condition 2	Reaction condition 3
Total	Alumina / g	10.0162	10.0024	10.0014	10.0089
	SiC16 / g	34.4309	34.3218	34.8132	34.4643
Bed 1	Alumina / g	2.5158	2.5019	2.5018	2.5011
	SiC16 / g	8.6077	8.5815	8.7015	8.6215
	SiC100 / g	3.0158	3.0772	3.0067	3.0184
Bed 2	Alumina / g	2.5061	2.5021	2.5017	2.5042
	SiC16 / g	8.6062	8.5805	8.704	8.6237
	SiC100 / g	3.0168	3.0422	3.0697	3.0091
Bed 3	Alumina / g	2.5073	2.5012	2.5097	2.5064
	SiC16 / g	8.6082	8.5807	8.7049	8.62.27
	SiC100 / g	3.0031	3.0276	3.0309	3.0004
Bed 4	Alumina / g	2.4977	2.5053	2.4954	2.5070
	SiC16 / g	8.5981	8.58	8.6966	8.6208
	SiC100 / g	3.0027	3.0373	3.0219	3.0076

Appendix 3: Analysis results for the liquid products from the reference phosphorus removal test run

Table 1. Liquid product analysis results (1/2).

Sample name		Refer-ence P1	Refer-ence P2	Refer-ence P3	Refer-ence P4	Refer-ence P5	Refer-ence P6	Refer-ence P7	Refer-ence P8	Refer-ence P9
Density at 50 °C	kg/m3	890.04	890.35	890.43	890.49	890.55	890.58	890.62	890.67	890.63
Bromine Number	g Br/100 g				31.424				31.006	
Total nitrogen	mg/kg	151.975	153.665	153.201	152.223	152.41	152.571	155.557	156.914	155.388
Sodium (ICP-MS)	mg/kg	14.45	6.06	4.73	4.143	3.4	3.211	3.3	3.319	3.089
Magnesium (ICP-MS)	mg/kg	0.0579	0.0339	0.0337	0.0293	0.0278	0.0229	0.022	0.00459	0.00257
Silicon (ICP-MS)	mg/kg	0.306	0.345	0.353	0.349	0.407	0.427	0.409	0.37	0.389
Phosphorus (ICP-MS)	mg/kg	1.218	1.37	1.187	1.227	1.11	0.905	0.868	0.842	0.756
Potassium (ICP-MS)	mg/kg	0.201	0.105	0.188	0.0681	0.19	0.129	0.098	0.106	0.097
Calcium (ICP-MS)	mg/kg	0.353	0.285	0.248	0.238	0.157	0.2623	0.166	0.147	0.252
Iron (ICP-MS)	mg/kg	1.55	0.518	0.385	0.307	0.248	0.179	0.177	0.158	0.139
Sulphur, MWDXRF	mg/kg	11.36	11.28	10.92	11.88	11.34	11.32	11.01	11.66	11.35
Total chlorides	mg/kg	6.35	6.725	6.725	6.66	6.545	6.655	6.565	6.45	6.495
Total Acid Number (TAN)	mg KOH/g	18.33	16.19	15.45		14	13.7	13.6	13.4	13.3

Appendix 3: Analysis results for the liquid products from the reference phosphorus removal test run

Table 1. Liquid product analysis results (2/2).

Sample name		Refer-ence P9	Refer-ence P10	Refer-ence P11	Refer-ence P12	Refer-ence P13	Refer-ence P14
Density at 50 °C	kg/m3	890.63	890.58	890.69	890.72	890.73	890.65
Bromine Number	g Br/100 g				31.988		
Total nitrogen	mg/kg	155.388	155.965	155.451	155.775	155.456	156.307
Sodium (ICP-MS)	mg/kg	3.089	2.89	2.849	2.83	3.015	3.069
Magnesium (ICP-MS)	mg/kg	0.00257	0.0107	0.00303	0.00354	0	0.00578
Silicon (ICP-MS)	mg/kg	0.389	0.427	0.41	0.399	0.371	0.272
Phosphorus (ICP-MS)	mg/kg	0.756	0.826	0.692	0.691	0.663	0.632
Potassium (ICP-MS)	mg/kg	0.097	0.121	0.092	0.147	0.0637	0.0783
Calcium (ICP-MS)	mg/kg	0.252	0.389	0.116	0.193	0.162	0.377
Iron (ICP-MS)	mg/kg	0.139	0.144	0.122	0.127	0.122	0.142
Sulphur, MWDXRF	mg/kg	11.35	12.77	11.51	11.92	11.98	11.77
Total chlorides	mg/kg	6.495	6.72	7.005	6.675	6.53	6.585
Total Acid Number (TAN)	mg KOH/g	13.3	13.1	13	13	12.8	15.33

Appendix 4: Analysis results for the liquid products from the condition change phosphorus removal test runs

Table 1. Liquid product analysis results of low temperature test run.

Sample name		Low temperature P1	Low temperature P2	Low temperature P3	Low temperature P4	Low temperature P5	Low temperature P6	Low temperature P7
Density at 50 °C	kg/m3	891.05	891.06	891.05	891.04	891.04	891.06	891.04
Total nitrogen	mg/kg	155.416	155.428	156.226	155.566	155.718	157.594	157.494
Sodium (ICP-MS)	mg/kg	7.64	4.912	4.317	4.068	3.257	3.267	2.97
Magnesium (ICP-MS)	mg/kg	0.05459	0.0304	0.0238	0.0266	0.018	0.0256	0.0236
Silicon (ICP-MS)	mg/kg	0.528	0.4058	0.383	0.507	0.411	0.568	0.618
Phosphorus (ICP-MS)	mg/kg	1.652	1.707	1.73	1.772	1.623	2.161	2.59
Potassium (ICP-MS)	mg/kg	0.2	0.0786	0.0927	0.11	0.293	0.632	0.818
Calcium (ICP-MS)	mg/kg	0.444	0.321	0.344	0.2949	0.287	0.269	0.248
Iron (ICP-MS)	mg/kg	1.467	0.529	0.354	0.261	0.26	0.156	0.12
Sulphur, MWDXRF	mg/kg	12.93	13.66	14.37	13.97	14.52	15.57	15.39
Total chlorides	mg/kg	6.125	6.5	6.655	6.52	6.57	6.065	6.12
Total Acid Number (TAN)	mg KOH/g	12.66	13.77	13	13.64	12.82	13.22	13.15

Appendix 4: Analysis results for the liquid products from the condition change phosphorus removal test runs

Table 2. Liquid product analysis results of low pressure test run.

Sample name		Low pressure P1	Low pressure P2	Low pressure P3	Low pressure P4	Low pressure P5	Low pressure P6	Low pressure P7	Low pressure P8	Low pressure P9	Low pressure P10	Low pressure P11
Density at 50 °C	kg/m3	889.81	890.32	890.33	890.53	890.52	890.63	890.91	890.64	890.67	890.69	890.74
Total nitrogen	mg/kg	151.873	150.802	151.374	148.967	149.558	148.288	152.516	153.87	152.958	153.408	152.104
Sodium (ICP-MS)	mg/kg	13.93	6.013	5.645	5.39	3.495	3.23	3.06	2.739	2.403	2.518	2.33
Magnesium (ICP-MS)	mg/kg	0.045	0.0926	0.0284	0.0182	0.0186	0.01546	0.0132	0.00676	0.01089	0.01016	0.01968
Aluminium (ICP-MS)	mg/kg	23.94	0.107	5.94	4.474	3.213	2.206	1.23	1.064	1.252	1.184	1.1
Silicon (ICP-MS)	mg/kg	0.253	0.566	0.668	0.671	0.689	1.237	0.7125	0.6044	0.483	0.464	0.509
Phosphorus (ICP-MS)	mg/kg	1.149	8.074	1.691	1.623	1.204	1.098	1.397	1.548	1.039	0.929	0.742
Potassium (ICP-MS)	mg/kg	0.2946	4.055	0.343	0.2048	0.154	0.193	0	0	0	0	0.08686
Calcium (ICP-MS)	mg/kg	0.333	0.446	0.22	0.1946	0.142	0.131	0.192	0.1639	0.123	0.1259	0.129
Iron (ICP-MS)	mg/kg	1.423	0.116	0.508	0.395	0.307	0.243	0.1946	0.151	0.1256	0.1428	0.136
Sulphur, MWDXRF	mg/kg	11.08	12.16	12.48	12.19	11.47	11.89	12.75	8.99	11.58	11.64	11.5
Total chlorides	mg/kg	5.92	6.605	6.59	6.615	6.275	6.415	6.205	5.99	5.915	6.08	6.095
Total Acid Number (TAN)	mg KOH/g	20.71	17.39	18.66	14.88	15.28	14.18	12.03	12.54	11.68	12.47	12.47

Appendix 4: Analysis results for the liquid products from the condition change phosphorus removal test runs

Table 3. Liquid product analysis results of low feed rate test run.

Sample name		Low feed rate P1	Low feed rate P2	Low feed rate P3	Low feed rate P4	Low feed rate P5	Low feed rate P6	Low feed rate P7	Low feed rate P8	Low feed rate P9	Low feed rate P10
Density at 50 °C	kg/m3	889.72	889.99	890.22	890.31	890.36	890.39	890.39	890.44	890.48	890.08
Total nitrogen	mg/kg	146.069	146.701	147.357	146.981	145.946	146.335	146.119	145.587	144.828	144.459
Sodium (ICP-MS)	mg/kg	21.06	11.448	7.92	5.166	5.33	5.027	3.565	3.127	3.226	3.155
Magnesium (ICP-MS)	mg/kg	0.06482	0.034	0.01748	0.0188	0.02571	0.014	0.019748	0.01892	0.01438	0.009682
Aluminium (ICP-MS)	mg/kg	59.32	22.82	11.83	7.944	6.87	6.248	5.733	4.956	4.443	4.257
Silicon (ICP-MS)	mg/kg	0.1484	0.126	0.215	0.156	0.258	0.261	0.321719	0.321	0.352	0.358
Phosphorus (ICP-MS)	mg/kg	1.195	1.16	0.927	0.766	0.818	0.713	0.55269	0.437	0.457	0.506
Potassium (ICP-MS)	mg/kg	0.167	0.07489	0	0.107	0.047	0	0.1023	0.129	0.116	0.1545
Calcium (ICP-MS)	mg/kg	0.326	0.174	0.1086	0.06057	0.09056	0.04167	0.16	0.101	0.109	0.112
Iron (ICP-MS)	mg/kg	1.826	0.79	0.4789	0.348	0.31	0.287	0.24	0.224	0.203	0.187
Sulphur, MWDXRF	mg/kg	11.85	12.08	10.76	11.63	11.89	12.37	11.71	12.01	11.86	12.14
Total chlorides	mg/kg	5.98	6.51	7.225	6.47	6.62	6.59	5.745	6.29	6.42	6.395
Total Acid Number (TAN)	mg KOH/g	22.4	19	17.6	16.3	16.3	15.7	21.35	20.72	20.84	20.76

Appendix 5: XRD diffractograms of γ-alumina from phosphorus removal reference test run

Figure 1. Aluminium phosphates were detected on the surface of the spent γ-alumina in the extrudates from the first two guard beds.

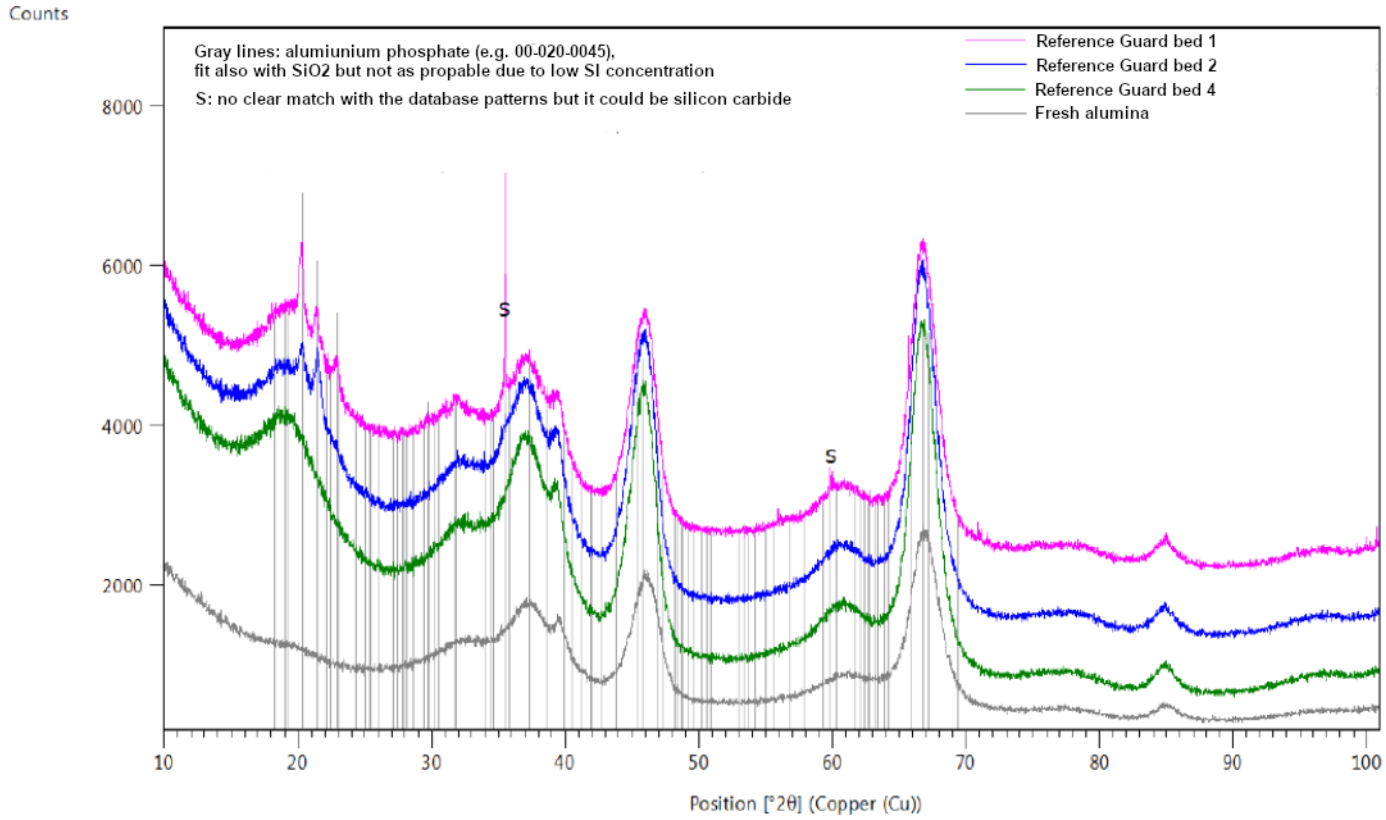

Appendix 6: EDS scan of the surface of spent γ-alumina in phosphorus removal test runs

Table 1. Content of different elements on the surface of spent alumina from reference, low temperature and low pressure test runs.

Sample name		Reference Guard bed 1	Reference bed 2	Reference bed 4	Low tempera-ture Guard bed 1	Low tem-pature Guard bed 2	Low tem-pature Guard bed 4	Low pressure Guard bed 1	Low pressure Guard bed 2	Low pressure Guard bed 4
Sodium (EDS)	wt-%	5.5	3.1	1.0	4.5	1.7	0.8	9.8	6.0	1.5
Aluminum (EDS)	wt-%	10.7	30.6	39.5	14.7	32.7	37.4	12.6	21.1	38.3
Silicon (EDS)	wt-%	5.0	0.3	0.8	8.9	0.3	0.5	3.5	0.4	0.3
Phosphorus (EDS)	wt-%	15.6	8.1	0.4	7.1	4.7	2.6	20.6	13.6	2.1
Sulfur (EDS)	wt-%	1.0	0.9	0.2	1.3	0.2	0.2	1.1	0.4	0.2
Potassium (EDS)	wt-%	4.3	1.2	0.0	3.2	1.4	0.9	6.7	1.8	0.3
Calcium (EDS)	wt-%	0.2	0.1	0.0	0.1	0.0	0.0	0.3	0.1	0.0
Titanium (EDS)	wt-%				0.2	0.0	0.1			
Vanadium (EDS)	wt-%				0.5					
Chromium (EDS)	wt-%						0.1			
Iron (EDS)	wt-%	0.1	0.0	0.0	0.1	0.1	0.2	0.2	0.1	0.0
Nickel (EDS)	wt-%						0.2			

Appendix 7: EDS MAP of extrudates from phosphorus removal reference test run

Figure 1. Content of potassium, sulphur and sodium on the surface of γ-alumina extrudate marked with purple, yellow and red respectively. Calcium content on the impurity layer on the surface of extrudates marked with blue.

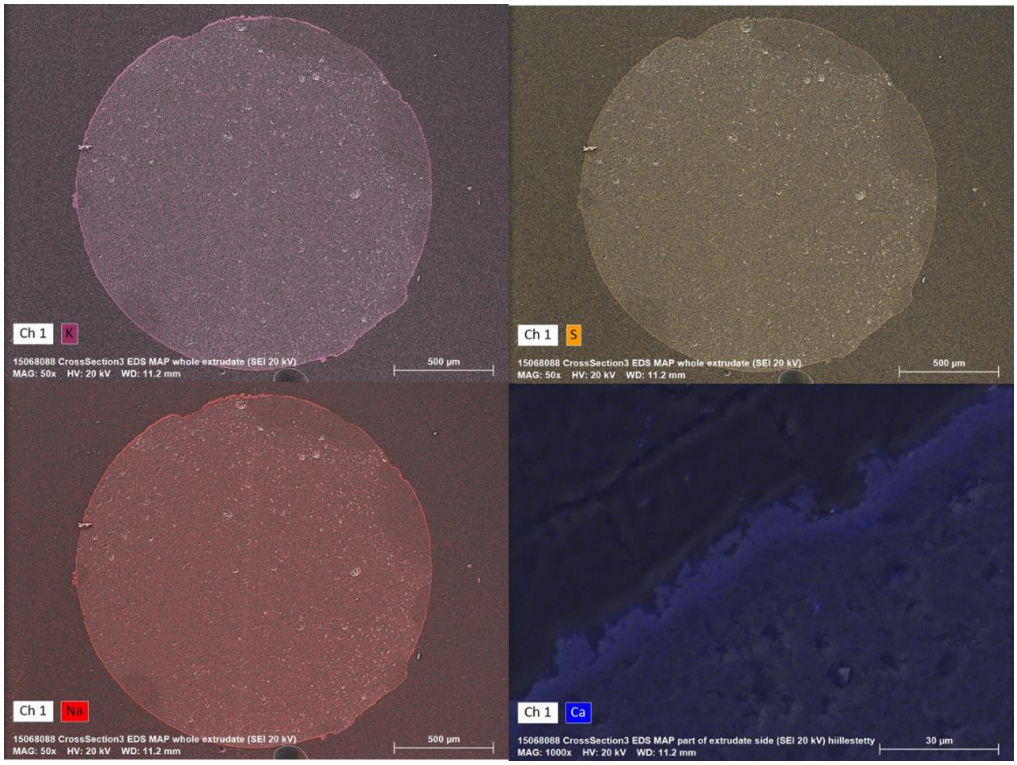

Appendix 8: SEM-EDS linescan profile of the spent γ-alumina from phosphorus removal reference test run

Figure 1. Linescan of the alumina extrudate. High content of phosphorus can be seen on the rim of the extrudates.

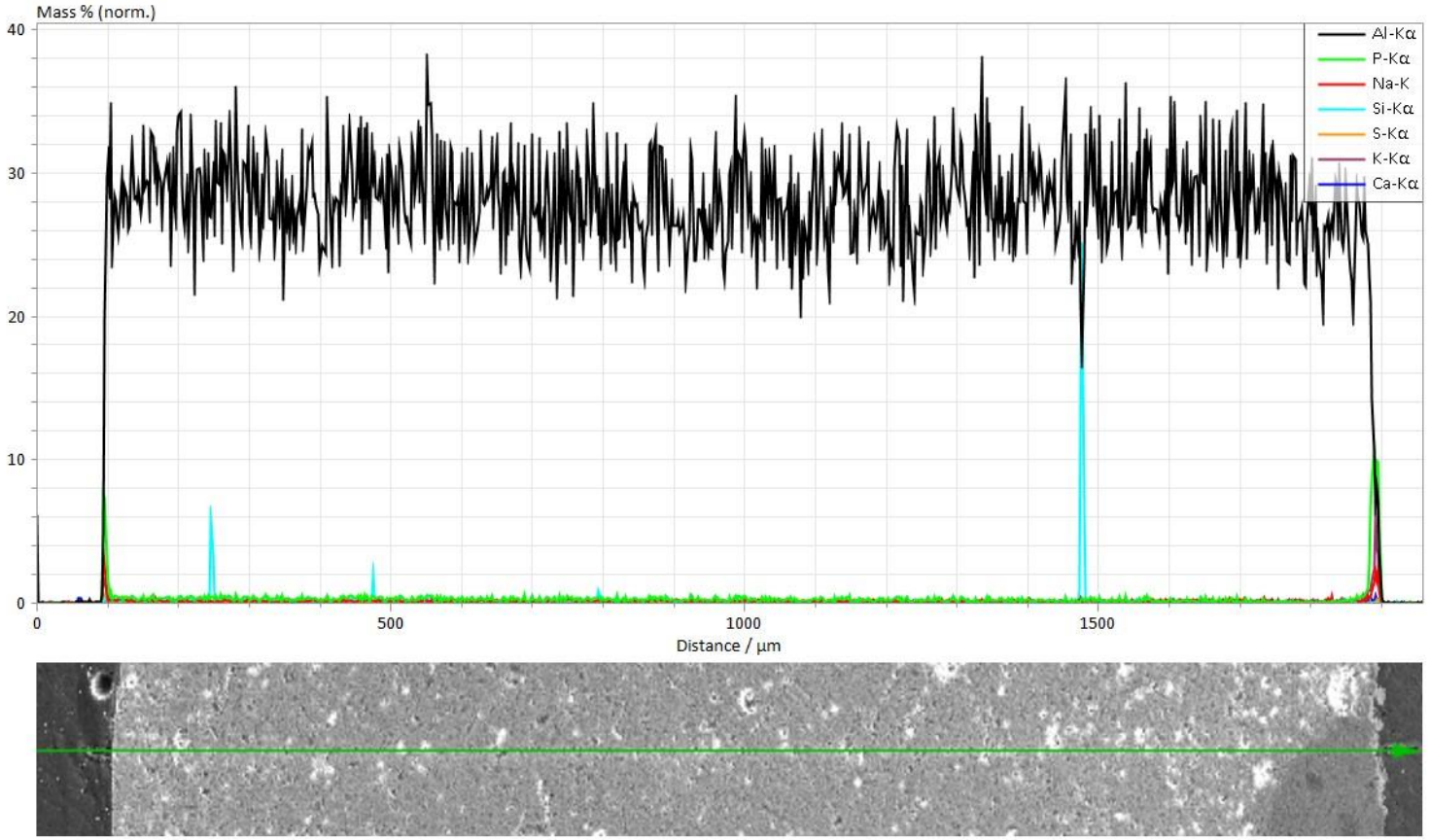

Appendix 9: XRD diffractograms of spent γ-alumina from phosphorus removal low temperature test run

Figure 1. No changes to fresh sample are seen.

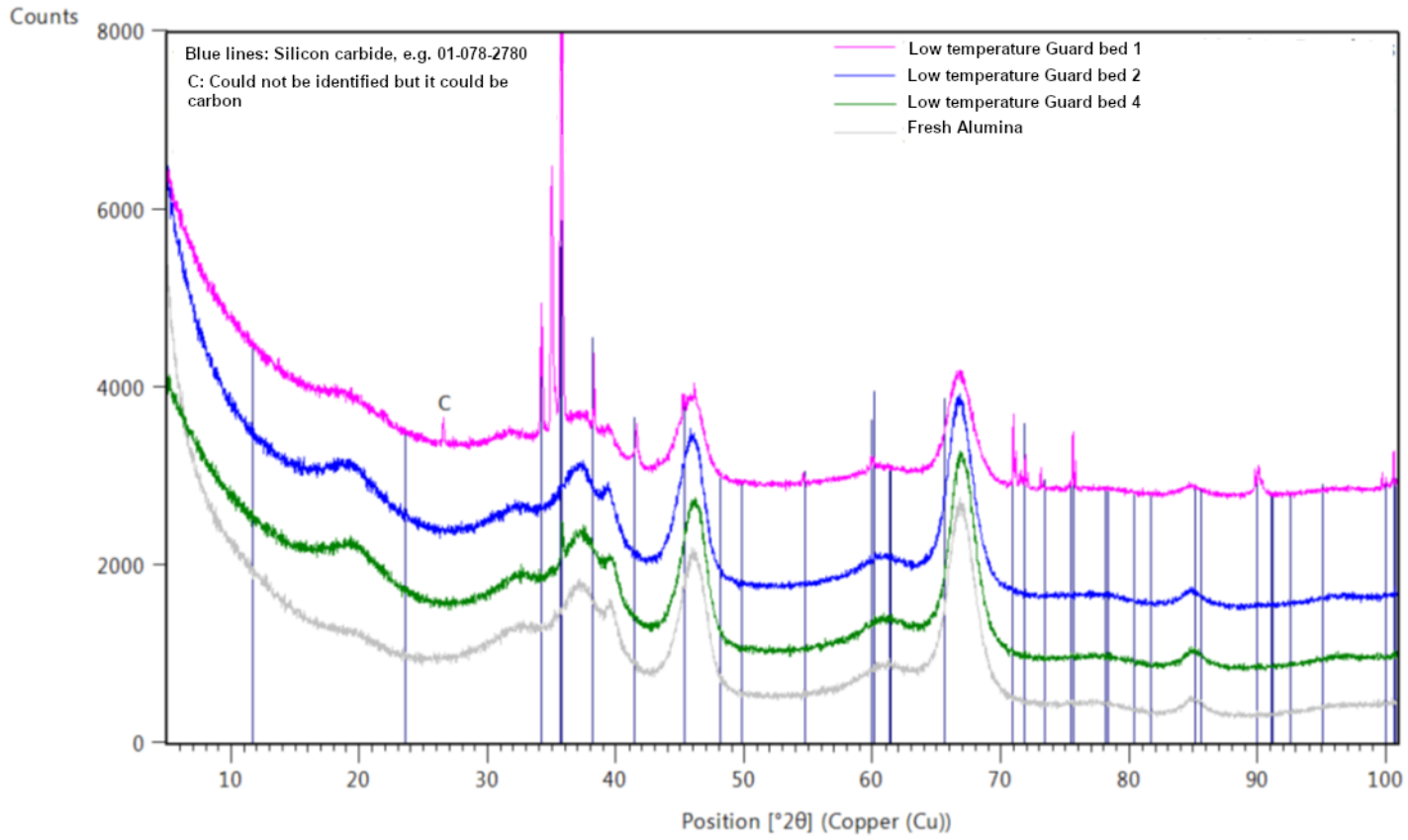

Appendix 10: Analysis results for the liquid products from the reference silicon removal test run

Table 1. Liquid product analysis results (1/2).

Sample name		Refer-ence P1	Refer-ence P2	Refer-ence P3	Refer-ence P4	Refer-ence P5	Refer-ence P6	Refer-ence P7	Refer-ence P8	Refer-ence P9
Density at 50 °C	kg/m3	956.7	956.6	956.6	956.4	956.5	956.4	956.4	956.1	956.5
Total nitrogen	mg/kg	519.561	522.487	512.158	511.409	520.199	515.817	539.099	537.287	538.848
Sodium (ICP-MS)	mg/kg	18.098	11.72	10.449	6.296	5.848	5.74	4.679	4.502	4.308
Magnesium (ICP-MS)	mg/kg	0.0466	0.0313	0.0189	0.0136	0	0	0.00375	0.00295	0
Aluminium (ICP-MS)	mg/kg	208	167	131	93.76	81.79	76.4	69	64	57
Silicon (ICP-MS)	mg/kg	15.66	16.97	17.41	16.96	16.92	16.72	16.34	16.71	15.79
Phosphorus (ICP-MS)	mg/kg	1.71	1.68	1.786	1.558	1.506	1.48	1.26	1.578	1.527
Potassium (ICP-MS)	mg/kg	0.156	0.209	0.168	0.326	0.1427	0.128	0.183	0.11	0.131
Calcium (ICP-MS)	mg/kg	0.463	0.38	0.348	0.326	0.293	0.197	0.336	0.427	0.311
Iron (ICP-MS)	mg/kg	6.057	5.87	5.79	5.399	5.21	4.96	4.811	6.51	6.587
Sulphur, MWDXRF	mg/kg	2105	2109	2116	2107	2109	2117	2116	2131	2129
Total chlorides	mg/kg	2.71	3.045	3	3.065	3.165	2.955	2.825	2.89	2.92
Total Acid Number (TAN)	mg KOH/g	79.4	77.9	76.1	75.4	77.3	78.8	87.53	92.09	88.26

Appendix 10: Analysis results for the liquid products from the reference silicon removal test run

Table 2. Liquid product analysis results (2/2).

Sample name		Refer-ence P10	Refer-ence P11	Refer-ence P12	Refer-ence P13
Density at 50 °C	kg/m3	956.2	956	956.1	956.2
Total nitrogen	mg/kg	537.461	541.846	537.969	534.546
Sodium (ICP-MS)	mg/kg	3.713	3.897	3.783	3.27
Magnesium (ICP-MS)	mg/kg	0.00389	0	0	0
Aluminium (ICP-MS)	mg/kg	58	54	53	49
Silicon (ICP-MS)	mg/kg	16.59	16.29	16.37	15.71
Phosphorus (ICP-MS)	mg/kg	1.664	1.502	1.361	1.317
Potassium (ICP-MS)	mg/kg	0.191	0.147	0.187	0.156
Calcium (ICP-MS)	mg/kg	0.336	0.382	0.267	0.4089
Iron (ICP-MS)	mg/kg	6.714	6.268	6.032	5.249
Sulphur, MWDXRF	mg/kg	2117	2130	2116	2123
Total chlorides	mg/kg	2.975	2.985	2.585	2.665
Total Acid Number (TAN)	mg KOH/g	95.17	89.08	96.43	89.62

Appendix 11: Analysis results for the liquid products from the condition change silicon removal test runs

Table 1. Liquid product analysis results of low temperature test run.

Sample name		Low tempera-ture P1	Low tempera-ture P2	Low tem-perature P3	Low tem-perature P4	Low tem-perature P5	Low tem-perature P6
Density at 50 °C	kg/m3	956.26	956.12	956.38	956.28	956.29	956.27
Total nitrogen	mg/kg	539.446	543.388	547.79	547.595	543.587	547.72
Sodium (ICP-MS)	mg/kg	17.91	4.123	3.061	2.664	2.54	17.78
Magnesium (ICP-MS)	mg/kg	0.104	0.00748	0	0	0	0
Aluminium (ICP-MS)	mg/kg	16	15.05	14.69	14.3	14.22	14.47
Silicon (ICP-MS)	mg/kg	15.59	15.05	14.69	14.307	14.22	14.47
Phosphorus (ICP-MS)	mg/kg	1.66	1.752	1.631	1.415	1.77	1.77
Potassium (ICP-MS)	mg/kg	0.501	0.425	0.362	0.391	0.505	0.51
Calcium (ICP-MS)	mg/kg	0.333	0.01352	0.03549	0	0.0366	0.1
Iron (ICP-MS)	mg/kg	2.609	1.866	1.334	1.176	1.962	2.18
Sulphur, MWDXRF	mg/kg	2141.49	2139.23	2156.98	2143.61	2130.81	2135.88
Total chlorides	mg/kg	4.55	4.4	4.295	4.61	4.625	4.59
Total Acid Number (TAN)	mg KOH/g	84.5	75.67	80.29	71.93		

Appendix 11: Analysis results for the liquid products from the condition change silicon removal test runs

Table 2. Liquid product analysis results of low pressure test run.

Sample name		Low pressure P1	Low pressure P2	Low pressure P3	Low pressure P4	Low pressure P5	Low pressure P6	Low pressure P7	Low pressure P8	Low pressure P9	Low pressure P10	Low pressure P11
Density at 50 °C	kg/m3	956.54	956.09	955.27	956.44	956.4	956.32	956.33	956.09	956.28	956.4	956.42
Total nitrogen	mg/kg	533.629	529.139	530.555	533.889	533.474	534.832	536.092	538.373	542.354	539.865	534.799
Sodium (ICP-MS)	mg/kg	20.74	9.265	7.517	0.402	0.897	4.71	5.084	5.13	4.8	4.921	4.76
Magnesium (ICP-MS)	mg/kg	0.122	0.0436	0.02216	0.0295	0.032	0.0182	0.03377	0.01018	0.03205	0.03187	0.02977
Aluminium (ICP-MS)	mg/kg	195	81	63.79	60.38	53.36	44.87	39.46	36.92	37.3	36.46	34.63
Silicon (ICP-MS)	mg/kg	17.04	16.78	17.96	17.43	16.6	16.29	18.138	17.93	17.99	18.13	18.145
Phosphorus (ICP-MS)	mg/kg	1.434	1.39	1.423	1.324	1.26	1.169	1.118	0.9196	1.961	1.98	1.69
Potassium (ICP-MS)	mg/kg	0.246	0.117	0.148	0.149	0.103	0.0913	0.06935	0	0.055	0.08697	0.064606
Calcium (ICP-MS)	mg/kg	0.587	0.224	0.167	0.236	0.185	0.103	0.067	0	0.2476	0.363	0.324
Iron (ICP-MS)	mg/kg	7.133	5.937	5.7	5.89	5.33	4.24	3.3469	2.546	7.691	9.144	7.629
Sulphur, MWDXRF	mg/kg	2080.94	2096.11	2086.82	2086.15	2080.57	2081.31	2085.02	2090.52	2121.995	2104.93	2128.095
Total chlorides	mg/kg	3.85	4.33	4.275	4.215	4.22	4.04	4.08	4.195	3.74	3.865	3.645
Total Acid Number (TAN)	mg KOH/g	77.81	75.91	75.71	76.53	76.11	81.87	75.97	79.56	76.13	77.47	77.26

Appendix 11: Analysis results for the liquid products from the condition change silicon removal test runs

Table 3. Liquid product analysis results of low feed rate test run.

Sample name		Low feed rate P0	Low feed rate P1	Low feed rate P2	Low feed rate P3	Low feed rate P4	Low feed rate P5	Low feed rate P6	Low feed rate P7	Low feed rate P8	Low feed rate P9	Low feed rate P10
Density at 50 °C	kg/m3	956.86	958.01	957.41	957.02	956.76	956.58	956.84	956.75	956.71	956.56	956.29
Total nitrogen	mg/kg	534.813	536.025	533.623	535.536	537.589	539	537.482	527.406	537.596	537.527	537.549
Sodium (ICP-MS)	mg/kg	145	68.9	39.6	21.05	16.4	14	12.893	10.8	9.75	9.196	7.894
Magnesium (ICP-MS)	mg/kg	1.071	0.436	0.195	0.062	0.037	0.005	0.009	0.026	0.013	0.003	0
Aluminium (ICP-MS)	mg/kg	986	734	614	373	274	247	231	207	188	179	171
Silicon (ICP-MS)	mg/kg	15.1	17.4	17.5	18	19.3	18.87	18.862	19.5	19.5	19.75	19.9
Phosphorus (ICP-MS)	mg/kg	1.041	0.717	0.68	0.745	0.983	0.933	0.907	0.921	0.834	0.845	0.739
Potassium (ICP-MS)	mg/kg	1.089	0.595	0.284	0.19	0.175	0.155	0.161	0.158	0.111	0.113	0.093
Calcium (ICP-MS)	mg/kg	5.615	2.1	1.078	0.529	0.484	0.426	0.493	0.357	0.314	0.321	0.316
Iron (ICP-MS)	mg/kg	26.4	10.1	5.418	3.447	4.111	4.032	4.124	4.256	4.027	3.789	3.507
Sulphur, MWDXRF	mg/kg	1990.445	1736.31	2041.61	2077.87	2066.84	2075.385	2096.33	2101.67	2082.665	1958.255	1858.125
Total chlorides	mg/kg	3.48	3.215	3.5	3.235	3.425	3.59	3.645	3.635	4.92	3.695	3.035
Total Acid Number (TAN)	mg KOH/g	69.7	71.9	73.2	78.59	77.33	74.46	81.33	77.52	75.58	75.06	79.39

Appendix 12: XRD diffractograms of γ-alumina from silicon removal test run

Figure 1. No changes compared to the fresh alumina are seen.

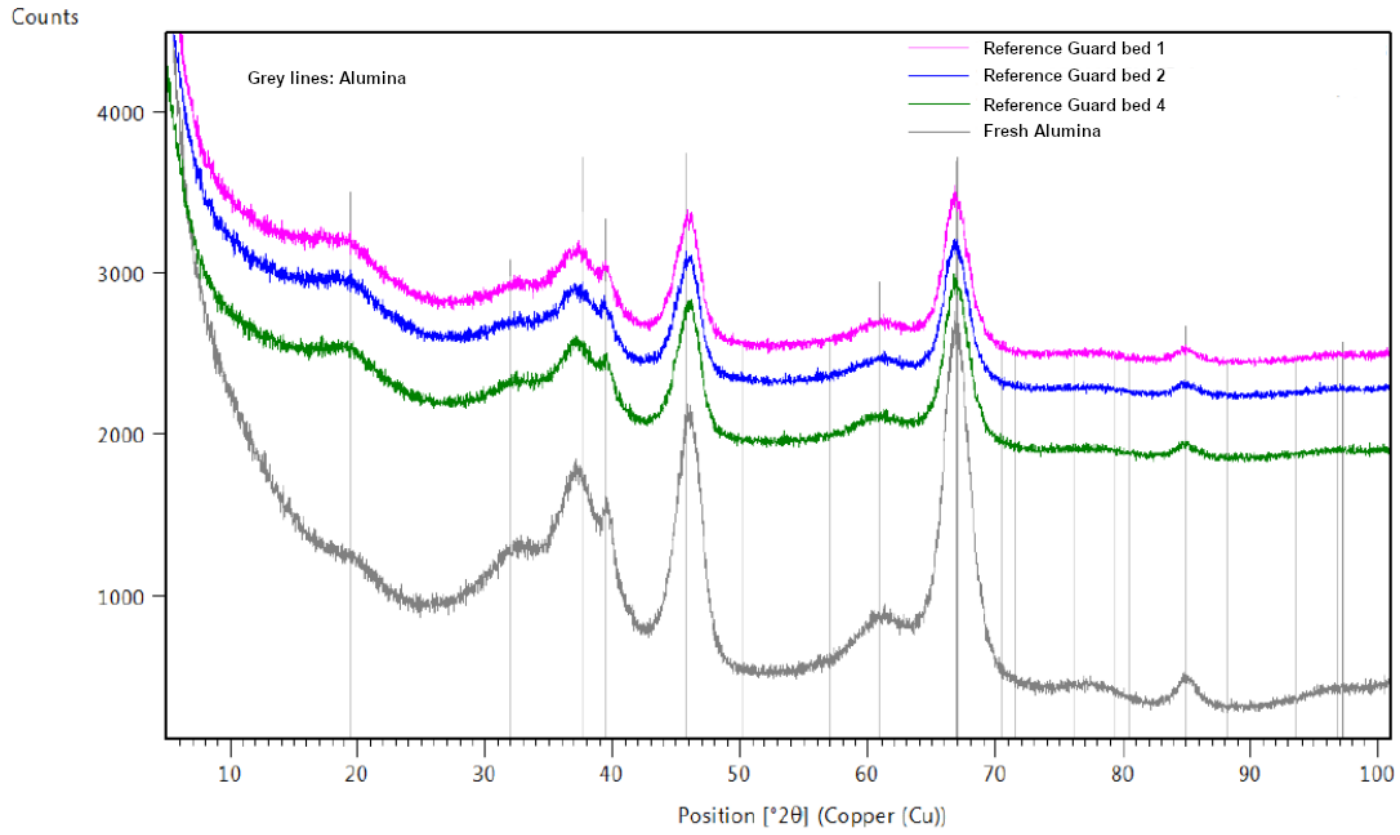

Appendix 13: EDS scan of the surface of spent γ-alumina in silicon removal test runs

Table 1. Content of different elements on the surface of spent alumina from reference, low temperature and low pressure test runs.

Sample name		Reference Guard bed 1	Reference bed 2	Reference bed 4	Low temperature Guard bed 1	Low temperature Guard bed 2	Low temperature Guard bed 4	Low pressure Guard bed 1	Low pressure Guard bed 2	Low pressure Guard bed 4
Sodium (EDS)	wt-%	0.1	0.1	0.1	0.5	0.7	0.3	0.5	1.7	0.1
Aluminum (EDS)	wt-%	23.3	33.7	31.8	35.6	35.5	38.9	45.8	34.5	36.9
Silicon (EDS)	wt-%	0.2	0.3	0.3	0.2	0.2	0.3	0.4	0.7	0.4
Phosphorus (EDS)	wt-%	5.2	0.7	0.7	1.0	0.7	0.4	0.3	1.3	0.8
Sulfur (EDS)	wt-%	0.8	0.4	0.3	0.3	0.3	0.3	0.1	0.4	0.4
Potassium (EDS)	wt-%	0.1	0.0	0.0	0.2	0.2	0.1	0.0	0.2	0.0
Calcium (EDS)	wt-%				0.0	0.0	0.0	0.0	0.1	0.0
Titanium (EDS)	wt-%	0.0	0.0	0.0						
Iron (EDS)	wt-%	0.2	0.1	0.1	0.3	0.3	0.3	0.0	0.0	0.1